THE USE OF INHIBITORS TO STABILIZE FOLDED CONFORMATIONS OF ENZYMES

By

STEPHEN P. REID
B.Sc., The University of British Columbia, 2000

A THESIS SUBMITTED IN PARTIAL FULFILLMENT OF
THE REQUIREMENTS OF THE DEGREE OF
MASTER OF SCIENCE
in
THE FACULTY OF GRADUATE STUDIES
(Department of Chemistry)

We accept this thesis as conforming
to the required standard

THE UNIVERSITY OF BRITISH COLUMBIA
March 2004
© Stephen P. Reid, 2004

Library Authorization

In presenting this thesis in partial fulfillment of the requirements for an advanced degree at the University of British Columbia, I agree that the Library shall make it freely available for reference and study. I further agree that permission for extensive copying of this thesis for scholarly purposes may be granted by the head of my department or by his or her representatives. It is understood that copying or publication of this thesis for financial gain shall not be allowed without my written permission.

Stephen Reid
Name of Author *(please print)*

31/03/2004
Date (dd/mm/yyyy)

Title of Thesis: The Use of Inhibitors to Stabilize Folded Conformations of Enzymes

Degree: M.Sc.

Year: 3/2004

Department of Chemistry
The University of British Columbia
Vancouver, BC Canada

Abstract

Tay Sachs and Gaucher diseases are lysosomal storage disorders that are caused by deficiencies in the lysosomal enzymes β-hexosaminidase A and glucocerebrosidase, respectively. The glycolipid substrates of deficient β-hexosaminidase A and glucocerebrosidase accumulate in lysosomal neurons, resulting in neurodegenerative disorders. The enzyme deficiencies are caused by heritable amino acid point mutations that result in unstable and potentially misfolded enzymes. The mutant enzymes, although catalytically active in many cases, are destroyed by cellular quality control mechanisms in the endoplasmic reticulum (ER).

A potential therapy for adult chronic Tay Sachs disease and Gaucher disease is the use of enzyme inhibitors as chemical chaperones. To act as a chemical chaperone the enzyme-specific inhibitor must stabilize the folded conformation of the enzyme and thus prevent enzyme destruction by cellular quality control mechanisms. The enzyme/inhibitor complex can then be transferred from the ER to the lysosome where the substrate concentration is significantly high that some enzyme activity is restored. In the chronic adult disease forms, only 10 % of normal enzyme activity is required for a patient to become asymptomatic.

A competitive inhibitor for β-hexosaminidase A, NAG-thiazoline, was synthesized and shown to be a potent inhibitor of β-hexosaminidase A and the related enzyme β-hexosaminidase B, with K_i values of 270 nM and 190 nM, respectively. Chemical denaturation studies showed that NAG-thiazoline stabilizes a bacterial hexosaminidase from *Streptomyces plicatus* (*Sp. Hex.*) and human β-hexosaminidase B against guanidine hydrochloride denaturation. Thermal denaturation studies showed that NAG-thiazoline stabilizes *Sp. Hex.*, β-hexosaminidase B, and β-hexosaminidase A against thermal denaturation. These results provide a chemical explanation for recent results from collaborator Dr. Mike Tropak (The Hospital for Sick Children, Toronto), which showed that NAG-thiazoline increases β-hexosaminidase A activity in Tay Sachs fibroblasts.

A mechanism based inactivator for glucocerebrosidase, 2-deoxy-2-fluoro-β-D-glucopyranosyl fluoride, was synthesized and shown to stabilize glucocerebrosidase against guanidine hydrochloride denaturation. *N*-Octyl-1-epivalienamine was synthesized and shown to be a potent competitive inhibitor of glucocerebrosidase with

a K_i value of 75 nM and to stabilize glucocerebrosidase against thermal denaturation. These results show that 2-deoxy-2-fluoro-β-D-glucopyranosyl fluoride and *N*-octyl-1-epivalienamine stabilize the folded conformation of glucocerebrosidase and may act as chemical chaperones in therapies for Gaucher disease.

An additional study was performed in which the synthetic capacity of a glycosynthase developed from a β-glucuronidase from *Thermotoga maritima* was explored. Using α-D-glucopyranuronosyl fluoride or α-D-galactopyranuronosyl fluoride as donors, and pNP-glucoside, pNP-xyloside, and pNP-cellobioside as acceptors, the E476A β-glucuronidase mutant catalyzed the formation of six novel oligosaccharides.

Table of Contents

Abstract ii

Table of Contents iv

List of Figures vii

List of Tables ix

List of Schemes x

List of Abbreviations xi

Acknowledgments xiii

1 General Introduction **1**

1.1 Glycosidases 1

1.1.1 The Catalytic Mechanism of Retaining β-Glycosidases 2

1.1.2 The Anchimeric Assistance Mechanism 5

1.1.3 Glycosidase Inhibitors 8

1.1.4 Mechanism Based Inactivators 9

1.2 Lysosomal Storage Disorders 10

1.2.1 Tay Sachs Disease 13

1.2.1.1 The Human Hexosaminidases 13

1.2.1.2 The Cause of the Deficiency in Hex A 16

1.2.2 Gaucher Disease 17

1.2.2.1 Glucocerebrosidase 18

1.2.3 Therapies for Lysosomal Storage Disorders 19

1.2.3.1 The Chemical Chaperone Approach 19

1.3 Aims of this Thesis 21

2 The Stabilizing Effect of NAG-Thiazoline on Family 20 Hexosaminidases **22**

2.1 NAG-Thiazoline: a Competitive Inhibitor of Family 20 Hexosaminidases 22

2.2 The Synthesis of NAG-Thiazoline 24

2.3 Inhibition Results 25

2.4 Denaturation Experiments 31

2.4.1 Sp. Hex. Thermal Denaturation Studies 32

2.4.2 Sp. Hex. Guanidine Hydrochloride Denaturation Studies 33

2.4.3 Hex B Thermal Denaturation Studies 37

2.4.4 Hex B Guanidine Hydrochloride Denaturation Studies 38

2.4.5 Hex A Denaturation Studies 41

2.5 Conclusion/Future Outlook 42

3 The Stabilizing Effect of 2-Deoxy-2-Fluoro-β-D-Glucopyranosyl Fluoride and *N*-Octyl-1-Epivalienamine on Glucocerebrosidase 43
- 3.1 Stabilization of Glucocerebrosidase by a Mechanism-Based Inactivator 43
  - *3.1.1 The Synthesis of 2-Deoxy-2-Fluoro-β-D-Glucopyranosyl Fluoride* 45
  - *3.1.2 Inactivation of Glucocerebrosidase with 2-Deoxy-2-Fluoro-β-D-Glucosyl Fluoride.* 46
  - *3.1.3 Denaturation Studies with Glucocerebrosidase in the Presence and Absence of 2-Deoxy-2-Fluoro-β-D-Glucosyl Fluoride* 47
- 3.2 Stabilization of Glucocerebrosidase by a Competitive Inhibitor 51
  - *3.2.1 N-Octyl-1-Epivalienamine: a Competitive Inhibitor of Glucocerebrosidase* 51
  - *3.2.2 The Inhibition of Glucocerebrosidase by N-Octyl-1-Epivalienamine* 53
  - *3.2.3 Denaturation Studies with Glucocerebrosidase in the Presence and Absence of N-Octyl-1-Epivalienamine.* 54
- 3.3 Conclusion 56

4 The Development of a Glucuronidase Glycosynthase 57
- 4.1 Introduction 57
  - *4.1.1 Backgound on Glycosynthases* 57
  - *4.1.2 Thermotoga maritima* 59
  - *4.1.3 β-Glucuronidases* 59
- 4.2 Development of a Glucuronosynthase from the β-Glucuronidase from *Thermotoga maritima* 60
  - *4.2.1 Synthesis of Donor Sugars: α-D-Glucopyranuronosyl Fluoride and α-D-Galactopyranuronosyl fluoride* 61
  - *4.2.2 Glucuronosynthase Reactions* 62
  - *4.2.3 Attempts to Synthesize Glycosaminoglycan Fragments* 66
- 4.3 Conclusion 70

5 Materials and Methods 71
- 5.1 Enzymology 71
  - *5.1.1 Sp. Hex. Kinetics* 71
  - *5.1.2 Human β-Hexosaminidase A and B Kinetics* 71
    - 5.1.2.1 Determination of k_{cat}/K_m Values for pNP-GlcNAc and pNP-GalNAc 72
  - *5.1.3 Glucocerebrosidase Kinetics* 73
  - *5.1.4 Competitive Inhibition* 73
  - *5.1.5 Inactivation of Glucocerebrosidase* 74
  - *5.1.6 Thermal Denaturation Experiments* 74
  - *5.1.7 Guanidine Hydrochloride Denaturation Experiments* 76
  - *5.1.8 General Procedure for Glucuronidase Glycosynthase Reactions* 78
- 5.2 Syntheses 79

5.2.1 General Synthesis 79
5.2.2 Generous Gifts 79
5.2.3 NAG-Thiazoline ***(2.2)*** 80
5.2.4 2-Deoxy-2-Fluoro-β-D-Glucopyranosyl Fluoride ***(3.3)*** 82
5.2.5 N-Octyl-1-Epivalienamine ***(3.6)*** 84
5.2.6 α-D-Galactopyranuronosyl Fluoride ***(4.6)*** 86
5.2.7 α-D-Glucopyranuronosyl Fluoride ***(4.9)*** 89
5.2.8 General Procedure for Derivitization of Glycosynthase Products 90
5.2.9 Assignment of Protons in ^{1}*H NMR Spectra of Derivatized Glycosynthase Products* 91
5.2.10 Characterization of Glycosynthase Products 91

Appendix 95
References 96

List of Figures

Figure 1.1 Diagram showing the glycone and aglycone components of a D-glucoside, and the numbering scheme used for carbohydrates in this thesis 1

Figure 1.2 Stereochemical outcome of reactions catalyzed by inverting and retaining glycosidases 2

Figure 1.3 The ion pair intermediate proposed by Phillips 4

Figure 1.4 Examples of competitive inhibitors of glycosidases 9

Figure 1.5 Diagram of terminal *N*-acetyl-β-D-glucosamine (**1.6**) and *N*-acetyl-β-D-galactosamine (**1.7**) residues 14

Figure 1.6 Diagram of 4-methylumbelliferyl β-D-*N*-acetylglucosamine-6-sulfate (**1.8**) (MUGS) 15

Figure 1.7 Diagram of *N*-butyl deoxynojirimycin (**1.9**) 19

Figure 1.8 Diagram of compounds **1.10-1.12** 20

Figure 2.1 Diagram showing the oxazolinium ion intermediate and NAG-thiazoline (**2.2**) 22

Figure 2.2 Diagram of 4-methylumbelliferyl 2-thioacetamido glucoside (**2.3**) 23

Figure 2.3 Diagram of GalNAc-isofagomine·HCl (**2.4**) 24

Figure 2.4 Diagram of 4-methylumbelliferyl β-D-*N*-acetylglucosaminide (MUG) (**2.5**) 26

Figure 2.5 Dixon plots for a series of family 20 inhibitors 28

Figure 2.6 Diagram of pNP-GlcNAc (**2.8**) and pNP-GalNAc (**2.9**) 29

Figure 2.7 The folded and unfolded states of a protein 31

Figure 2.8 The relative activity of *Sp. Hex.* in the presence or absence of NAG-thiazoline during thermal denaturation at 55 °C 33

Figure 2.9 The intrinsic fluorescence spectrum of *Sp. Hex.* in buffer and in 5 M guanidine hydrochloride 34

Figure 2.10 The intrinsic fluorescence spectrum of *Sp. Hex.* in the absence and presence of NAG-thiazoline 34

Figure 2.11 Chemical denaturation of *Sp. Hex.* in the absence and presence of NAG-thiazoline, as monitored by intrinsic fluorescence 35

Figure 2.12 The CD spectrum of *Sp. Hex* 36

Figure 2.13 Chemical denaturation of *Sp. Hex.* in the absence and presence of NAG-thiazoline, as monitored by CD spectrometry 37

Figure 2.14 The relative activity of Hex B in the presence or absence of NAG-thiazoline during thermal denaturation at 60 °C 38

Figure 2.15 The intrinsic fluorescence spectrum of folded and denatured Hex B 39

Figure 2.16 The intrinsic fluorescence spectrum of Hex B incubated with NAG-thiazoline, folded and denatured 39

Figure 2.17 Chemical denaturation of Hex B in the absence and presence of NAG-thiazoline, as monitored by intrinsic fluorescence (λ_{max}) 40

Figure 2.18 The relative activity of Hex A in the presence or absence of thiazoline during thermal denaturation at 56 °C 41

Figure 3.1 Diagram of 2-deoxy-2-fluoro-β-D-glucopyranosyl fluoride (**3.3**) 43

Figure 3.2 The time-dependent inactivation of glucocerebrosidase at room temperature by 2-deoxy-2-fluoro-β-D-glucopyranosyl fluoride (**3.3**) 47
Figure 3.3 The intrinsic fluorescent spectra of folded and denatured glucocerebrosidase 48
Figure 3.4 Chemical denaturation of glucocerebrosidase in the absence and presence of 2-deoxy-2-fluoro-β-D-glucopyranosyl fluoride (inactivator), as monitored by intrinsic fluorescence at a fixed wavelength of 330 nm 49
Figure 3.5 Chemical denaturation of glucocerebrosidase in the absence and presence of 2-deoxy-2-fluoro-β-D-glucopyranosyl fluoride (inactivator), as monitored by intrinsic fluorescence at λ_{max} 49
Figure 3.6 Diagram of *N*-octyl-1-epivalienamine (**3.6**) and 1-epivalienamine (**3.7**) 51
Figure 3.7 Dixon plot for the inhibition of glucocerebrosidase by *N*-octyl-1-epivalienamine 54
Figure 3.8 Lineweaver-Burk plot for glucocerebrosidase inhibition by *N*-octyl-1-epivalienamine 54
Figure 3.9 The relative activity of glucocerebrosidase in the presence or absence of *N*-octyl-1-epivalienamine during thermal denaturation at 53 °C 55
Figure 4.1 The structures of glucuronic acid (**4.1**) and hyaluronic acid (**4.2**) 59
Figure 4.2 Diagram of UDP-glucuronic acid 60
Figure 4.3 Diagram of 2-deoxy-2-fluoro-β-D-glucopyranuronosyl fluoride 61
Figure 4.4 Diagram of α-D-galactopyranuronosyl fluoride (**4.6**) and α-D-glucopyranuronosyl fluoride (**4.9**) 61
Figure 4.5 The compounds that did not function as acceptors for the E476A glucuronosynthase 67
Figure 4.6 Molecular model of *T. maritima* β-glucuronidase with bound 2-deoxy-2-fluoro galactosyl moiety 69
Figure 4.7 Space-filled model of *T. maritima* β-glucuronidase 69

List of Tables

Table 2.1 K_i values for a series of family 20 glycosidase inhibitors 27

Table 2.2 Family 20 hexosaminidase substrate specificities 30

Table 4.1 E476A Glucuronidase glycosynthase reaction yields 64

Table 4.1 E476A Glucuronidase glycosynthase products selected for characterization 65

Table 5.1 Concentrations and temperatures used during thermal denaturation experiments 75

Table 5.2 Concentrations used during guanidine hydrochloride denaturation experiments 77

List of Schemes

Scheme 1.1 The mechanism of a retaining β-glucosidase 3

Scheme 1.2 The mechanism of family 20 β-hexosaminidases 7

Scheme 1.3 Inactivation of a retaining β-glucosidase with 2,4-dinitrophenyl 2-deoxy-2-fluoro-β-D-glucopyranoside (**1.5**) 10

Scheme 1.4 The degradation of gangliosides by lysosomal enzymes 12

Scheme 1.5 The reaction catalyzed by lysosomal human β-hexosaminidase A 15

Scheme 1.6 The reaction catalyzed by glucocerebrosidase 18

Scheme 2.1 The synthesis of NAG-thiazoline (**2.2**) 25

Scheme 3.1 Inactivation of a retaining β-glycosidase with 2-deoxy-2-fluoro-β-D-glucopyranosyl fluoride (**3.3**) 44

Scheme 3.2 The synthesis of 2-deoxy-2-fluoro-β-D-glucopyranosyl fluoride (**3.3**) 46

Scheme 3.3 The synthesis of *N*-octyl-1-epivalienamine (**3.6**) 53

Scheme 4.1 a. A trans-glycosylation reaction 58

b. A glycosynthase reaction 58

Scheme 4.2 The synthesis of galactopyranuronosyl fluoride (**4.6**) 62

Scheme 4.3 A glycosynthase reaction catalyzed by the E476A mutant of β-glucuronidase 63

Scheme 4.4 The acetylation and esterification of compound 4.13 66

List of Abbreviations

Abg:	*Agrobacterium sp.* β-glucosidase
Ar:	Aryl
a.u.:	Absorbance units
Bn:	Benzyl
CD:	Circular dichroism
CHO:	Chinese hamster ovary
CMC:	Critical micelle concentration
COSY:	Correlation spectroscopy
DNP:	Dinitrophenyl
E. coli	*Escherichia coli*
ER:	Endoplasmic reticulum
F:	Folded
GalNAc:	*N*-acetylgalactosamine
GalNAc-isofagamine:	(2*R*,3*R*,4*S*,5*R*)-2-acetamido-3,4-dihydroxy-5-hydroxymethyl-piperidine
GlcNAc:	*N*-acetylglucosamine
GlcNAc-6-SO$_4^-$:	*N*-acetylglucosamine-6-sulfate
GMP:	Good manufacturing practices
h:	Hour(s)
Hex A:	β-Hexosaminidase A
Hex B:	β-Hexosaminidase B
Hex S:	β-Hexosaminidase S
I:	Inhibitor
$k_{\text{cat}}/k_{\text{non}}$:	Ratio of rate constants for catalyzed and non-catalyzed reactions
$k_{\text{H}}/k_{\text{D}}$:	Ratio of rate constants for protio and deutero substrates
K_{i}:	Inhibition constant
K_{m}:	Michaelis constant of a substrate
LC-MS/MS:	Liquid chromatography-tandem mass spectrometry
M:	Moles per litre
min:	Minutes
MUG:	4-methylumbelliferyl-β-D-*N*-acetylglucosaminide
MUGS:	4-Methylumbelliferyl-β-D-*N*-acetylglucosamine-6-sulfate
m/z:	Mass to charge ratio
NAGal-thiazoline:	(3a*R*,5*S*,6*S*,7*R*,7a*R*)-5-(acetoxymethyl-6,7-diacetoxy-2-methyl-5,6,7,7a-tetrahydro-3a*H*-pyrano[3,2-*d*]thiazole)
NAG-thiazoline:	(3a*R*,5*R*,6*S*,7*R*,7a*R*)-5-(acetoxymethyl-6,7-diacetoxy-2-methyl-5,6,7,7a-tetrahydro-3a*H*-pyrano[3,2-*d*]thiazole)

NMR:	Nuclear magnetic resonance
OAc:	Acetate
PET:	Positron emission tomography
pNP:	*para*-nitrophenyl
pNP-GalNAc:	*para*-nitrophenyl β-D-*N*-acetylgalactosaminide
pNP-GlcNAc:	*para*-nitrophenyl β-D-*N*-acetylglucosaminide
RT:	Room temperature
s:	Seconds
S:	Substrate
Sp. Hex.:	β-Hexosaminidase from *Streptomyces plicatus*
T:	Temperature
THF:	Tetrahydrofuran
TFA:	Trifluoroacetic acid
TLC:	Thin layer chromatography
U:	Unfolded
UDP:	Uridine diphosphate
UV:	Ultraviolet light
v:	Reaction velocity
V_{max}:	Maximum reaction velocity
Vis:	Visible light
XylNAc-isofagamine:	(2*R*,3*R*,4*R*)-2-acetamido-3,4-dihydroxy-piperidine
λ_{max}:	Wavelength of maximum fluorescence
ΔN:	Difference in refractive index

Acknowledgements

I would like to thank my supervisor, Professor Stephen Withers, for his great knowledge and enthusiasm towards science, and for creating a great environment for working and learning. I also thank my collaborators at the Hospital for Sick Children in Toronto: Dr. Don Mahuran, Dr. Mike Tropak, and Brigitte Rigat. I thank Professor R.V. Stick (The University of Western Australia) and Professor Spencer Knapp (Rutgers, New Jersey) for providing compounds. I extend my gratitude to the staff at the UBC NMR facility for technical assistance: Lianne Darge, Marietta Austria and Dr. Nick Burlinson. Thanks to McIntosh group member Dr. Mark Okon for running a 600 MHz NMR. I thank the staff at the UBC mass spectrometry lab and Dr. Fred Rosell for assistance with CD spectroscopy. In the Withers group I'd like to thank Karen Rupitz for assistance with enzyme kinetics and Shouming He for assistance with mass spectrometry. I would also like to thank my summer student, Fathima Shaikh for allowing me to learn some supervision skills and doing a nice job on some syntheses.

I am seriously indebted to many people who provided invaluable advice and guidance along the way, and became my good friends. I would like to thank all Withers group members that I have had the pleasure of working with, past and present. I must give extra thanks to Dr.'s Andrew Watts, Michael Jahn, Chris Tarling, Hongming Chen, David Vocadlo, Carl Rye, Tanja Wrodnigg, Ian Greig, Hannes Muellegger, James Macdonald, Mark Vaughn, and soon to be Dr.'s Dave Dietrich, Luke Lairson, Omid Hekmat, Seung Lee, David Poon, and Brian Rempel.

Finally I thank my non-scientist friends in Vancouver, Calgary and elsewhere, and my family for continuing love and support in my adventures.

1 General Introduction

1.1 Glycosidases

To the average person the word carbohydrate brings to mind spaghetti and maybe a 'carb free' diet. To a scientist, carbohydrates have countless important roles, such as involvement in cell-cell interactions, protein signaling, and as the monomeric units found in cellulose and starch. Along with nucleotides and amino acids, carbohydrates are the molecules most important for carrying out the tasks responsible for life itself.

Carbohydrates in living systems are synthesized, metabolized, transferred, and modified with the help of enzymes. Glycosidases catalyze the cleavage of the glycosidic bond, that is the C-O bond between the glycone (carbohydrate) and the aglycone (may or may not be a carbohydrate) (Figure 1.1).

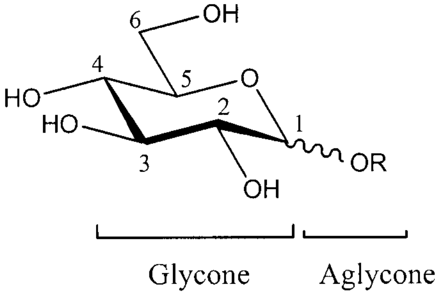

Figure 1.1 Diagram showing the glycone and aglycone components of a D-glucoside, and the numbering scheme used for carbohydrates in this thesis.

The reactions carried out by glycosidases can be classified according to three criteria:

1. *The structure of the glycone.* A particular glycosidase usually demonstrates maximum activity on a specific glycone. For example a galactosidase more rapidly cleaves a galactoside than a glucoside.
2. *The anomeric configuration of the glycone.* Each glycosidase specifically catalyzes the cleavage of either α or β glycosidic linkages.

3. *The stereochemical outcome of the reaction catalyzed.* A glycosidase may catalyze the cleavage of the glycosidic bond with either retention or inversion of configuration of the anomeric centre (Figure 1.2).

In addition, Henrissat has developed a system classifying glycosidases into 92 different families based on amino acid sequence similarities (http://afmb.cnrs-mrs.fr/CAZY/)[1]. Members of each family have the same three-dimensional fold and catalyze reactions with the same stereochemical outcome.

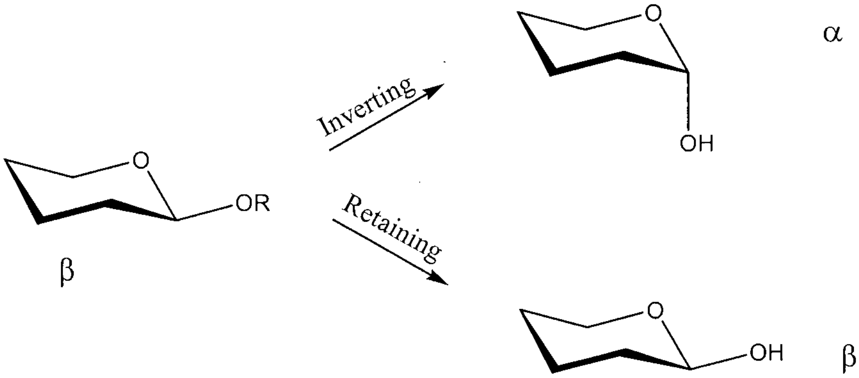

Figure 1.2 Stereochemical outcome of reactions catalyzed by inverting and retaining glycosidases.

The ability of glycosidases to enhance reaction rates is truly remarkable. The glycosidic bond is extremely stable; for example the glycosidic bond in cellulose has a half-life of 5 million years under physiological conditions. Enzymes are able to catalyze the cleavage of glycosidic bonds with rate enhancements[2] (k_{cat}/k_{non}) of up to 10^{17}, an amazing feat considering that an enzyme is simply a polymer of amino acids.

1.1.1 The Catalytic Mechanism of Retaining β-Glycosidases

The mechanism of retaining β-glycosidases, first proposed in 1953 by Koshland, [3] requires the presence of two carboxylic acid groups in the active site. One carboxylic acid group acts as a general acid/base catalyst, and the other acts as the catalytic nucleophile (Scheme 1.1). In the first step of the mechanism, the glycosylation step, the catalytic nucleophile attacks the anomeric center. The mechanism proceeds through an oxocarbenium ion transition state in which the sugar adopts a distorted conformation with partial positive charge on the anomeric carbon and the endocyclic oxygen. The general acid/base residue aids the departure of the aglycone by protonating the glycosidic oxygen. The glycosidic bond is broken and a glycosyl enzyme intermediate, in which the sugar is covalently bound to the enzyme, is formed. In the second step, the deglycosylation step, an incoming nucleophile, water or another carbohydrate (in the case of transglycosylation), attacks the anomeric centre with general base catalysis from the general acid/base residue. A second oxocarbenium ion transition state is formed, again forming partial positive charge on the anomeric carbon and the endocyclic oxygen. Finally, the glycosyl enzyme intermediate is released and the product is formed with overall retention of anomeric configuration.

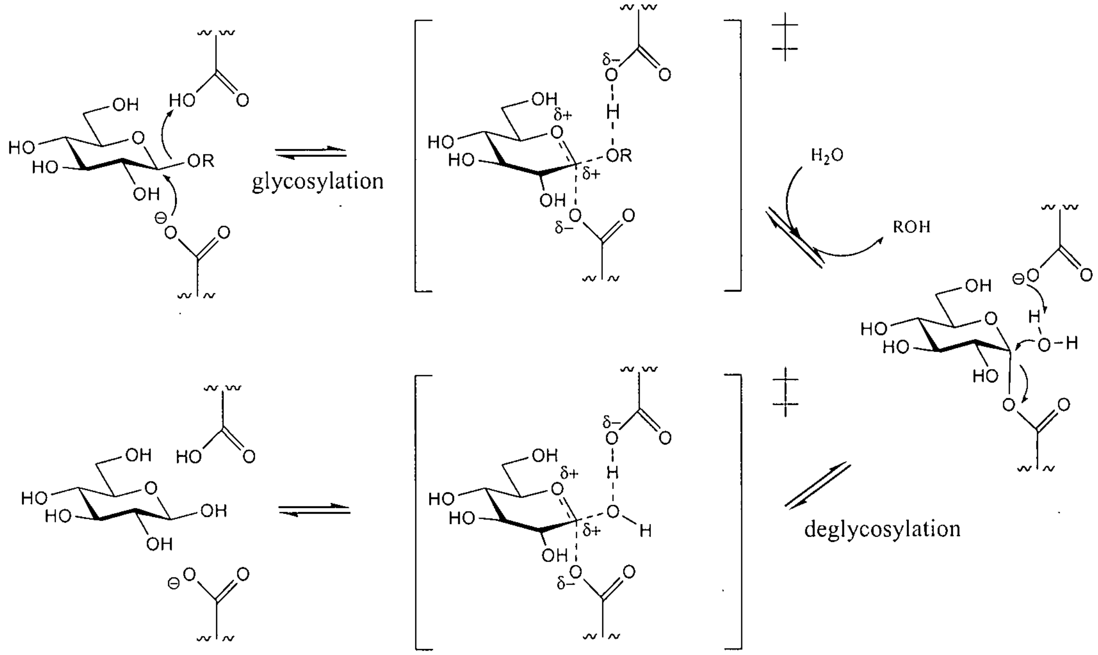

Scheme 1.1 The mechanism of a retaining β-glucosidase.

The double displacement mechanism for retaining β-glycosidases is now widely accepted due to considerable experimental evidence, but historically this was not always the case. An alternative mechanism, proposed by Phillips,[4] involved an

sp^2 hybridized ion-pair intermediate rather than a glycosyl-enzyme intermediate (Figure 1.3).

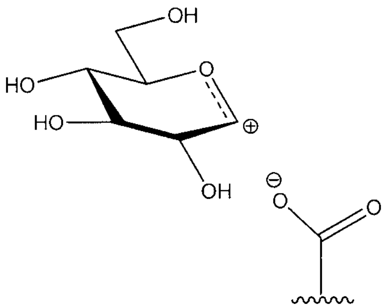

Figure 1.3. The ion pair intermediate proposed by Phillips.[4]

Early evidence against the ion pair mechanism came in the form of kinetic isotope effects. Sinnott and Souchard found that when an activated substrate for which independent studies had shown that the second step was rate-limiting was used, (k_H/k_D) > 1, indicating that the second (deglycosylation) step involved a decrease in hybridization from intermediate to transition state (sp^3 to sp^2-like).[5] If the mechanism did in fact proceed through an ion pair, an inverse kinetic isotope effect would be expected since the ion pair intermediate is sp^2 hybridized, and an increase in hybridization would be needed to reach the more sp^3-like transition state. Further evidence for the double displacement mechanism has been provided by X-ray crystallography. The X-ray crystal structures of numerous retaining β-glycosidases have been published which show the presence of two carboxylic acid residues in the active site, positioned approximately 5 Å apart, a space suitable for the proposed mechanism to take place.[6] In several cases the covalent intermediate has been trapped using a deactivated substrate, which has allowed identification of the catalytic nucleophile through X-ray crystallography,[7] and through proteolytic digestion followed by LC-MS/MS analysis of the fragments.[8,9] Mutagenesis studies in which the acid/base carboxyl group was replaced with a different amino acid have shown that the glycosylation step was slowed for substrates with poor leaving groups which need acid catalysis for departure (reviewed by Zechel and Withers).[10] The deglycosylation step was also slowed considerably for all substrates, since base catalysis was not available to aid the incoming nucleophile. For substrates with reactive leaving groups, the glycosylation step was not affected. However the deglycosylation step was slowed, resulting in accumulation of the covalent intermediate and resulting in unusually low substrate K_m values and high initial reaction rates in the pre-steady state. The addition of nucleophilic anions such as azide, formate and acetate resulted in an increase in rate of cleavage of the glycosyl enzyme intermediate, thus of steady state rates for activated substrates. No such 'rescue' was seen with wild-type enzymes.

In order for the acid/base residue to function as an acid catalyst in the glycosylation step and a base catalyst in the deglycosylation step, the pK_a of the carboxylic acid must change during the course of the reaction. A ^{13}C NMR titration study on a xylanase from *Bacillus circulans* showed that the pK_a of the acid/base residue dropped from 6.7 to 4.2 from the glycosylation to step to the deglycosylation step, indicating that the acid/base carboxylate undergoes "pK_a cycling" in order to act as both an acid and a base catalyst.[11]

The results of a study on a β-glycosidase from *Agrobacterium sp.* (Abg)[12] are also consistent with a double displacement mechanism. A Brønstead plot (log k_{cat} vs. pK_a) for a series of aryl β-glucosides showed a biphasic, concave downward Brønstead relationship, indicating that the deglycosylation step is rate limiting for active substrates, and the glycosylation step is rate limiting for less active substrates. The same study also demonstrated that there are normal ($k_H/k_D > 1$) α secondary deuterium kinetic isotope effects for both the glycosylation and deglycosylation steps, as was the case in the earlier study by Sinnott and Souchard.

1.1.2 The Anchimeric Assistance Mechanism

The body of evidence summarized above provides excellent evidence that retaining β-glycosidases proceed through a double displacement mechanism. However, there is a class of β-glycosidases that employ an intramolecular catalytic nucleophile rather than an enzymatic nucleophile. The family 20 hexosaminidases proceed through an anchimeric assistance mechanism in which the substrate 2-acetamido group acts as the catalytic nucleophile (Scheme 1.2).[13] As is the case in the standard double displacement mechanism, two carboxylic acid groups (labeled A and B) are present in the active site. In this case however, neither carboxylate acts as the catalytic nucleophile. Instead the oxygen atom on the 2-acetamido group attacks the anomeric centre in the glycosylation step. The mechanism proceeds through an oxocarbenium ion transition state in which the sugar adopts a distorted conformation with partial positive charge on the anomeric carbon, endocyclic oxygen and the nitrogen of the acetamido group. General acid catalysis from carboxylic acid B aids the departure of the aglycone, the glycosidic bond is broken, and an oxazolinium ion intermediate is formed. Carboxylate A stabilizes the positive charge that forms on the nitrogen in the oxazolinium ion intermediate. In the deglycosylation step, general base catalysis from carboxylate B aids the incoming nucleophile, in this case water, to attack the anomeric centre and the mechanism proceeds through a second oxocarbenium ion intermediate to give the hydrolyzed product with retention of anomeric configuration.

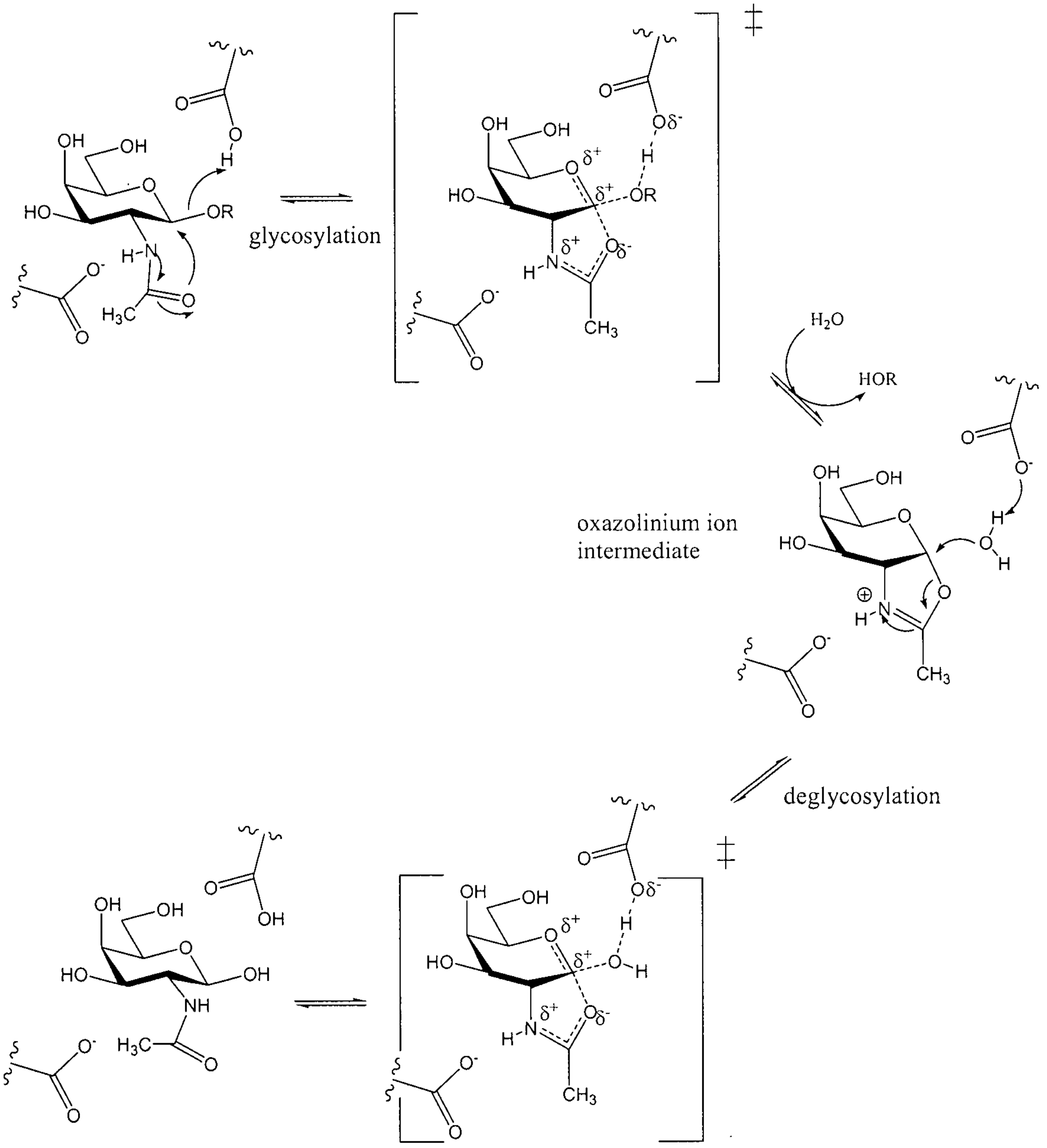
glycosylation
H₂O
HOR
oxazolinium ion intermediate
deglycosylation

Scheme 1.2 The mechanism of family 20 β-hexosaminidases.

1.1.3 Glycosidase Inhibitors

Glycosidase inhibitors are useful tools for probing enzyme mechanism. Since competitive inhibitors interact with the active site, kinetic and structural studies can provide information about the interactions involved in catalysis. Enzymes essentially function by lowering the activation energy of a chemical reaction by stabilizing the transition state. To achieve this, enzymes must bind the transition state even better than the ground state.[14] In this vein, competitive glycosidase inhibitors are often designed to mimic at least one feature of the oxocarbenium ion transition state.

In addition to providing insight into enzyme mechanism, glycosidase inhibitors have the potential to act as drugs in many diseases, such as HIV,[15] influenza,[16] and cancer.[17]

Nitrogen-containing sugar mimics (Figure 1.4) are potent inhibitors of many glycosidases.[18,19] Acarbose[20] **(1.1)**, a natural product, is a transition state mimic that is a potent α-amylase inhibitor and is used as a treatment for diabetes mellitus.[21] The key unit of acarbose is the carba-sugar at the non-reducing end, termed 'valienamine'.[22] Because of the double bond, the molecule adopts a flattened conformation, while the nitrogen provides the ability to carry positive charge, thus mimicking the proposed oxocarbenium ion-like transition state.

Nojirimycin[23] **(1.2)**, another natural product, and its related analogs, contain a nitrogen atom in place of the endocyclic oxygen found in sugars. Sugar mimics like nojirimycin which contain an endocyclic nitrogen are termed 'aza-sugars'. When charged, the nitrogen binds tightly to the active site, which contains various amino acids positioned to stabilize the positive oxocarbenium ion-like transition state. Despite the tight binding qualities of nojirimycins, studies comparing the changes in free energy associated with binding of substrates and related inhibitors have shown that the nojirimycins are not true transition state analogs.[24]

Another class of aza-sugars are the isofagomines, which contain a nitrogen atom at the pseudo anomeric centre that can accommodate the positive charge found at the anomeric centre in the oxocarbenium ion-like transition state. The discovery that the natural product Siastatin B[25] **(1.3)** was a potent sialidase inhibitor inspired the synthesis of isofagomine[26] **(1.4)** and related derivatives.[27,28] Interestingly, the nojirimycin class of inhibitors are generally potent inhibitors of α-glycosidases, while the isofagomine class of inhibitors are generally potent inhibitors of β-glycosidases.[29]

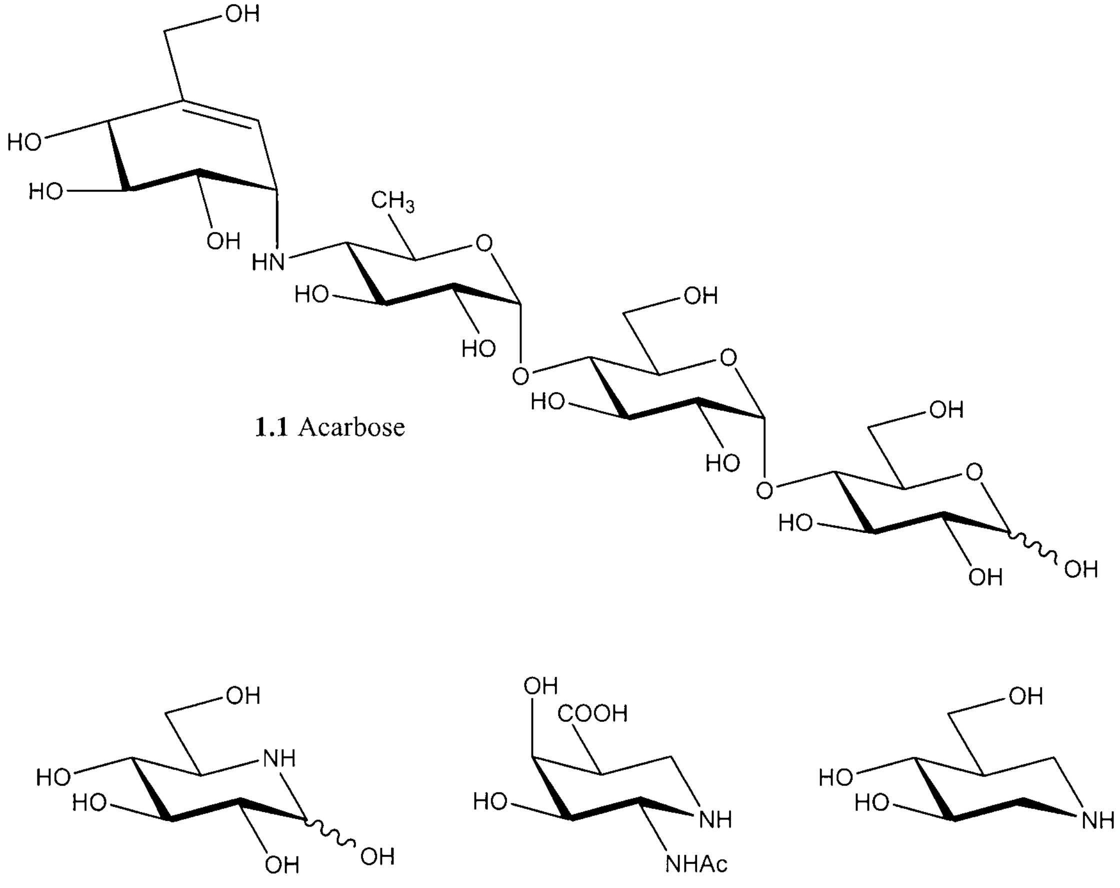

1.1 Acarbose

1.2 Nojirimycin

1.3 Siastatin B

1.4 Isofagomine

Figure 1.4 Examples of competitive glycosidase inhibitors.

1.1.4 Mechanism Based Inactivators

Mechanism-based inactivators react with a key catalytic residue in the active site irreversibly or with an extremely slow turnover rate. In 1987 the Withers group introduced a novel class of mechanism-based inactivators, the 2-deoxy-2-fluoroglucosides.[30] The first such inactivator was 2,4-dinitrophenyl 2-deoxy-2-fluoro-β-D-glucopyranoside (**1.5,** Scheme 1.3). This compound has an electronegative fluorine atom at C-2, which destabilizes the oxocarbenium ion-like transition states for both the glycosylation and deglycosylation steps. The incorporation of a highly reactive leaving group at C-1 speeds up the glycosylation step sufficiently to overcome the destabilizing effect caused by the fluorine at C-2, and the glycosyl-enzyme intermediate is formed. The deglycosylation step is slowed down sufficiently to allow accumulation of the glycosyl enzyme intermediate, resulting in rapid, time-dependent inactivation.

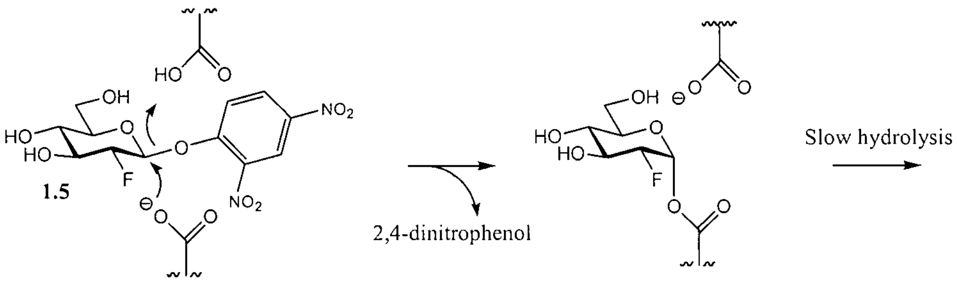

Scheme 1.3 Inactivation of a retaining β-glucosidase with 2,4-dinitrophenyl 2-deoxy-2-fluoro-β-D-glucopyranoside **(1.5)**.

This technique has proven useful in identifying the catalytic nucleophiles of several enzymes through X-ray crystallography,[7] and through proteolytic digestion followed by LC-MS/MS analysis of the fragments.[8,9]

1.2 Lysosomal Storage Disorders

Lysosomes are the organelles within the cell responsible for destruction and recycling of cellular components. The degradation of cellular components within the lysosome is carried out by various lysosomal enzymes. Lysosomal storage disorders are caused by deficiencies in lysosomal enzymes, which results in accumulation of the deficient enzyme's substrate.

One class of molecules that are recycled in the lysosome are gangliosides, which are glycosphingolipids consisting of a ceramide unit attached to an oligosaccharide chain. Gangliosides are attached to animal cell membranes through their hydrophobic ceramide moiety. The hydrophilic oligosaccharide chains extend into the extracellular space, where they are involved in cell differentiation and cell-cell interactions. The highest ganglioside content has been found in the brain.[31]

Gangliosides are degraded in an orderly fashion by specific enzymes within the lysosome (Scheme 1.4). A deficiency in any one of these enzymes results in disease due to accumulation of the particular ganglioside associated with that enzyme.[32] Scheme 1.4 shows the degradation of gangliosides by enzymes in the lysosome, and the diseases associated with each enzyme deficiency.

This thesis focuses on two of the lysosomal enzymes, β-hexosaminidase A and glucocerebrosidase, and the diseases associated with these enzymes, Tay Sachs and Gaucher disease.

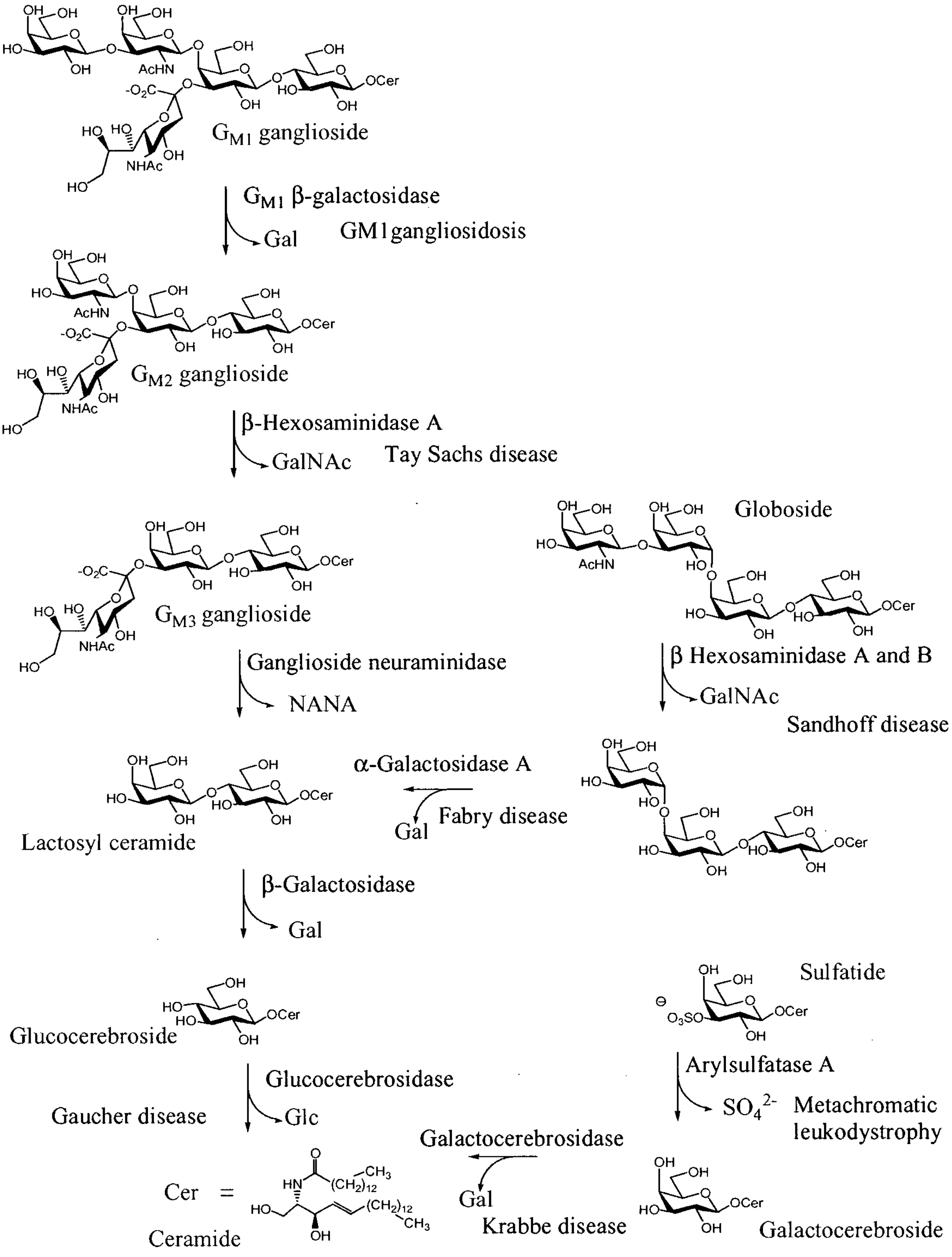
GM1 ganglioside
GM1 β-galactosidase
Gal
GM1gangliosidosis
GM2 ganglioside
β-Hexosaminidase A
GalNAc
Tay Sachs disease
Globoside
GM3 ganglioside
Ganglioside neuraminidase
NANA
β Hexosaminidase A and B
GalNAc
Sandhoff disease
Lactosyl ceramide
α-Galactosidase A
Gal
Fabry disease
β-Galactosidase
Gal
Glucocerebroside
Sulfatide
Glucocerebrosidase
Glc
Gaucher disease
Arylsulfatase A
SO4 2-
Metachromatic leukodystrophy
Galactocerebrosidase
Gal
Krabbe disease
Cer =
Ceramide
Galactocerebroside
OCer

Scheme 1.4 The degradation of gangliosides by lysosomal enzymes. Enzymes are shown in blue, and the diseases associated with each enzyme deficiency are shown in red. Adapted from Voet and Voet.[33]

1.2.1 Tay Sachs Disease

Dr. Warren Tay first described what would later be known as Tay Sachs disease in 1881. He observed a cherry-red spot on the retina of a mentally and physically retarded one-year-old child. The clinical symptoms first observed by Tay were observed again six years later by Bernhard Sachs and termed familial amaurotic idiocy.[34] The condition was named Tay Sachs disease after the clinicians that first described it.

Tay Sachs disease is caused by accumulation of a compound in the brains of patients, and in 1962 Lars Svennerholm identified that compound as G_{M2} ganglioside[35] (Scheme 1.5). In 1969 Okada discovered that a deficiency in the enzyme β-hexosaminidase A was the cause of the accumulation of G_{M2} ganglioside.[36]

The deficiency in β-hexosaminidase A is hereditary and most common among Ashkenazi Jews. Tay Sachs occurs at an estimated carrier rate of 1 in 300 in the general population and 1 in 35 among the Ashkenazi Jewish population.[31] There is currently no cure for Tay Sachs disease, though incidences of the disease have dropped due to international carrier detection programs.[37]

1.2.1.1 The Human Hexosaminidases

Hexosaminidases catalyze the cleavage of β-(1,4) linked *N*-acetylglucosamine **(1.6)** (GlcNAc) or *N*-acetylgalactosamine (GalNAc) **(1.7)** residues from the non-reducing end of oligosaccharides and glycoconjugates (Figure 1.5).

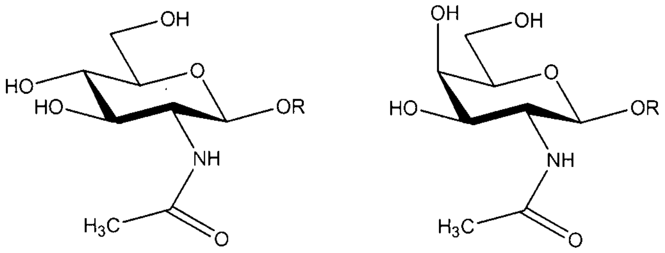

1.6 **1.7**

Figure 1.5 Diagram of terminal *N*-acetyl-β-D-glucosamine (**1.6**) and *N*-acetyl-β-D-galactosamine (**1.7**) residues. R = oligosaccharide or glycoconjuagate.

Unlike most glycosidases, which are specific for only one substrate, hexosaminidases catalyze the cleavage of both *N*-acetylglucosamine and *N*-acetylgalactosamine residues. The name 'hexosaminidase' encompasses both the glucosaminidase and galactosaminidase activity. Three β-hexosaminidase isozymes are found in human tissue. The isozymes are dimers composed of combinations of two subunits, α and β. β-Hexosaminidase A (Hex A) is a heterodimer composed of one α and one β subunit, and β-hexosaminidase B (Hex B) is a homodimer composed of two β subunits. The third isozyme is the rare β-hexosaminidase S (Hex S) composed of two α subunits. Only Hex A and Hex S are capable of efficiently hydrolyzing negatively charged substrates such as the artificial substrate 4-methylumbelliferyl β-D-*N*-acetylglucosamine-6-sulfate (MUGS) (**1.8**, Figure 1.6), while only Hex A is capable of cleaving the terminal GalNAc from the negatively charged G_{M2} ganglioside *in vivo* (Scheme 1.5). In order to do so Hex A requires a cofactor, the G_{M2} activator protein, which extracts G_{M2} ganglioside from the intralysosomal membrane and presents the terminal GalNAc residue to Hex A.[38] Both Hex A and Hex B are family 20 hexosaminidases which proceed through the anchimeric assistance mechanism (Scheme 1.2).

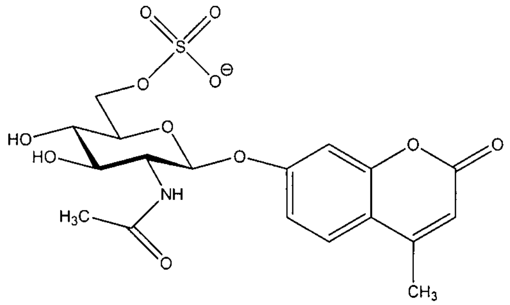

Figure 1.6 Diagram of 4-methylumbelliferyl β-D-*N*-acetylglucosamine-6-sulfate **(1.8)** (MUGS).

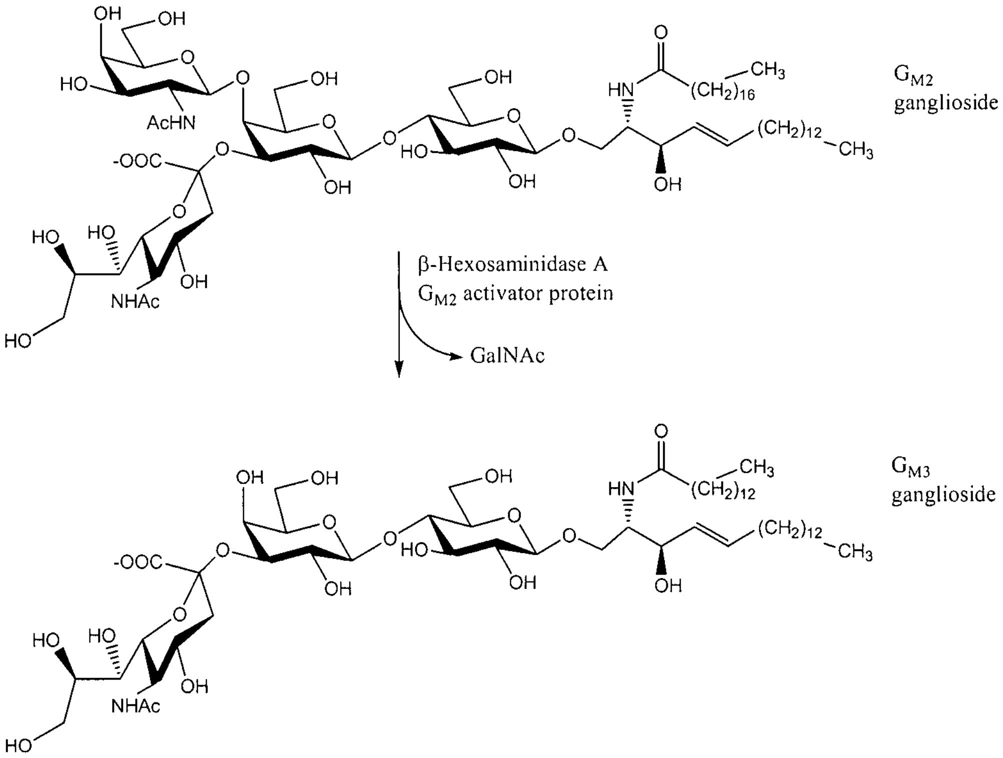
G_{M2} ganglioside
β-Hexosaminidase A
G_{M2} activator protein
GalNAc
G_{M3} ganglioside

Scheme 1.5 The reaction catalyzed by lysosomal human β-hexosaminidase A.

1.2.1.2 The Cause of the Deficiency in Hex A

The *HEXA* and *HEXB* genes encode the α and β subunits, respectively. Heritable naturally occurring point mutations in the *HEXA* gene result in mutant α subunits, which may result in an unstable, misfolded Hex A enzyme. Like many other proteins, Hex A is synthesized in the endoplasmic reticulum (ER). Misfolded and incompletely assembled proteins are common side-products of protein synthesis in the ER. While correctly folded proteins are secreted and go on to perform their function, misfolded and incompletely assembled proteins are retained in the ER and degraded through quality control mechanisms. Thus, unstable, potentially misfolded Hex A is not transported through the golgi apparatus to the lysosome, but instead is retained in the ER and destroyed by quality control mechanisms in the cell.[39] Consequently, the mutant Hex A, though catalytically active, does not reach its target substrate and G_{M2} ganglioside accumulates. Tay Sachs disease is the most common of three similar diseases known as the G_{M2} gangliosidoses. Mutations in the β subunit, encoded by the *HEXB* gene, cause Sandhoff disease. The third and most rare disease is known as the AB-variant form of G_{M2} gangliosidosis and is caused by mutations in the *GM2A* gene, which codes for the G_{M2} activator protein.

There are several different levels of severity and age of onset of Tay Sachs disease. The acute, infantile form is caused by mutations in the α subunit that prevent any Hex A from reaching the lysosome, and is characterized by rapidly progressing neurological deterioration beginning at 3-5 months of age and resulting in death by the age of 4 years.[37] The less severe adult onset form of Tay Sachs is characterized by slowly progressing neurodegenerative disorders. This milder phenotype is seen in mutations that allow only 1-5 % of wild-type Hex A activity. The majority of Ashkenazi Jewish patients with adult Tay Sachs disease have an αG269S mutation which causes the protein to be slightly unstable. Interestingly, mutations that allow for only 5-10 % of wild-type activity have been seen in patients who are asymptomatic[40]. Thus it is believed that a "critical threshold" of 5-10 % of wild-type Hex A activity is needed to prevent accumulation of G_{M2} ganglioside.[40]

The α and β subunits of Hex A are inactive as monomers. The recently published crystal structure for Hex B and modeling data for Hex A[41] provided insight into why this is the case. Although each subunit contains an active site, the crystal structure of Hex B showed that the two active sites are found at the interface of the two monomers, and that several residues from one subunit stabilize and structurally complete the active site residues of the other subunit. The α and β subunits share a primary structure that is 60 % identical, and most of the conservation between the subunits is found within their catalytic domains. Modeling studies showed that like Hex B, the active site of Hex A is found at the dimer interface. The modeling studies also showed a large groove at the αβ dimer interface where the G_{M2} activator protein likely docks, and that the active sites of the α and β subunits are essentially identical except for three amino acid changes: βAsp426 → αGlu394, βAsp452 → αAsn423, and βLeu453 → αArg424. The presence of an arginine residue (Arg424) in the α active site instead of the leucine residue (Leu453) appears to help create the electrostatic environment needed to accommodate negatively charged substrates such as G_{M2} ganglioside. This result is supported by previous kinetic studies that showed that an Arg424Gln mutation affected the enzyme's ability to remove GlcNAc-6-SO_4^- from an artificial substrate.[42] It was later shown that the same site in β-hexosaminidase A is responsible for binding both the 6-sulfate group on artificial substrates and the sialic acid moiety of G_{M2} ganglioside.[43]

1.2.2 Gaucher Disease

The second lysosomal storage disorder discussed in this thesis is Gaucher disease. Gaucher disease was named after French dermatologist Phillipe Gaucher, who described the first case of the disease in 1882 in his medical thesis.[44] It was found that cells of the spleen were peculiar due to a storage material, which was later characterized as glucosylceramide by another French scientist, Aghion.[44]

Gaucher disease is the most common of the lysosomal storage disorders, with a prevalence of 1/50 000 in the Caucasian population.[45] Like Tay Sachs disease, Gaucher disease is heritable and most common among Ashkenazi Jews. Like Tay Sachs disease, Gaucher disease is caused by point mutations resulting in unstable, misfolded enzymes that are destroyed by quality control mechanisms in the cell before they can reach their target substrates in the lysosome. Interestingly, the phenotypes for the disease are highly variable, though they are all caused by accumulation of glucosylceramide. Gaucher disease is classified into 3 types based on central nervous system involvement and age of onset.[44] Type 1 is characterized by the absence of central nervous system involvement, while type 2 is characterized by onset in infancy and rapidly progressing neurodegenerative disorders resulting in death before the age of 2 years. Type 3 is characterized by early childhood or adolescent onset and slowly progressing neurodegenerative disorders. All three types result in degrees of enlargement of the liver and spleen. The only currently available treatment for Gaucher disease is enzyme replacement therapy,[46] which is expensive with a cost of between $100 000 and $750 000 per patient per year, and is only effective towards type 1 Gaucher disease, since injected enzyme cannot cross the blood brain barrier.[47]

1.2.2.1 Glucocerebrosidase

Glucocerebrosidase, a retaining β-glycosidase from family 30, catalyzes the cleavage of the glycosidic bond in glucosylceramide with retention of anomeric configuration (Scheme 1.6).[48] The proposed mechanism for glucocerebrosidase is that shown for general retaining β-glycosidases in Scheme 1.1.

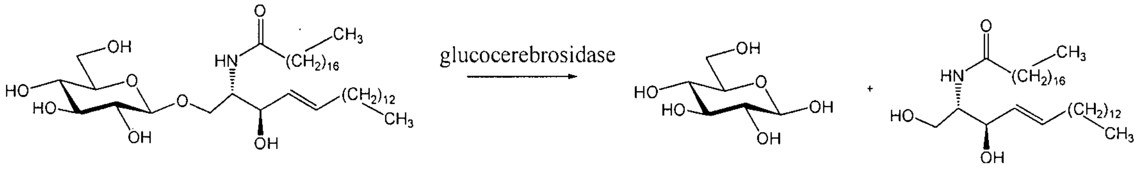

Scheme 1.6 The reaction catalyzed by glucocerebrosidase.

Glucocerebrosidase is a membrane-associated enzyme, which attaches to the negatively charged phospholipids on the lysosomal membrane once it is delivered from the ER to the lysosome. An activator protein, saposin C, induces a further conformational change rendering the enzyme active. Substrate docking with the recently published X-ray crystal structure of glucocerebrosidase shows that the ceramide chain does not appear to fit in the active site, suggesting that the ceramide chain either remains embedded in the lipid bilayer during catalysis or interacts with the saposin C cofactor. [49] Extensive kinetic characterization has shown that the enzyme requires detergents such as Triton X-100 and sodium taurocholate for activity *in vitro*.[50]

1.2.3 Therapies for Lysosomal Storage Disorders

Enzyme replacement therapy is proving to be an effective, albeit expensive, therapy for type 1 Gaucher disease.[47] The search for a more universal therapy has led to the study of 'substrate deprivation therapy': inhibition of the synthesis of glycosphingolipids. Blocking the ganglioside production pathway should theoretically prevent ganglioside accumulation. Indeed, *N*-(n-butyl)deoxynojirimycin (**1.9**, Figure 1.7), an inhibitor of the ceramide-specific glucosyl transferase involved in ganglioside synthesis, has shown promise in clinical trials as a therapy for Gaucher disease.[51] However, side-effects such as osmotic diarrhea were experienced due to inhibition of intestinal α-glucosidases and other glycosidases, and more importantly toxic effects were observed on the liver and spleen in treated humans.[52]

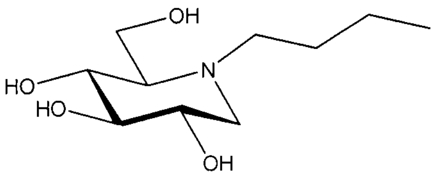

Figure 1.7 Diagram of *N*-(n-butyl)deoxynojirimycin (**1.9**).

1.2.3.1 The Chemical Chaperone Approach

The chemical chaperone approach brings to mind rescuing someone from themselves. The body's own internal watchdogs are responsible for preventing a slightly unstable, yet still catalytically active enzyme from fulfilling its all-important role. Studies of the quality control mechanisms in the ER have shown that there are ER chaperones and folding enzymes that assist the folding process and serve as retention anchors for immature proteins, preventing these immature proteins from being degraded. [39] This knowledge spawned the idea that an artificial or chemical chaperone could be introduced that could theoretically stabilize an unstable, misfolded protein and allow that protein to escape degradation by the quality control mechanisms. This concept has been applied to several systems,[53] including the most common protein mutation causing cystic fibrosis. The mutant cystic fibrosis transmembrane conductance regulator protein was stabilized by glycerol, allowing it to escape the quality control mechanisms in the ER, and restoring protein activity.[54]

The chemical chaperone approach has also been applied to lysosomal storage disorders. In the first case, 1-deoxy-galactonojirimycin **(1.10**, Figure 1.8**)** was found to enhance α-galactosidase A activity in Fabry lymphoblasts.[55] Later it was shown that *N*-(n-nonyl)deoxynojirimycin **(1.11)** increases glucocerebrosidase activity in Gaucher fibroblasts.[47] Most recently the galacto-like 4 epimer of *N*-octyl-1-epivalienamine **(1.12)** was shown to increase activity in a mouse model of G_{M1} gangliosidosis.[56]

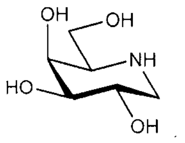

1.10

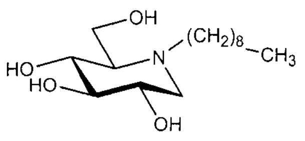

1.11

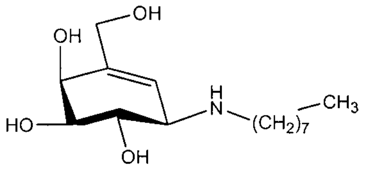

1.12

Figure 1.8 Diagram of compounds **1.10-1.12**.

In each of these cases an enzyme inhibitor was used to specifically target and stabilize the mutant enzyme in question. The binding of the inhibitor in the active site provides enough stabilization through non-covalent hydrogen bonding interactions to allow the mutant enzyme to pass the quality control mechanisms in the ER and reach the lysosome. The use of an enzyme inhibitor to increase enzyme activity seems counterintuitive. In this case, however, the inhibitor is tightly and specifically binding to the enzyme in the ER, then chaperoning the enzyme to the lysosome, where the concentration of the substrate is much higher than the concentration of the inhibitor (especially in cases where the substrate has accumulated). Once in the lysosome, some enzyme activity is restored when the substrate replaces the inhibitor in the active site. A modest increase of enzyme activity to only 5-10% of normal would be necessary for a Tay Sachs patient to be asymptomatic.[40] Side-effects should be minimal since the inhibitor is necessary at lower concentrations than the 'substrate deprivation therapy' approach where a larger dose is necessary to inhibit the ganglioside synthesizing enzymes.

1.3 Aims of this Thesis

The recent work published in this field has shown the potential for the use of enzyme inhibitors as chemical chaperones in lysosomal storage disorders. The goal of this thesis is ultimately to take the first steps towards chemical chaperone therapies for Tay Sachs and Gaucher diseases. The initial goal is to synthesize and test the inhibitory power of small molecule inhibitors for these enzymes. The second aim is to show that these inhibitors have the ability to stabilize the folded conformation of the enzyme and provide a biochemical explanation for the stabilizing effect provided by chemical chaperones. The third goal is to provide the compounds and chemical expertise to the group of collaborator Dr. Don Mahuran (Hospital for Sick Children, Toronto) in their ongoing research towards therapies for Tay Sachs and Gaucher disease.

2 The Stabilizing Effect of NAG-Thiazoline on Family 20 Hexosaminidases

2.1 NAG-Thiazoline: a Competitive Inhibitor of Family 20 Hexosaminidases

Until 1996 there was little evidence that family 20 hexosaminidases proceed through an anchimeric assistance mechanism instead of the standard double displacement mechanism. However, the work of Vocadlo, Withers *et. al.*[13] provided undeniable evidence that family 20 hexosaminidases do proceed through an anchimeric assistance mechanism. A stable analog of the proposed oxazolinium ion intermediate, NAG-thiazoline (systematic name (3a*R*,5*R*,6*S*,7*R*,7a*R*)-5-(acetoxymethyl-6,7-diacetoxy-2-methyl-5,6,7,7a-tetrahydro-3a*H*-pyrano[3,2-*d*]thiazole)) **(2.2)** was synthesized. As shown in Figure 2.1, NAG-thiazoline contains a sulfur atom in the place of the oxygen atom seen in the proposed oxazolinium ion intermediate. Inhibition studies showed that NAG-thiazoline is a powerful inhibitor of jack bean hexosaminidase (K_i = 280 nM),[13] and a hexosaminidase from *Streptomyces plicatus* (*Sp. Hex.*) (K_i = 20 μM).[57]

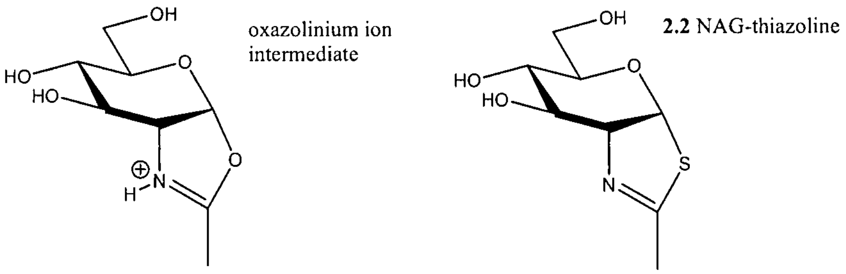
oxazolinium ion intermediate

2.2 NAG-thiazoline

Figure 2.1 Diagram showing the oxazolinium ion intermediate and NAG-thiazoline **(2.2)**.

Further support for the anchimeric assistance mechanism was provided when incubation of jack bean hexosaminidase with 4-methylumbelliferyl-2-thioacetamido-β-D-glucoside **(2.3,** Figure 2.2) resulted in release of 4-methylumbelliferone and time-dependent loss of enzyme activity. The loss of enzyme activity was shown to be due to the reversible build-up of NAG-thiazoline. These results suggested that the enzyme catalyzes the conversion of **2.3** to NAG-thiazoline, through nucleophilic attack of the thioacetamido group on the anomeric centre.

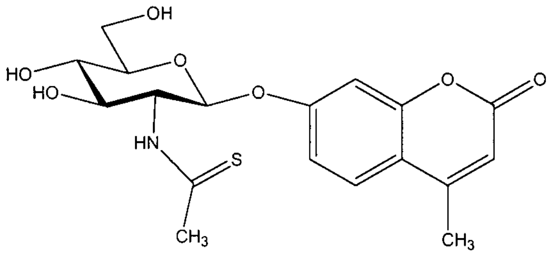

2.3

Figure 2.2 Diagram of 4-methylumbelliferyl-2-thioacetamido-β-D-glucoside (**2.3**).

Structural data from X-ray crystal structures of *Sp. Hex.*[58] and Hex B[41] with bound NAG-thiazoline have since provided insight into which residues are involved in the positioning of the 2-acetamido group for nucleophilic attack at the anomeric centre and the stabilization of the positive charge formed on the oxazolinium ring upon cyclization.

X-ray crystal structures of *Sp. Hex.*[59] and Hex B[41] with bound GalNAc-isofagomine (**2.4**, Figure 2.3), have also been published. Azasugars of the isofagomine class are generally strong inhibitors of β-retaining glycosidases, in part because of a strong electrostatic interaction that forms between the catalytic nucleophile and positively charged nitrogen at the pseudo anomeric centre.[59] Since family 20 hexosaminidases lack a catalytic nucleophile, isofagomine type azasugars were not expected to be powerful inhibitors of these enzymes. Surprisingly, GalNAc-isofagomine was found to be a powerful inhibitor of *Sp. Hex.* (K_i = 2.7 μM). In this case, however, the X-ray crystal structures with bound GalNAc-isofagomine have shown a strong electrostatic hydrogen-bonding interaction between the protonated nitrogen atom of the ring and the general acid-base residue.

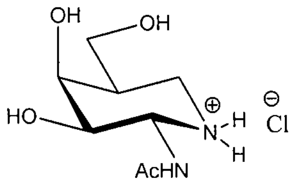

Figure 2.3 Diagram of GalNAc-isofagomine·HCl **(2.4)** (systematic name (2*R*,3*R*,4*S*,5*R*)-2-acetamido-3,4-dihydroxy-5-hydroxymethyl-piperidinium hydrochloride)

2.2 The Synthesis of NAG-Thiazoline

Although there are several other known family 20 hexosamidase inhibitors, NAG-thiazoline was selected as the best candidate for further studies, as its relatively easy synthesis allows for rapid and economical scale-up.

NAG-thiazoline was synthesized similarly to the published method (Scheme 2.1).[13] 2-Acetamido-2-deoxy-β-D-glucopyranose 1,3,4,6-tetra-acetate was refluxed with Lawesson's reagent in toluene to provide the cyclized per-*O*-acetylated thiazoline **(2.1)** in 70 % yield. The reaction with Lawesson's reagent creates the thio-acetamide, and heating promotes cyclization through an S_N2-like displacement of the β-OAc group by the thio-acetamide group. The per-*O*-acetylated thiazoline was then deprotected with sodium methoxide in methanol. Careful neutralization with glacial acetic acid provided the desired NAG-thiazoline product **(2.2)** in 75 % yield. Neutralization with the harsher Amberlite® H^+ IR 120 resin led to opening of the ring and formation of the hydrolysis product.

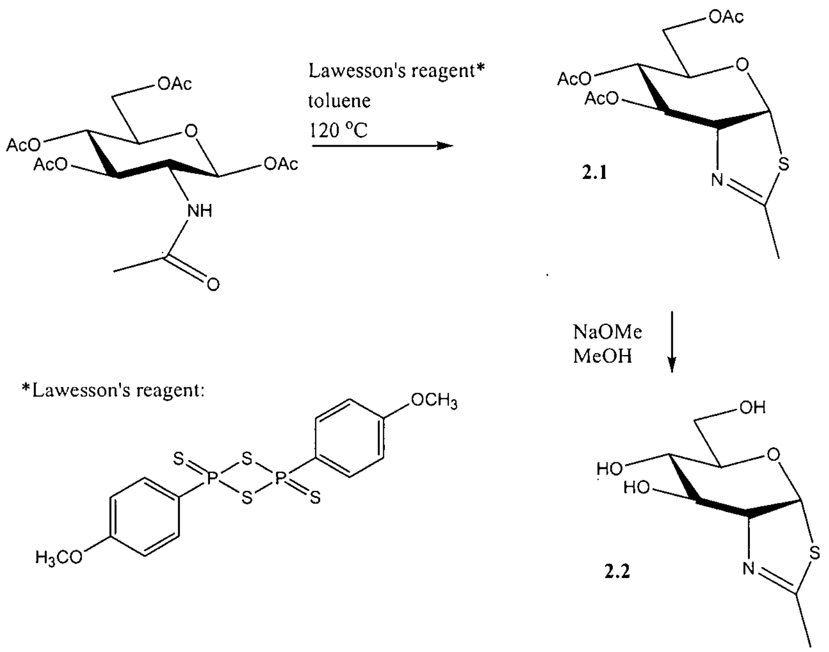

Scheme 2.1 The synthesis of NAG-thiazoline **(2.2)**.

2.3 Inhibition Results

Hex A and Hex B enzyme activity can be measured by monitoring the release of methylumbelliferone from the artificial substrate 4-methylumbelliferyl β-D-*N*-acetylglucosaminide (MUG) **(2.5)** by fluorescence (Figure 2.4). Alternatively, *para*-nitrophenyl β-D-*N*-acetylglucosaminide (pNP-GlcNAc) can be used as an artificial substrate for the human β-hexosaminidases using a spectrophotometric assay with a UV-Vis spectrometer. However the concentration of pNP-GlcNAc needed is in the milli-molar range, resulting in difficulties with substrate solubility and high background absorbances. The use of a fluorescent substrate overcomes these complications and allows the use of less enzyme, but requires a stopped assay. At the pH used for the assay (pH 4.5), methylumbelliferone is protonated and hence does not fluoresce. The enzyme/substrate mixture can be diluted into a solution of high pH and the fluorescence of this solution can then be measured. Although this assaying technique is labour intensive, it is effective, and hence was used for this study.

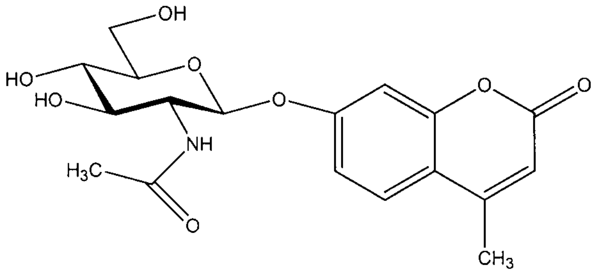

Figure 2.4 Diagram of 4-methylumbelliferyl β-D-*N*-acetylglucosaminide (MUG) **(2.5)**

NAG-thiazoline was tested as an inhibitor of Hex A and Hex B by measuring the rates of hydrolysis of MUG at a series of NAG-thiazoline concentrations. For the purpose of comparison, two other potential inhibitors were also tested in the same fashion: NAGal-thiazoline **(2.6)** (systematic name (3a*R*,5*S*,6*S*,7*R*,7a*R*)-5-(acetoxymethyl-6,7-diacetoxy-2-methyl-5,6,7,7a-tetrahydro-3a*H*-pyrano[3,2-*d*]thiazole)), and XylNAc-isofagomine·HCl **(2.7)** (systematic name (2*R*,3*R*,4*R*)-2-acetamido-3,4-dihydroxy-piperidinium hydrochloride). The structures of these compounds are shown in Table 2.1. NAGal-thiazoline is the galacto- version of NAG-thiazoline, and has a reported K_i value of 100 μM for *Sp. Hex.*[57] K_i values were obtained for the three inhibitors by fitting the data to the equation for competitive inhibition (Equation 2.1) using GraFit version 4.0.19.[60]

$$v = \frac{V_{\max} \cdot [S]}{K_m\left(1 + \frac{[I]}{K_i}\right) + [S]} \qquad \text{(Equation 2.1)}$$

The data can be graphically represented with Dixon plots (the inverse of the reaction rate vs. inhibitor concentration). The line for $1/V_{\max}$ intersects the lines representing different substrate concentrations at K_i = -[I]. The results of the inhibition studies are shown in Table 2.1, and the corresponding Dixon plots are shown in Figure 2.5.

Table 2.1 K_i values for a series of family 20 glycosidase inhibitors.

Name	Structure	*Sp. Hex.*	Hex B	Hex A
NAG-thiazoline **(2.2)**	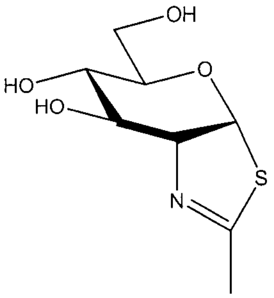	20 μM[56]	190 nM	270 nM
NAGal-thiazoline **(2.6)**	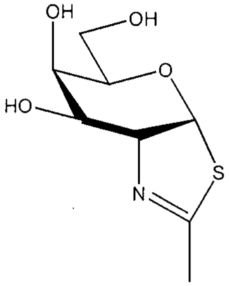	100 μM[56]	860 nM	820 nM
XylNAc-isofagomine·HCl **(2.7)**	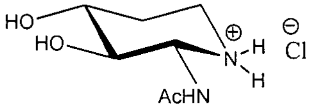 HO HO AcHN N H H ⊕ ⊖ Cl	38 μM	Not Done	90 μM

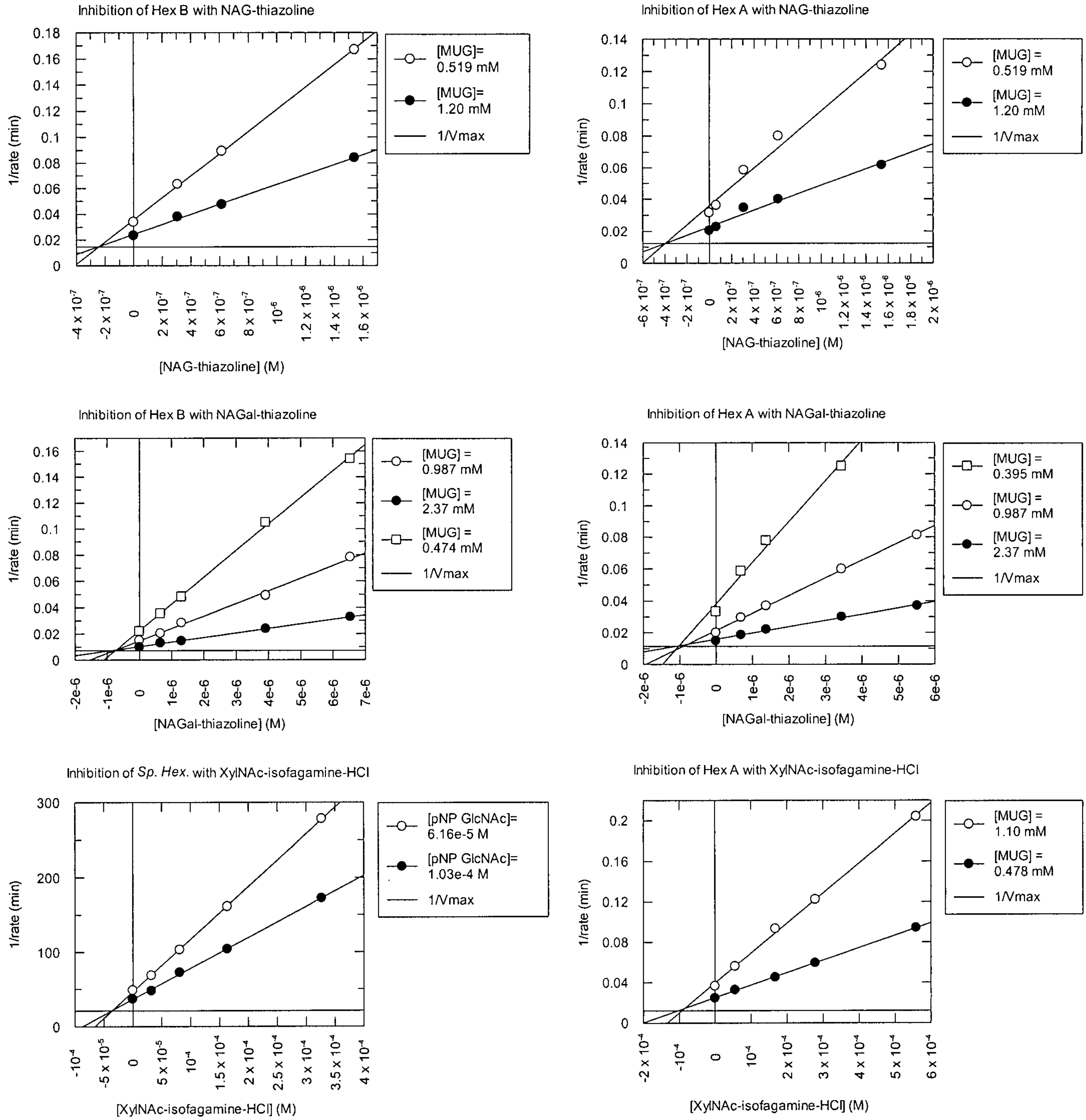

Figure 2.5 Dixon plots for a series of family 20 inhibitors.

As expected, NAG-thiazoline was found to be a potent competitive inhibitor of both Hex A and Hex B, with K_i values of 270 nM and 190 nM, respectively. K_i values for NAGal-thiazoline (820 nM for Hex A and 860 nM for Hex B) are approximately three fold higher. The previous work of Vocadlo[57] had shown that *Sp. Hex.* also binds NAG-thiazoline (K_i = 20 μM) tighter than NAGal-thiazoline (K_i = 100 μM).

The specificity constants (k_{cat}/K_m) for each enzyme for the artificial substrates *para*-nitrophenyl β-D-*N*-acetylglucosaminide (pNP-GlcNAc) (**2.8**, Figure 2.6) and *para*-nitrophenyl β-D-*N*-acetylgalactosaminide (pNP-GalNAc) (**2.9**, Figure 2.6) were examined to see whether the lower K_i for the thiazoline of gluco- configuration is paralleled by increased substrate specifity towards substrates of gluco- configuration.

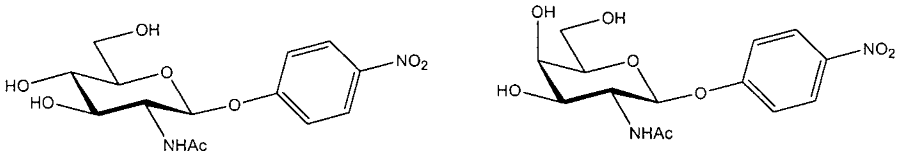

2.8 **2.9**

Figure 2.6 Diagram of pNP-GlcNAc (**2.8**) and pNP-GalNAc (**2.9**).

The specificity constants provide a means of comparison of the catalytic efficiency of an enzyme towards a substrate. A higher k_{cat}/K_m indicates a higher catalytic efficiency. For each enzyme, k_{cat}/K_m for pNP-GlcNAc is slightly higher than that for pNP-GalNAc, indicating that the enzymes show higher substrate specificity towards pNP-GlcNAc. While this difference is small, it is supported by results from two previously published studies that showed that both Hex A and Hex B are more active towards artificial substrates of the gluco- configuration.[36,61] Thus the increased selectivity towards NAG-thiazoline over NAGal-thiazoline parallels the increased substrate specificity for pNP-GlcNAc over pNP-GalNAc demonstrated by all three hexosaminidases.

Table 2.2 Family 20 hexosaminidase substrate specificities.

Enzyme	pNP-GlcNAc k_{cat}/K_m (x 10^5 $M^{-1}s^{-1}$)	pNP-GalNAc k_{cat}/K_m (x 10^5 $M^{-1}s^{-1}$)
Sp. Hex.[57]	37.0	6.70
Hex B	20.4	14.5
Hex A	5.25	4.10

XylNAc-isofagomine (**2.7**) was found to inhibit Hex A and *Sp. Hex.* with K_i values of 90 μM and 38 μM respectively. Comparison of the K_i values of XylNAc-isofagomine and NAG-thiazoline for Hex A (90 μM and 270 nM, respectively) reveals that NAG-thiazoline binds Hex A approximately 330 times tighter. While XylNAc-isofagomine is not a powerful inhibitor of Hex A, its related analog GalNAc-isofagomine (**2.4**, Figure 2.3) may be better. Previously published results for inhibition of *Sp. Hex.* by GalNAc-isofagomine (K_i = 2.7 μM)[59] indicate that GalNAc-isofagomine binds to *Sp. Hex.* tighter than the three inhibitors discussed here. However, the data in Table 2.1 shows that XylNAc-isofagomine binds to Hex A less tightly than to *Sp. Hex.* If the same trend holds, GalNAc-isofagomine will not be a tighter binder to Hex A than NAG- and NAGal-thiazoline. Regardless of the potential inhibitory power of GalNAc-isofagomine towards Hex A, the fact remains that the isofagomines are not trivial to synthesize (starting from an advanced precursor: 12 steps, 17 % overall yield for GalNAc-isofagomine),[59] which makes the thiazolines more attractive therapeutic candidates.

To summarize, NAG-thiazoline binds to Hex A approximately 3 times tighter than NAGal-thiazoline and 330 times tighter than XylNAc-isofagomine. Because of its ease of synthesis and tight-binding properties to Hex A, NAG-thiazoline was chosen for further studies.

2.4 Denaturation Experiments

Globular proteins such as *Sp. Hex.*, Hex A, and Hex B exist in equilibrium between the folded and unfolded states (Figure 2.7). The equilibrium can be shifted to the right, thereby denaturing the protein, by environmental changes such as rise in temperature, variation of pH, or the addition of chemical denaturants such as guanidine hydrochloride. Amino acid mutations, of course, can also have this effect. Protein denaturation may or may not be reversible. For example, proteins denatured with guanidine hydrochloride can often be refolded by removing the guanidine hydrochloride through dialysis, but proteins denatured with heat often aggregate and precipitate, becoming irreversibly unfolded. In the simplest model, unfolding is a cooperative two state process. In this model a protein that is 50 % unfolded has 50 % of the molecules folded and 50 % unfolded; unfolding intermediates are less stable than either the folded or unfolded states and therefore do not exist for a significant length of time.

$$\text{Folded (F)} \rightleftharpoons \text{Unfolded (U)} \longrightarrow \text{Irreversibly Unfolded}$$

Figure 2.7 The folded and unfolded states of a protein.

The idea of using an enzyme inhibitor as a chemical chaperone is centred on the hypothesis that the interactions that form between enzyme and inhibitor provide extra enzyme stability. Should this be the case, one might expect an enzyme with bound inhibitor to be slightly more stable and hence slightly more resistant to conditions that tend to denature proteins such as heat and chaotropic agents. To test this hypothesis, we set out to see whether NAG-thiazoline stabilizes family 20 β-hexosaminidases against thermal and chemical denaturation. Of greatest interest was to see whether NAG-thiazoline stabilizes Hex A towards denaturation. Project collaborators from the group of Dr. Don Mahuran (Hospital for Sick Children, Toronto) have successfully purified human Hex A that has been expressed in Chinese hamster ovary (CHO) cells. However, the purification proved difficult and only small quantities of Hex A were made available to us for this study. Ideally, experiments would be performed with Hex A containing a mutation such as the Gly269Ser mutation common in adult Tay Sachs disease. Unfortunately, mutant Hex A has proven sufficiently unstable that it has yet to be successfully purified. Hex B is more stable than Hex A[31] and has been purified in larger quantities. Thus initial studies were performed on the easily obtainable bacterial *Sp. Hex.*, and additional studies were performed with Hex B and where possible Hex A. Given that the three hexosaminidases are from the same family, it should be reasonable to extrapolate results from one to another.

2.4.1 Sp. Hex. Thermal Denaturation Studies

Thermal denaturation studies were performed by first determining a temperature at which the enzyme loses substantial activity within an hour. The enzyme was then incubated at this temperature in the presence or absence of inhibitor, and aliquots were removed at fixed time intervals and the enzyme activity was measured using the artificial substrate pNP-GlcNAc by UV/Vis spectrometry.

The concentration of NAG-thiazoline selected for all of the denaturation experiments was at least ten times its K_i value to ensure that the inhibitor occupied the vast majority of enzyme active sites. It was also ensured that the absolute concentration of NAG-thiazoline was always greater than the enzyme concentration. In all cases, when an aliquot of the enzyme/NAG-thiazoline mixture was diluted into a buffered solution of substrate for the kinetic assay, the dilution factor was large enough for the concentration of NAG-thiazoline to become significantly less than K_i so that a reaction rate could be measured.

Sp. Hex. thermal denaturation studies were performed by incubating the enzyme at a temperature of 55 °C. Aliquots were removed and the residual activity of *Sp. Hex.* was measured using the artificial substrate pNP-GlcNAc. A parallel experiment was performed in which *Sp. Hex.* was incubated in the presence of 240 μM NAG-thiazoline (K_i = 20 μM).

Figure 2.8 shows a plot of percent enzyme activity remaining against incubation time at 55 °C. The figure shows that *Sp. Hex.* retains more activity when incubated with NAG-thiazoline, indicating that the NAG-thiazoline stabilizes *Sp. Hex.* to thermal denaturation.

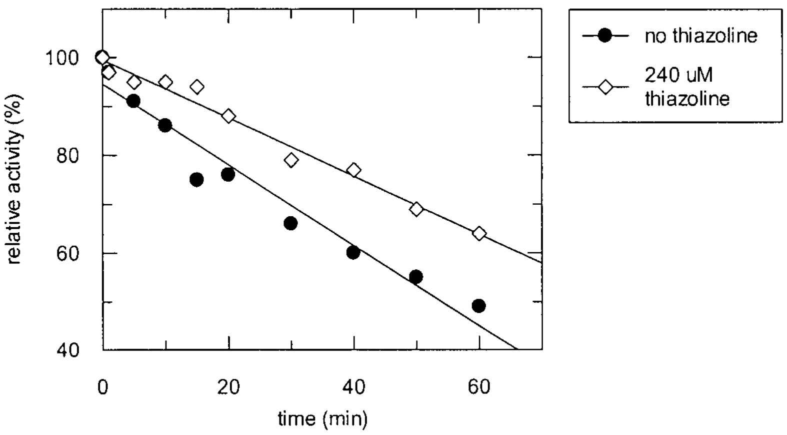

Figure 2.8 The relative activity of *Sp. Hex.* in the presence or absence of NAG-thiazoline during thermal denaturation at 55 °C.

2.4.2 Sp. Hex. Guanidine Hydrochloride Denaturation Studies

The resistance of *Sp. Hex.* to chemical denaturation was examined using guanidine hydrochloride as denaturant. The mechanism of action of chaotropic agents such as guanidine hydrochloride is not fully understood, although they are believed to disrupt hydrophobic interactions within the protein.[62]

In order to measure the degree of folding or unfolding, the intrinsic fluorescence of the enzyme was examined. The aromatic amino acids phenylalanine, tyrosine and tryptophan fluoresce when excited with radiation at the appropriate wavelength. Tyrosine and tryptophan absorb at wavelengths near 280 nm, which coincidentally is the wavelength where phenylalanine emits[62]. Additionally, tryptophan emission is much stronger than tyrosine emission. Consequently when a protein is excited near 280 nm, it is mainly the tryptophan emission that is observed. Protein unfolding often leads to a change in emission intensity and a shift in the wavelength of maximum emission to a higher wavelength. When in a hydrophobic environment such as the buried interior of a protein, tryptophan has an emission maximum near 320 nm. The fluorescence maximum of tryptophan in the unfolded state often approaches that of tryptophan in aqueous solution, with a maximum near 350 nm. The fluorescence emission spectrum of *Sp. Hex.* shows an emission maximum of 333 nm when folded and 356 nm when incubated in 5 M guanidine hydrochloride (Figure 2.9). Of note is that NAG-thiazoline seems to quench some of the fluorescence emission intensity when bound in the active site of the enzyme, though the curve maintains the same shape (Figure 2.10). The unfolded spectra in the absence or presence of NAG-thiazoline are identical. At a certain concentration of guanidine hydrochloride (2.5 M for *Sp. Hex.*), the fluorescence emission spectrum no longer changes with increasing guanidine hydrochloride concentrations, and thus the enzyme will be considered to be denatured.

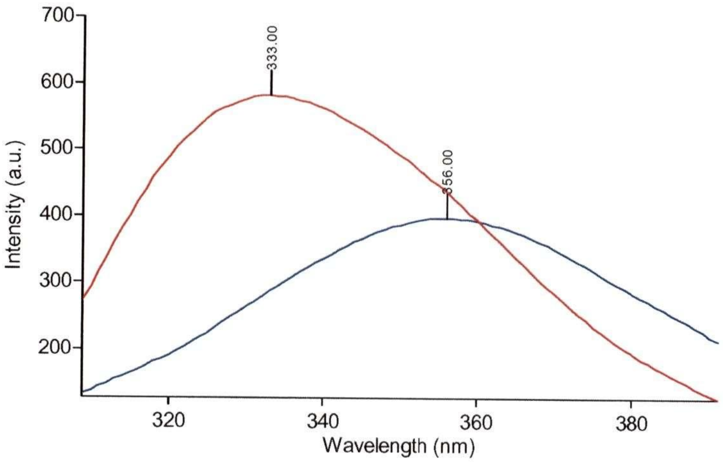

Figure 2.9 The intrinsic fluorescence spectrum of *Sp. Hex.* in buffer (red) and in 5 M guanidine hydrochloride (blue).

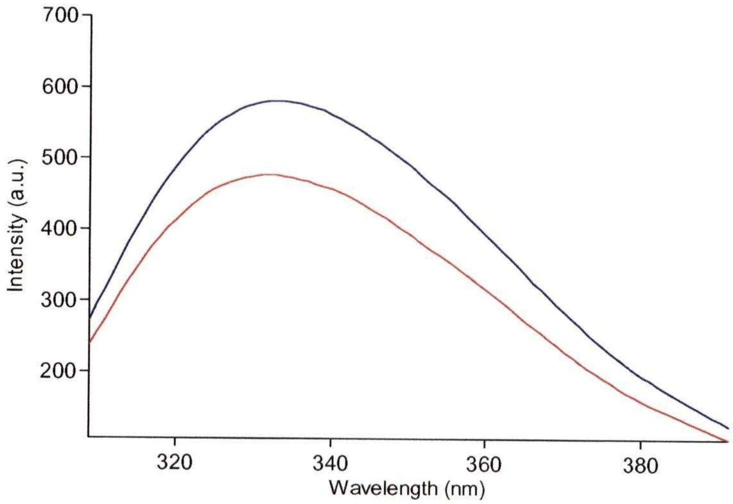

Figure 2.10 The intrinsic fluorescence spectrum of *Sp. Hex.* in the absence (blue) and presence (red) of NAG-thiazoline.

In order to create a denaturation curve, *Sp. Hex.* was incubated at a series of guanidine hydrochloride concentrations and the intrinsic enzyme fluorescence was measured at a fixed emission wavelength of 325 nm. At this wavelength the difference between the emission intensity of the spectra of the folded and unfolded enzyme is greatest.

A denaturation curve was created by plotting the percent fluorescence signal at 325 nm relative to the signal of the folded enzyme, against the concentration of guanidine hydrochloride (Figure 2.11). Comparison of the curves in the presence or absence of NAG-thiazoline shows that incubating *Sp. Hex.* with NAG-thiazoline caused the denaturation curve to shift to the right. In the absence of inhibitor *Sp. Hex.* began to unfold at a guanidine hydrochloride concentration of approximately 0.9 M and unfolded completely at a concentration of approximately 2 M. When pre-incubated with NAG-thiazoline, *Sp. Hex.* began to unfold at approximately 1.5 M guanidine hydrochloride and unfolded completely at approximately 2.5 M. Thus a higher concentration of guanidine hydrochloride is necessary to denature the enzyme when the inhibitor is bound.

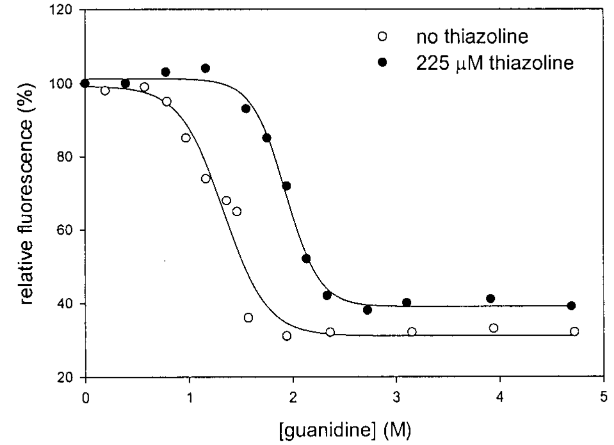

Figure 2.11 Chemical denaturation of *Sp. Hex.* in the absence and presence of NAG-thiazoline, as monitored by intrinsic fluorescence.

Another technique that can be used to monitor protein unfolding is circular dichroism (CD). The CD spectrum of folded *Sp. Hex.* is shown in Figure 2.12.

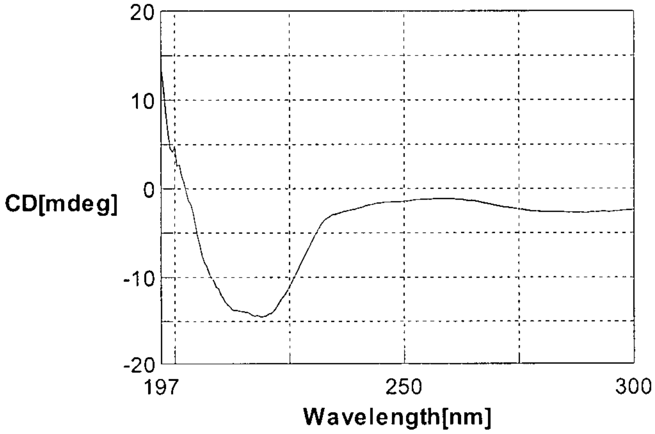

Figure 2.12 The CD spectrum of *Sp. Hex.*

Folded proteins generally have a strong CD signal at 222 nm, the characteristic wavelength of alpha helical content. The CD signal at this wavelength drops significantly in denatured proteins, which adopt a random coil.[62]

A denaturation curve was created by incubating *Sp. Hex.* at a series of guanidine hydrochloride concentrations and measuring the CD signal at 222 nm. The percent CD signal at 222 nm relative to the folded enzyme was plotted against the concentration of guanidine hydrochloride (Figure 2.13). As expected, the denaturation curve obtained is virtually identical to that obtained by fluorescence. When incubated with NAG-thiazoline, *Sp. Hex.* maintained a stronger CD signal at 222 nm in the 1-3 M guanidine range, again suggesting that NAG-thiazoline stabilizes *Sp. Hex.* against guanidine hydrochloride denaturation.

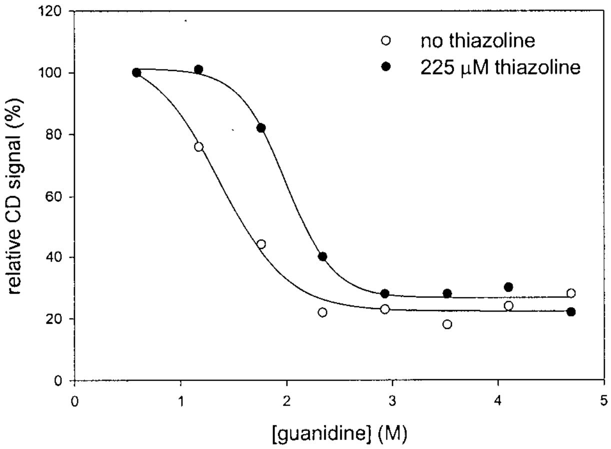

Figure 2.13 Chemical denaturation of *Sp. Hex.* in the absence and presence of NAG-thiazoline, as monitored by CD spectrometry.

2.4.3 Hex B Thermal Denaturation Studies

For the thermal denaturation study with Hex B, the enzyme was incubated at 60 °C and the activity was measured using the artificial substrate 4-methylumbelliferyl β-D-*N*-acetylglucosaminide (**2.5**, Figure 2.4). Figure 2.14 shows that over 30 minutes Hex B retained more activity when pre-incubated with NAG-thiazoline, demonstrating the ability of NAG-thiazoline to provide a stabilizing effect.

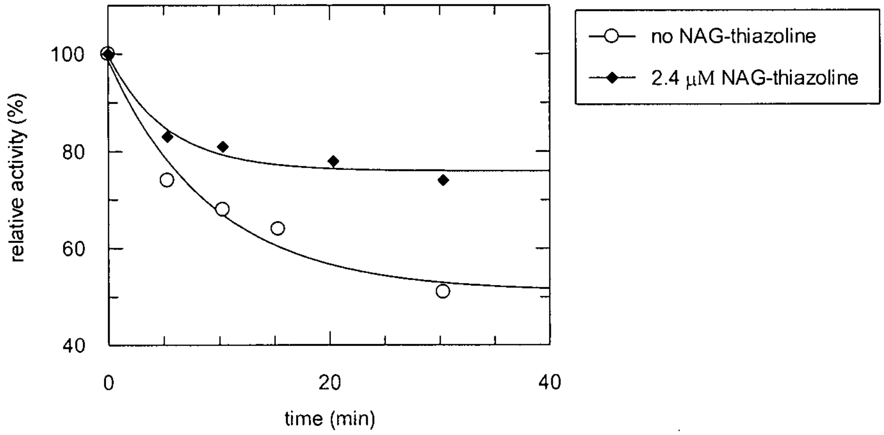

Figure 2.14 The relative activity of Hex B in the presence or absence of NAG-thiazoline during thermal denaturation at 60 °C.

2.4.4 Hex B Guanidine Hydrochloride Denaturation Studies

In addition to the thermal denaturation study, a guanidine denaturation study was undertaken with Hex B. The degree of folding/unfolding was measured by intrinsic fluorescence. As was the case with *Sp. Hex.*, the fluorescence emission spectrum shifted to the right with increasing guanidine concentrations (Figure 2.15). In this case it was not possible to follow the enzyme unfolding at a fixed wavelength because the spectra of the partially unfolded states maintained a high fluorescence emission signal at wavelengths near 325 nm (the wavelength used for the *Sp. Hex.* study). This was particularly troublesome when the enzyme was incubated with NAG-thiazoline since the inhibitor was again found to partially quench the fluorescence, in this case causing the fluorescence emission at 325 nm to be very similar for the folded and partially unfolded enzymes (Figure 2.16).

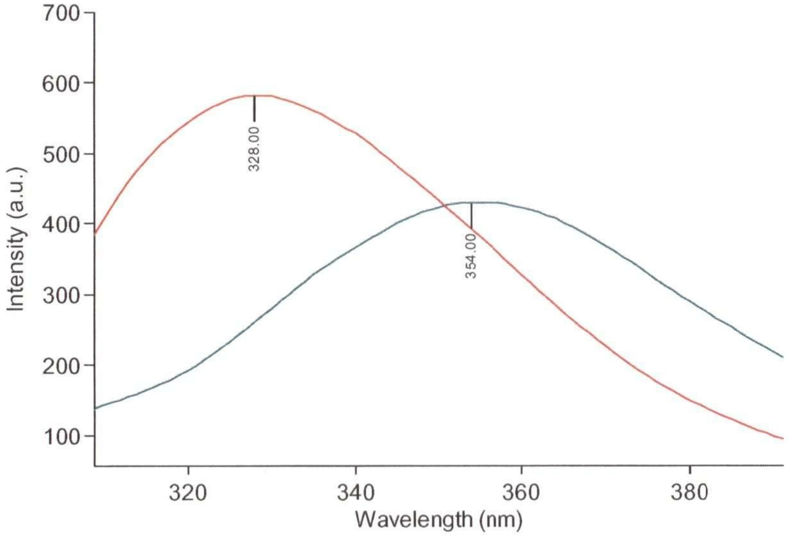

Figure 2.15 The intrinsic fluorescence spectrum of folded (red) and denatured (green) Hex B.

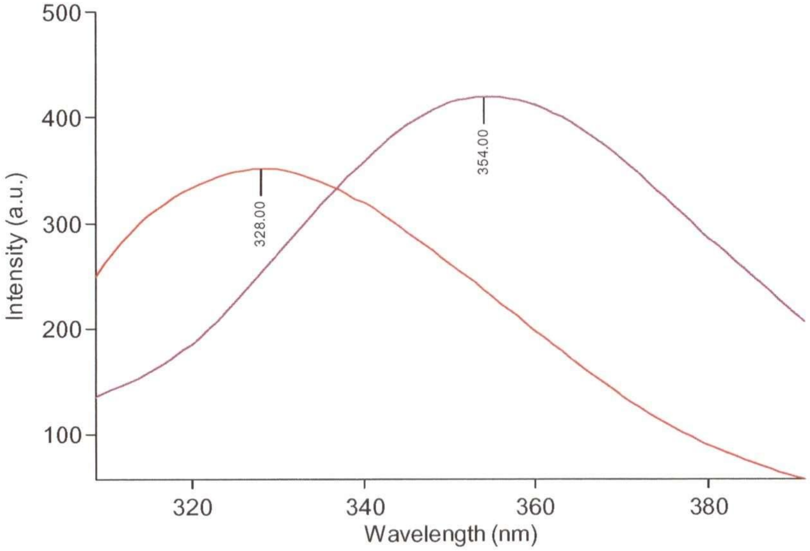

Figure 2.16 The intrinsic fluorescence spectrum of Hex B incubated with NAG-thiazoline, folded (red) and denatured (purple).

An alternative to examining the fluorescence at a fixed wavelength is to monitor the change in wavelength of maximum fluorescence (λ_{max}). As the enzyme unfolds, the wavelength of maximum fluorescence shifts to the right. The fact that NAG-thiazoline quenches fluorescence does not significantly affect this parameter.

Figures 2.15 and 2.16 show that the λ_{max} for folded Hex B is 328 nm in the absence or presence of NAG-thiazoline. A denaturation curve was obtained by plotting the wavelength of maximum fluorescence against the concentration of guanidine hydrochloride (Figure 2.17).

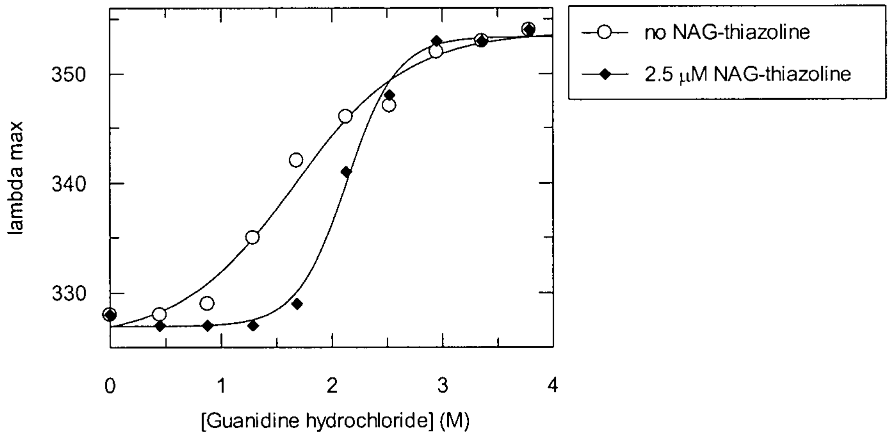

Figure 2.17 Chemical denaturation of Hex B in the absence and presence of NAG-thiazoline, as monitored by intrinsic fluorescence (λ_{max}).

The denaturation curve of enzyme that was pre-incubated with NAG-thiazoline is shifted to the right relative to the denaturation curve of the free enzyme. The stabilizing effect of the NAG-thiazoline is particularly noticeable at guanidine hydrochloride concentrations below 2 M. Below 2 M guanidine hydrochloride, the enzyme pre-incubated with NAG-thiazoline maintains a λ_{max} below 330 nm, indicating that the enzyme remains completely folded. In the absence of NAG-thiazoline, the enzyme begins to denature significantly at guanidine hydrochloride concentrations higher than 1 M. Above 3 M guanidine hydrochloride, both the free enzyme and the enzyme pre-incubated with NAG-thiazoline have the same λ_{max}, indicating that the denaturing conditions are powerful enough to overpower the stabilizing effect of NAG-thiazoline.

2.4.5 Hex A Denaturation Studies

Unfortunately there was insufficient Hex A to perform a chemical denaturation study using guanidine hydrochloride. Had sufficient enzyme been available, it may have been possible to gather enough data points to noticeably see the denaturation of each sub-unit separately in the dissociation curve. The α subunit is slightly less stable than the β subunit[37] and thus should denature before the β subunit. Such a study was not possible, but a thermal denaturation study, which required much less enzyme, was possible. The study was performed at 56 °C, a temperature slightly lower than the 60 °C used for the Hex B study. The lower temperature was necessary because the less stable Hex A denatured very quickly at 60 °C. Figure 2.18 shows that in the absence of NAG-thiazoline, Hex A retains less than 30 % of enzymatic activity when incubated at 56 °C for 30 minutes. However, in the presence of NAG-thiazoline, Hex A retains approximately 60 % of enzymatic activity when incubated at 56 °C for 30 minutes. The data indicates that Hex A retains more activity over a 30 minute period when pre-incubated with NAG-thiazoline, suggesting that NAG-thiazoline stabilizes Hex A against thermal denaturation.

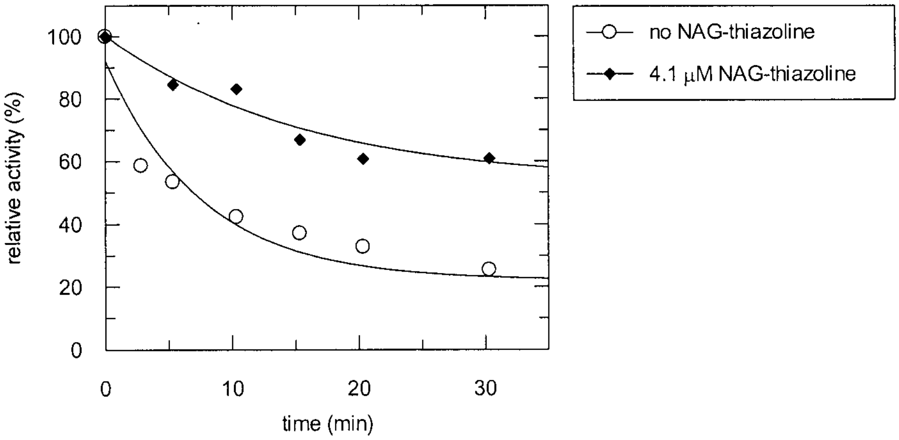

Figure 2.18 The relative activity of Hex A in the presence or absence of NAG-thiazoline during thermal denaturation at 56 °C.

2.5 Conclusion/Future Outlook

The results of the studies with *Sp. Hex.*, Hex B and Hex A presented here show that NAG-thiazoline stabilizes these enzymes against denaturation. These results provide some insight into why a competitive inhibitor may act as a chemical chaperone in a therapy for a lysosomal storage disorder. Further studies by collaborator Dr. Mike Tropak (Hospital for Sick Children, Toronto) with adult Tay Sachs and Sandhoff fibroblasts have shown that NAG-thiazoline has a stabilizing effect with the mutant enzymes in cell lines.[63] Tropak showed that NAG-thiazoline increases Hex A activity above the critical threshold of 10 % of wild type activity in adult Tay Sachs and Sandhoff fibroblasts. Tropak also showed that the increased Hex A activity is in fact found in the lysosome, indicating that NAG-thiazoline is chaperoning the mutant Hex A from the ER to the lysosome. These extremely promising results have been further boosted by studies with mice in which large doses of NAG-thiazoline have been administered without any resulting toxicity effects. Mahuran and Tropak are planning on contracting out a quality assured (GMP) large-scale synthesis of NAG-thiazoline for continued studies with mice, and potentially monkeys. If no complications or major side effects are detected, NAG-thiazoline could soon be tested on humans as a therapy for Tay Sachs disease.

3 The Stabilizing Effect of 2-Deoxy-2-Fluoro-β-D-Glucopyranosyl Fluoride and *N*-Octyl-1-Epivalienamine on Glucocerebrosidase

3.1 Stabilization of Glucocerebrosidase by a Mechanism-Based Inactivator

The deficient enzyme in Gaucher disease is glucocerebrosidase, a family 30 retaining β-glycosidase that operates through the standard double displacement mechanism (see Scheme 1.1). Glucocerebrosidase is a 497 amino acid membrane-associated glycoprotein with a mass of 59-67 kDa, depending upon the state of glycosylation.[44] As is the case with Tay Sachs disease and Hex A, we believe that an enzyme inhibitor could provide enough stabilization to allow an unstable mutant glucocerebrosidase to escape the quality control mechanisms in the ER and reach its substrate, glucosylceramide, in the lysosome. Unfortunately, glucocerebrosidase containing a Gaucher-causing mutation was not available for this study. However, a relatively large amount of wild-type enzyme was available, thanks to the donation of used vials from a patient currently undergoing enzyme replacement therapy. Each vial contains approximately 100 µL of 1.4 mg/mL leftover enzyme. Due to the abundance of enzyme, there was no need to do initial studies with a bacterial enzyme.

A previous study had shown that glucocerebrosidase was covalently inactivated by 2-deoxy-2-fluoro-β-D-glucopyranosyl fluoride (2FβF) (**3.3**, Figure 3.1).[64]

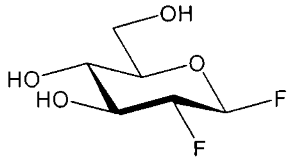

Figure 3.1 Diagram of 2-deoxy-2-fluoro-β-D-glucopyranosyl fluoride **(3.3)**

2-Deoxy-2-fluoro-D-glycosyl fluorides[65] function on the same principle as the original 2-fluoro mechanism based inactivators[30] (mechanism shown in Scheme 1.3), but the 2,4-dinitrophenyl leaving group has been replaced by a fluoride, which is also a good leaving group (Scheme 3.1). The catalytic nucleophile displaces the β-fluoride and forms a covalent bond with the 2-deoxy-2-fluoro-D-glucosyl moiety. Once labelled by the inactivator, the enzyme was proteolytically digested and through LC-MS/MS analysis of the fragments the catalytic nucleophile was identified as glutamate 340.[64]

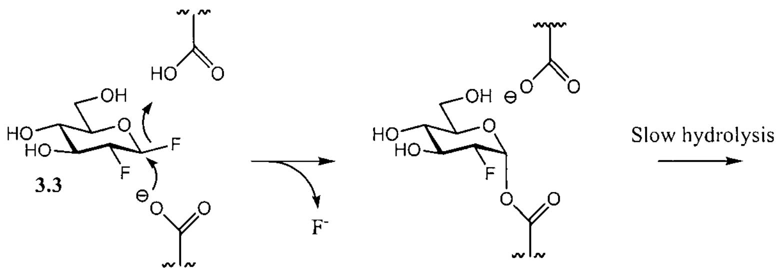

Scheme 3.1 Inactivation of a retaining β-glycosidase with 2-deoxy-2-fluoro-β-D-glucopyranosyl fluoride (**3.3**).

2-Deoxy-2-fluoro-β-D-glucopyranosyl fluoride (**3.3**) was considered as a good candidate for a chemical chaperone since the inactivator forms a covalent bond to the enzyme within the active site, possibly stabilizing the enzyme significantly. A previous study in the Withers lab had shown that β-glucosidases from *Agrobacterium faecalis* and *Caldocellum saccharolyticum* were stabilized against urea denaturation by a 2-deoxy-2-fluoro-D-glucosyl moiety bound in the active site.[66] Another important consideration is that 2-deoxy-2-fluoro-β-D-glucopyranosyl fluoride has been shown to reach organs such as the brain, spleen, liver and kidney when injected into rats and to inhibit the enzymes therein.[67] Also important is that this inhibited β-glycosidase activity was restored within 48 hours, showing that the trapped glycosyl enzyme intermediate was slowly turned over via hydrolysis or transglycosylation. Thus in theory if the compound was administered to a patient, it would reach the target organs, and the free glucocerebrosidase enzyme would be released from the glycosyl enzyme intermediate within a reasonable time scale. Another advantage of the use of a fluorine-containing inactivator is the option of incorporation of ^{18}F, which would allow monitoring of the location of the labeled enzyme through positron emission tomography (PET). In a previous study in the Withers laboratory, John McCarter successfully labelled a β-glucosidase from *Agrobacterium sp.* (Abg) with 2-deoxy-2-[^{18}F]fluoro-β-D-mannopyranosyl [^{18}F]fluoride and performed preliminary *in vivo* PET imaging studies with rats.[68] In a later study, Alexander Wong attempted to radiolabel glucocerebrosidase with 2,6-dideoxy-2-fluoro-6-[^{18}F]-fluoro-β–D-glucopyranosyl fluoride.[69,70] Although the cold version of compound was found to inactivate the enzyme, the radiolabelling of glucocerebrosidase with the ^{18}F compound was not successful. Despite the fact that the initial attempt to radiolabel glucocerebrosidase did not succeed, the successful radiolabeling of Abg by McCarter has shown the potential for this technique, and the possibility of radiolabeling glucocerebrosidase with an ^{18}F compound remains.

3.1.1 The Synthesis of 2-Deoxy-2-Fluoro-β-D-Glucopyranosyl Fluoride

2-Deoxy-2-fluoro-β-D-glucopyranosyl fluoride **(3.3)** was synthesized according to literature methods (Scheme 3.2).[71,72] Tri-*O*-acetyl-D-glucal was reacted with acetic anhydride/acetic acid and Selectfluor® at 60 °C to provide a mixture of three compounds; the α- and β- anomers of the gluco isomer, and the α-manno isomer. The gluco and manno compounds were separated by column chromatography with some difficulty providing a mixture of the α and β gluco isomers in a poor yield of 10 %. This material was then converted to the α-bromide **(3.1)** with 80 % yield using HBr/acetic acid. The bromide was displaced with silver fluoride to provide the β-fluoride **(3.2)** in 70 % yield. Deprotection was carried out with sodium methoxide in methanol to provide 2-deoxy-2-fluoro-β-D-glucopyranosyl fluoride **(3.3)** in 85 % yield.

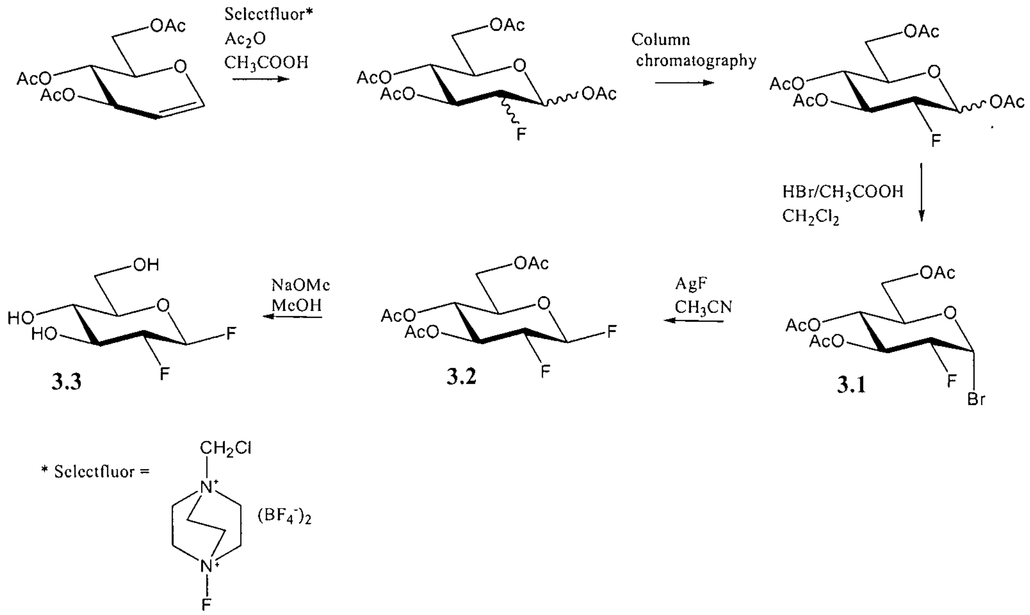
OAc
AcO
AcO
O
Selectfluor*
Ac_2O
CH_3COOH
OAc
AcO
AcO
O
OAc
F
Column
chromatography
OAc
AcO
AcO
O
OAc
F
HBr/CH_3COOH
CH_2Cl_2
OH
HO
HO
O
F
F
3.3
NaOMe
MeOH
OAc
AcO
AcO
O
F
F
3.2
AgF
CH_3CN
OAc
AcO
AcO
O
F
Br
3.1
* Selectfluor =
CH_2Cl
N^+
N^+
F
$(BF_4^-)_2$

Scheme 3.2 The synthesis of 2-deoxy-2-fluoro-β-D-glucopyranosyl fluoride **(3.3)**

3.1.2 Inactivation of Glucocerebrosidase with 2-Deoxy-2-Fluoro-β-D-Glucopyranosyl Fluoride

Glucocerebrosidase was incubated with an excess of 2-deoxy-2-fluoro-β-D-glucopyranosyl fluoride at room temperature. Aliquots of the enzyme/inactivator mixture were removed after 45 minutes, 3 hours, and 16 hours and enzyme activity was monitored using the artificial substrate 2,4-dinitrophenyl β-D-glucopyranoside (2,4-DNP-glucopyranoside). A continuous spectrophotometric assay was used to monitor the release of 2,4-dinitrophenol at 400 nm. Figure 3.2 shows that glucocerebrosidase was inactivated in a time-dependent fashion, and that after 16 hours the enzyme had lost 90 % of its activity.

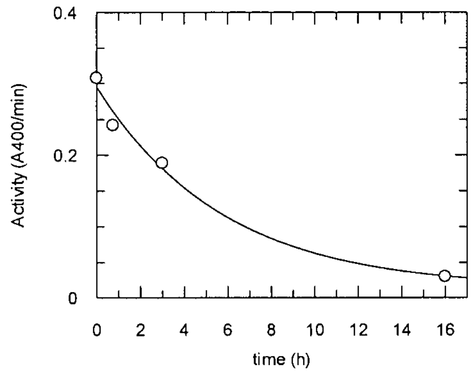

Figure 3.2 The time-dependent inactivation of glucocerebrosidase at room temperature by 2-deoxy-2-fluoro-β-D-glucopyranosyl fluoride (**3.3**). [Glucocerebrosidase] = 0.44 μM. [2-deoxy-2-fluoro-β-D-glucopyranosyl fluoride] = 2.5 mM

3.1.3 Denaturation Studies with Glucocerebrosidase in the Presence and Absence of 2-Deoxy-2-Fluoro-β-D-Glucopyranosyl Fluoride

Ideally, the stabilizing effect of 2-deoxy-2-fluoro-β-D-glucopyranosyl fluoride on glucocerebrosidase could be measured with both thermal and chemical denaturation studies like those performed previously with the hexosaminidases. However, performing a thermal denaturation study by monitoring enzyme activity is complicated by the fact that 2-deoxy-2-fluoro-β-D-glucopyranosyl fluoride is a covalent inactivator and not a competitive inhibitor like NAG-thiazoline. In the case of a competitive inhibitor, the inhibitor is held in the active site through non-covalent interactions. By diluting the enzyme/inhibitor mixture so that [I] << K_i, a large proportion of active sites become vacant, allowing the substrate to enter the active site, and making an assay for enzyme activity using an artificial substrate possible. However, in the case of a covalent inactivator like 2-deoxy-2-fluoro-β-D-glucopyranosyl fluoride, the inactivator is covalently linked in the active site, and remains covalently linked even after dilution. Thus the substrate cannot replace the inactivator in the active site and an assay for enzyme activity is not possible. Consequently thermal enzyme denaturation cannot be measured by monitoring enzyme activity.

However, a chemical denaturation study analogous to those performed with the hexosaminidases is possible. Intrinsic fluorescence was chosen over CD spectroscopy as the method of choice to monitor enzyme unfolding since it requires the use of less enzyme. Figure 3.3 shows the intrinsic fluorescence spectra of folded and denatured glucocerebrosidase.

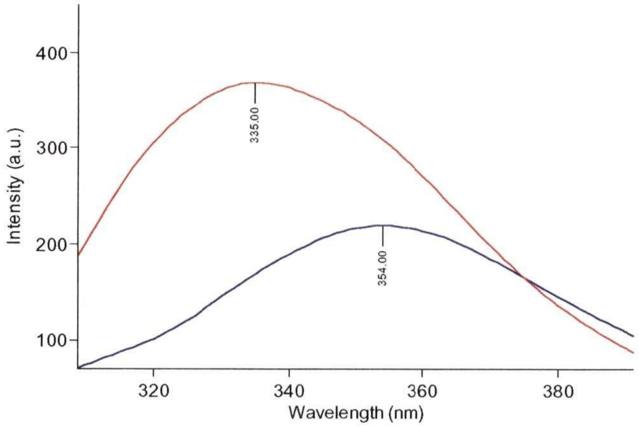

Figure 3.3 The intrinsic fluorescent spectra of folded (red) and denatured (blue) glucocerebrosidase.

As was the case for the hexosaminidases, the intrinsic fluorescence spectrum of denatured glucocerebrosidase is decreased in fluorescence intensity and is shifted to the right, with a higher λ_{max}. When the flurorescence spectra of glucocerebrosidase incubated in various concentrations of guanidine hydrochloride are examined, a trend is apparent. As the concentration of guanidine hydrochloride increases, λ_{max} shifts to the right and the fluorescence signal decreases in intensity as the tryptophan residues move from the hydrophobic buried interior of the folded protein to the solvent exposed denatured state. A denaturation curve can be created by either plotting the fluorescence intensity at a fixed wavelength or λ_{max} against guanidine hydrochloride concentration. In this case, both the fluorescence emission at a fixed wavelength of 330 nm (Figure 3.4) and the wavelength of maximum fluorescence (λ_{max}) (Figure 3.5) were examined. The fixed wavelength of 330 nm was chosen because it is at this wavelength that the difference in fluorescence intensity between the folded and unfolded spectra is greatest.

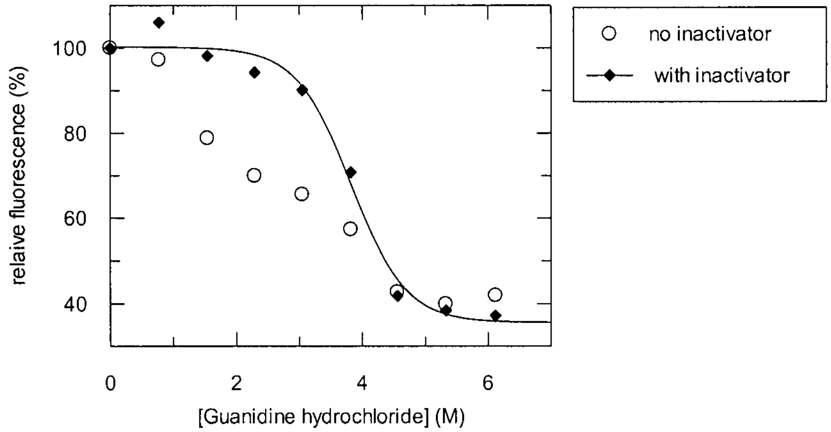

Figure 3.4 Chemical denaturation of glucocerebrosidase in the absence and presence of 2-deoxy-2-fluoro-β-D-glucopyranosyl fluoride (inactivator), as monitored by intrinsic fluorescence at a fixed wavelength of 330 nm.

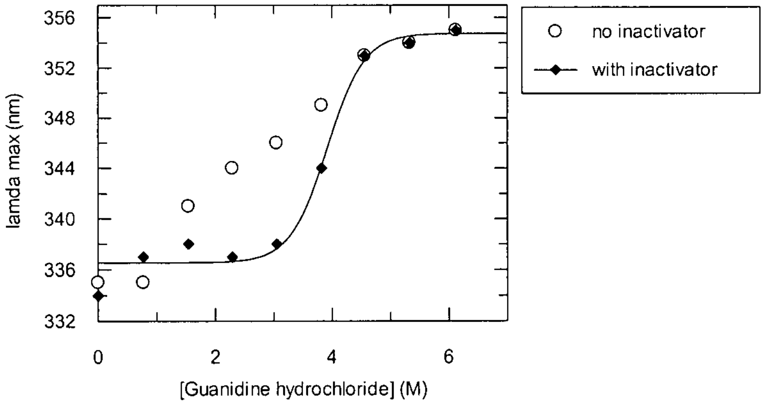

Figure 3.5 Chemical denaturation of glucocerebrosidase in the absence and presence of 2-deoxy-2-fluoro-β-D-glucopyranosyl fluoride (inactivator), as monitored by intrinsic fluorescence at λ_{max}.

Examining Figure 3.4 first, in the absence of the 2-deoxy-2-fluoro-D-glucosyl moiety (which forms after incubating glucocerebrosidase with 2-deoxy-2-fluoro-β-D-glucopyranosyl fluoride) the relative fluorescence at 330 nm drops rapidly above 1 M guanidine hydrochloride, indicating that the enzyme begins to unfold at these low guanidine hydrochloride concentrations. However, in the presence of the 2-deoxy-2-fluoro-D-glucosyl moiety the relative fluorescence at 330 nm stays near 100 % up to 3

M guanidine hydrochloride, indicating that the enzyme remains mainly folded in this range of guanidine hydrochloride concentrations.

Figure 3.5 shows that in the absence of the 2-deoxy-2-fluoro-D-glucosyl moiety, the λ_{max} increases rapidly above 1 M guanidine hydrochloride. This increase in λ_{max} is the result of more tryptophan residues becoming exposed to solvent, indicating that the protein is beginning to unfold. In the presence of the 2-deoxy-2-fluoro-D-glucosyl moiety, λ_{max} remains near 336 nm up to 3 M guanidine hydrochloride, indicating that the tryptophan residues remain sheltered from solvent as in the completely folded enzyme.

Interestingly, in both Figure 3.4 and 3.5, the data for denaturation after pre-incubation with 2-deoxy-2-fluoro-β-D-glucopyranosyl fluoride fit the equation for a sigmoidal curve, as expected for a cooperative two state unfolding process. However, in the absence of the 2-deoxy-2-fluoro-D-glucosyl moiety, the data do not fit a sigmoidal curve. Instead the relationship seems more linear. This could be because glucocerebrosidase, a membrane-associated protein, may be resistant to complete denaturaton as is the case for some other membrane-associated proteins[73]. Guanidine hydrochloride, which is believed to act by disrupting hydrophobic interactions within the folded protein,[74] may not be able to penetrate the long sequences of hydrophobic amino acid residues present in some membrane-associated proteins. Another consideration is that the buffer used for kinetics and the unfolding studies with glucocerebrosidase contains detergents such as thesit and sodium taurocholate, which are hydrophobic in nature. For full enzyme activity, these detergents must be present at or above their critical micelle concentration (CMC).[50] It has been shown that certain detergents present at concentrations higher than their critical micelle concentration stabilize partially folded protein intermediates[75]. The fact that the data obtained after pre-incubation with 2-deoxy-2-fluoro-β-D-glucopyranosyl fluoride does fit a sigmoidal curve suggests that over the guanidine hydrochloride range of 0 to 3 M, the 2-deoxy-2-fluoro-D-glucosyl moiety stabilizes the enzyme sufficiently to keep the enzyme completely folded. At concentrations higher than 3 M, the conditions are powerful enough to unfold the enzyme completely, essentially skipping the unfolded intermediates seen in the absence of the 2-deoxy-2-fluoro-D-glucosyl moiety, and approximating a cooperative two-state unfolding process.

Regardless of the explanation for the shapes of the curves, both Figures 3.4 and 3.5 clearly show that the presence of the 2-deoxy-2-fluoro-D-glucosyl moiety in the active site stabilizes glucocerebrosidase against denaturation in the 0 to 4 M guanidine hydrochloride concentration range.

3.2 Stabilization of Glucocerebrosidase by a Competitive Inhibitor

3.2.1 N-Octyl-1-Epivalienamine: a Competitive Inhibitor of Glucocerebrosidase

Having tested the stabilizing effect of a covalent enzyme inactivator, it was of interest to see how a competitive inhibitor would compare. In a study by the group of Ogawa[76], a series of *N*-alkyl-β-valienamines were synthesized and tested as inhibitors of mouse liver glucocerebrosidase. The study showed that *N*-octyl-1-epivalienamine **(3.6)** was the most potent mouse liver glucocerebrosidase inhibitor of those inhibitors tested. The 1-epivalienamine unit (**3.7**) is an isomer of the valienamine unit present in the naturally occurring compound acarbose (Figure 1.4). The attachment of an octyl chain to the amine provides the lipophilicity present in glucosylceramide, the natural substrate for glucocerebrosidase. A collaboration with the group of Professor R. V. Stick (the University of Western Australia), provided tetra-*O*-benzyl-1-epivalienamine (**3.4**, Scheme 3.4) (systematic name (1*R*,4*R*,5*S*,6*S*)-4,5,6-tribenzyloxy-3-(benzyloxymethyl)-cyclohex-2-enylamine), an advanced precursor to *N*-octyl-1-epivalienamine. The synthesis of tetra-*O*-benzyl-1-epivalienamine is lengthy, requiring 12 steps.[77]

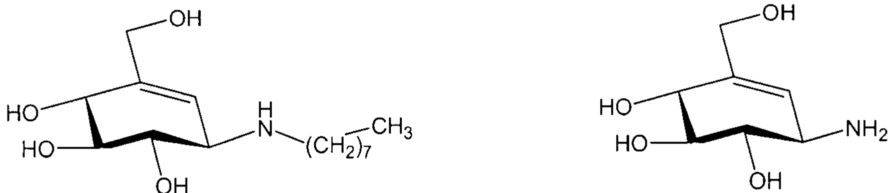

3.6

3.7

Figure 3.6 Diagram of *N*-octyl-1-epivalienamine (**3.6**) and 1-epivalienamine (**3.7**).

Initially the synthesis of the *N*-octyl product was attempted following the scheme published by Ogawa[76] in which the free amine was reacted with octanoyl chloride, creating an amide bond. The amide bond was then reduced using lithium aluminum hydride. Unfortunately, the desired product was not achieved, perhaps due to our use of benzyl ether protecting groups rather than the isopropylidene group used by Ogawa. There is precedent in the literature for lithium aluminum hydride causing hydrogenolysis of a primary benzyl ether group, resulting in the alcohol.[78]

An alternate strategy towards the synthesis of *N*-octyl-1-epivalienamine had to be employed. Tetra-*O*-benzyl-1-epivalienamine **(3.4)** was treated with octyl aldehyde in the presence of a reducing agent in an attempted reductive amination (Scheme 3.3). Water was distilled off with a Dean Stark apparatus, driving the equilibrium from the hemi-aminal to the imine. Addition of sodium borohydride in the same pot reduced the imine to the amine to provide the *N*-octyl product **(3.5)** with an overall yield of 65 %. Deprotection was carried out with sodium and liquid ammonia in THF (a Birch reduction), to afford the deprotected *N*-octyl-1-epivalienamine **(3.6)**. The Birch reduction reaction was quenched with ammonium chloride, causing the final product to be contaminated with sodium chloride and excess ammonium chloride. Unfortunately, the *N*-octyl-1-epivalienamine proved to be very difficult to purify from these salts. A combination of Sep-Pak® C-18 resin and ion exchange columns was necessary to eliminate the salts.

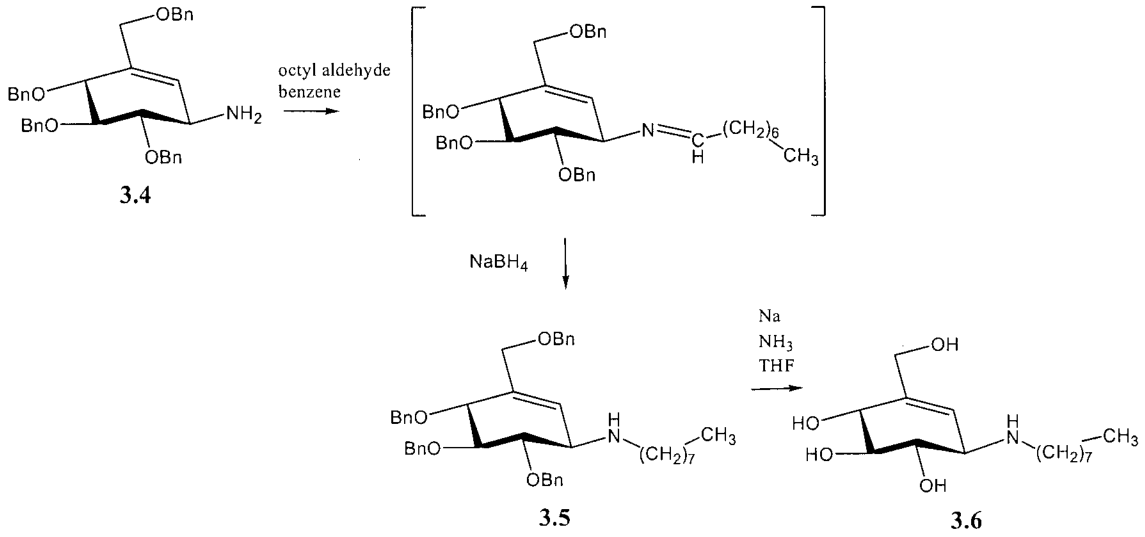

Scheme 3.3 The synthesis of *N*-octyl-1-epivalienamine (**3.6**).

3.2.2 The Inhibition of Glucocerebrosidase by N-Octyl-1-Epivalienamine

The inhibition of glucocerebrosidase by *N*-octyl-1-epivalienamine was measured by monitoring enzyme activity using the artificial substrate 2,4-DNP-glucopyranoside at a series of *N*-octyl-1-epivalienamine concentrations. The data were fit to the equation for competitive inhibition (Equation 2.1, p. 26), revealing that *N*-octyl-1-epivalienamine is a potent inhibitor of human glucocerebrosidase with a K_i value of 75 nM. A graphical representation of the data is shown in Figure 3.7 (Dixon plot). A Lineweaver-Burk plot (the inverse of reaction rate vs. the inverse of substrate concentration for different inhibitor concentrations) (Figure 3.8) can be used to verify that the inhibition is competitive. The Michaelis-Menten equation rearranges to:

$$\frac{1}{v_o} = \left(\frac{K_m}{V_{\max}}\right)\frac{1}{[S]} + \frac{1}{V_{\max}} \qquad \text{(Equation 3.1)}$$

Thus a plot of $1/v_o$ versus $1/[S]$ will have a slope of K_m/V_{max}, and an intercept of $1/V_{max}$. For competitive inhibitors, V_{max} remains constant, and the lines on the Lineweaver-Burk plot intersect at the same spot on the Y axis. Figure 3.8 shows that this is the case for glucocerebrosidase inhibition by *N*-octyl-1-epivalienamine, indicating that the inhibition is indeed competitive.

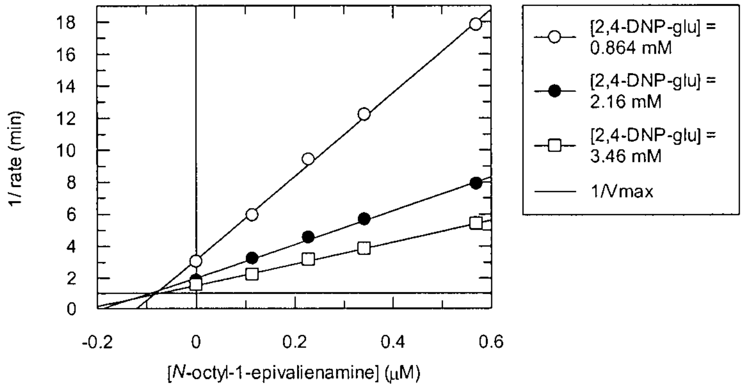

Figure 3.7 Dixon plot for the inhibition of glucocerebrosidase by *N*-octyl-1-epivalienamine.

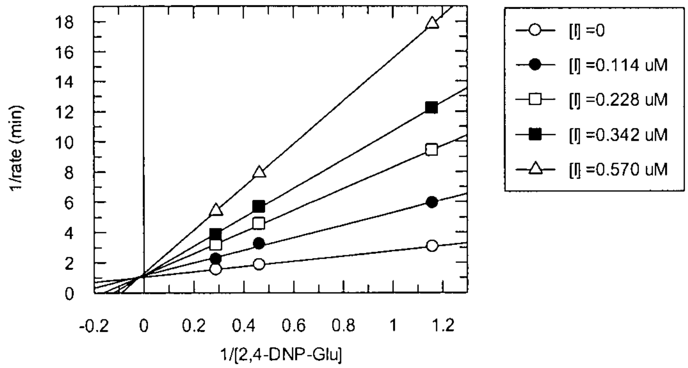

Figure 3.8 Lineweaver-Burk plot for glucocerebrosidase inhibition by *N*-octyl-1-epivalienamine.

3.2.3 Denaturation Studies with Glucocerebrosidase in the Presence and Absence of N-Octyl-1-Epivalienamine

A chemical denaturation study using guanidine hydrochloride and monitoring unfolding by fluorescence was performed. Interestingly, the enzyme pre-incubated with *N*-octyl-1-epivalienamine did not show increased resistance to guanidine hydrochloride denaturation. An explanation for this unexpected result is that the guanidine hydrochloride may be interacting with the *N*-octyl-1-epivalienamine and preventing it from binding as tightly. This could be due to the fact that guanidine hydrochloride is hydrophobic in nature, as is the octyl chain in *N*-octyl-1-epivalienamine.

Although *N*-octyl-1-epivalienamine does not protect glucocerebrosidase against guanidine hydrochloride-induced denaturation, the following study showed that it does provide a stabilizing effect against thermal denaturation and this is probably more relevant to the physiological situation. Glucocerebrosidase was incubated at 53 °C in the presence and absence of *N*-octyl-1-epivalienamine, and the residual activity at a series of time points was measured using the artificial substrate 2,4-DNP-glucopyranoside. Figure 3.9 shows that in the absence of *N*-octyl-1-epivalienamine, enzyme activity dropped rapidly; with almost zero detectable activity after 30 minutes. The data was fit to a first order decay equation, which provided a calculated half-life of 5.6 minutes. In the presence of *N*-octyl-1-epivalienamine, loss of activity was gradual, and the calculated half-life is 32 minutes. The data demonstrates that *N*-octyl-1-epivalienamine has a substantial stabilizing effect when glucocerebrosidase is incubated at an elevated temperature over time. This result shows that although no stabilizing effect against guanidine hydrochloride-induced denaturation could be detected, *N*-octyl-1-epivalienamine does have an ability to protect glucocerebrosidase against thermal denaturation.

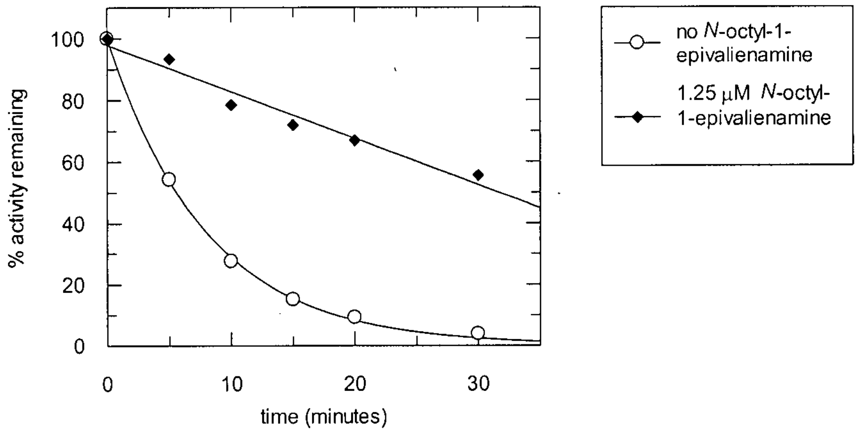

Figure 3.9 The relative activity of glucocerebrosidase in the presence or absence of *N*-octyl-1-epivalienamine during thermal denaturation at 53 °C.

3.3 Conclusion

The results presented here indicate that both a mechanism based inactivator (2-deoxy-2-fluoro-β-D-glucopyranosyl fluoride) and a competitive inhibitor (*N*-octyl-1-epivalienamine) stabilize glucocerebrosidase against denaturation. Both compounds could potentially function as chemical chaperones in therapies for Gaucher disease. Further studies with Gaucher fibroblasts are necessary to evaluate the ability of these inhibitors to enhance mutant glucocerebrosidase activity in the lysosome. The presence of the octyl chain would increase the specificity of *N*-octyl-1-epivalienamine towards glucocerebrosidase over other glycosidases, reducing the potential for side effects, and could also help the compound cross cellular membranes. However the difficulty of synthesis of *N*-octyl-1-epivalienamine would result in a costly therapy, although likely less costly than the presently used enzyme replacement therapy. In contrast, 2-deoxy-2-fluoro-β-D-glucopyranosyl fluoride is relatively easy to synthesize, but would likely have less specificity for glucocerebrosidase. This may or may not be a problem since the inhibitor is being used at sub-inhibitory concentrations needed to provide the modest increase in enzyme activity to remove disease symptoms. If need be, the fluoride at C-1 could be replaced with an activated lipophilic chain, in an effort to increase the specificity of the compound towards glucocerebrosidase.

4 The Development of a Glucuronidase Glycosynthase

4.1 Introduction

4.1.1 Background on Glycosynthases

Oligosaccharides are of considerable therapeutic interest,[79] with disease targets including metabolic and cardiovascular diseases, and cancer. Unfortunately, the chemical synthesis of oligosaccharides is hampered by the tedious use of protecting groups and the challenge of controlling the stereochemistry of the anomeric linkage.[80] This difficulty has hindered the development of oligosaccharides for use as therapeutics.

The problems faced with chemical synthesis can be overcome by the use of enzymes, which have built-in regio- and stereo-selectivity. Glycosyl transferases, which catalyze the transfer of a glycoside from an activated donor sugar to a saccharide acceptor, are the obvious best candidates. However, the donor is usually a nucleotide sugar, and the cost of nucleotide donor sugars is a limitation for industrial use.[81] Another possibility is the use of glycosidases 'run in reverse' in transglycosylation reactions. The glycosyl enzyme intermediate in the standard double displacement mechanism can be intercepted with an acceptor sugar instead of water, creating a transglycosylation product instead of a hydrolysis product (Scheme 4.1a). This is achieved by using donor sugars with good leaving groups to increase the concentration of glycosyl enzyme, and adding a high concentration of acceptor sugar. The effective concentration of water can also be reduced with the use of co-solvents. However, this technique suffers from poor yields since the oligosaccharide product of the transglycosylation reaction is a substrate for the enzyme.

The Withers group found a solution to this problem with the introduction of glycosynthases in 1998 (Scheme 4.1b).[82] The catalytic glutamate nucleophile in a retaining glycosidase from *Agrobacterium sp.* (Abg) was replaced with an alanine residue, resulting in a correctly folded but hydrolytically inactive enzyme. However, the mutant enzyme was able to catalyze the formation of β-(1,4) linkages between α-glucopyranosyl fluoride and a variety of acceptors. The α-glucosyl fluoride donor, which is of the opposite anomeric configuration to that of the regular substrate, mimics the glycosyl-enzyme intermediate found in the reaction pathway of retaining β-glycosidases. The acceptor binds in such a way that the 4-hydroxyl is positioned for nucleophilic attack on the anomeric center. General base catalysis is provided by the catalytic acid/base residue, increasing the nucleophilicity of the acceptor hydroxyl group. Fluoride, a good leaving group, departs and the glycosidic bond is formed, creating an oligosaccharide product.

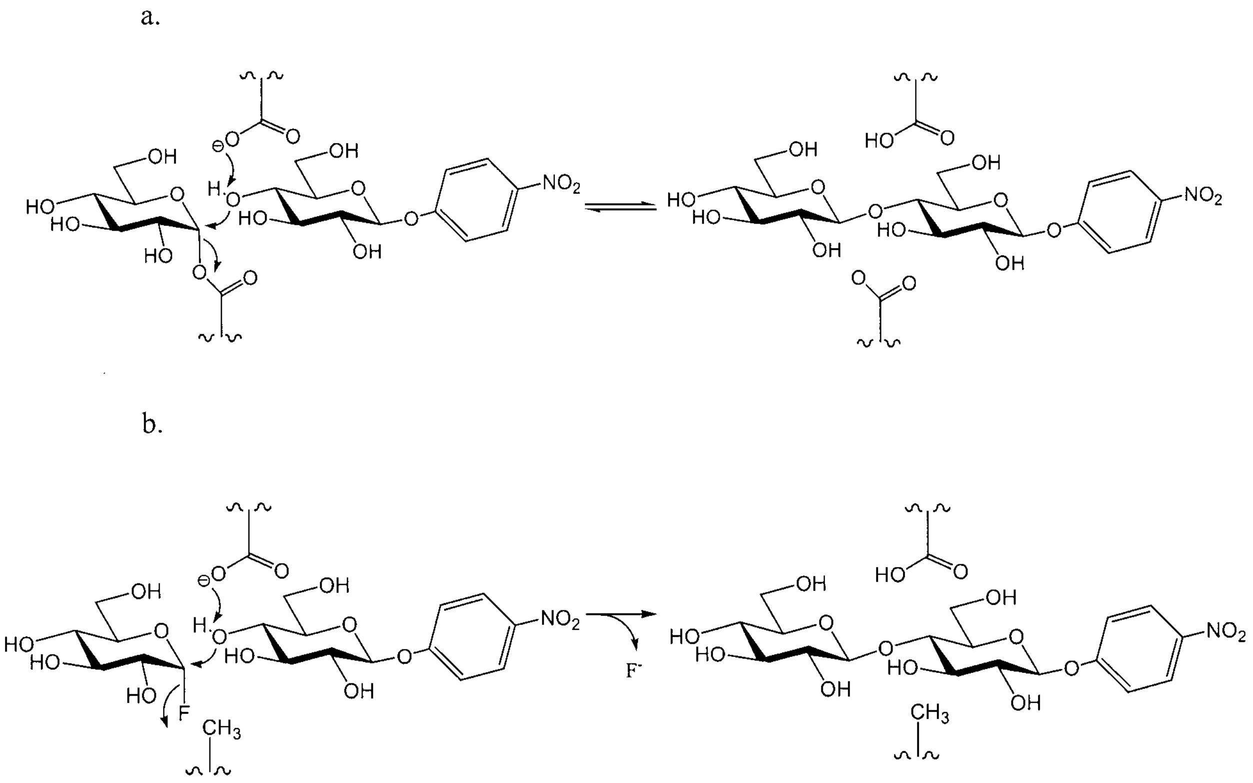

Scheme 4.1 a. A trans-glycosylation reaction.
b. A glycosynthase reaction.

The obvious advantage of this technique is that the oligosaccharide product is not a substrate for the hydrolytically inactive glycosynthase enzyme, and as a consequence yields are very good (70-90 %). Another advantage is that the glycosyl fluoride donors are relatively simple and inexpensive to synthesize. The glycosynthase technique has since been applied to other glycosidases by the Withers group and by others to create a variety of products and linkages, which have been catalogued in a review by Williams and Withers.[83]

At present, however, there are no reported glycosynthases that can incorporate glucuronic acid residues into oligosaccharides. The work presented here describes the first such glycosynthase, developed from a glucuronidase from *Thermotoga maritima.*

4.1.2 Thermotoga maritima

T. maritima is a thermophilic bacterium isolated from geothermally heated marine sediment with an optimum growth temperature of 80 °C.[84] The complete genomic sequence of *T. maritima* has been reported.[85] Numerous enzymes have been purified from *T. maritima*, including several glycosidases that are resistant to high temperatures, denaturing agents, and alcohols.[86] This resistance to harsher conditions has created interest in thermophilic enzymes due to their potential application in biotechnology and in industrial processes that require stability at high temperatures.

4.1.3 β-Glucuronidases

Family 2 β-glucuronidases are retaining β-glycosidases that catalyze the removal of glucuronic acid (**4.1**, Figure 4.1) units from the non-reducing end of oligosaccharides. Glucuronic acid has several important biological roles. It is a component of glycosaminoglycans, which are found in the ground substance that makes up the extracellular spaces in cartilage, tendon, skin, and blood vessel walls. One such glycosaminoglycan is hyaluronic acid (**4.2**, Figure 4.1), which consists of β-(1-4) linked repeating units of glucuronic acid β-(1-3) linked to *N*-acetyl-D-glucosamine, and is used for eye surgeries and other medicinal applications.[87]

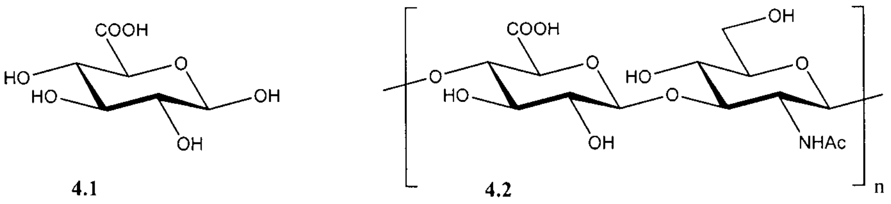

Figure 4.1. The structures of glucuronic acid (**4.1**) and hyaluronic acid (**4.2**).

Another glucuronic acid-containing glycosaminoglycan is heparin, which inhibits enzymes involved in blood coagulation and is widely used as an anti-coagulant in surgery.[88] Glucuronic acid also plays a key role in drug metabolism. Drugs are often metabolized through the transfer of glucuronic acid from UDP-glucuronic (Figure 4.2) acid to the drug. This transfer of glucuronic acid is a detoxification reaction that terminates the activity of the drug and results in excretion.[89]

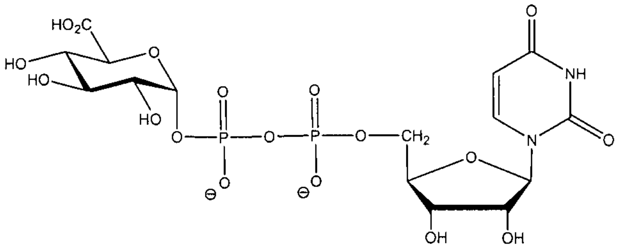

Figure 4.2 Diagram of UDP-glucuronic acid

The creation of a glycosynthase from a glucuronidase (a glucuronosynthase) would provide the ability to incorporate glucuronic acid monosaccharides into oligosaccharides thus creating the possibility of synthesizing glycosaminoglycans, glucuronoconjugates, or potential drugs. The chemical synthesis of such compounds involves the use of cumbersome protecting group manipulations[90] and complications due to the formation of side-products.[91] A glucuronidase from *T. maritima* was selected for conversion into a glucuronosynthase in the hope that the thermophilic properties of *T. maritima* would lead to a robust glycosynthase useful for a range of applications.

4.2 Development of a Glucuronosynthase from the β-Glucuronidase from *Thermotoga maritima*

The development of a glucuronosynthase was a collaborative effort with undergraduate student Jiyoung Hwang and post-doctoral fellow Dr. Hamzah Mohd. Salleh. The β-glucuronidase from *T. maritima* was cloned, overexpressed in *Escherichia coli*, and purified by Jiyoung Hwang. Dr. Hamzah Mohd. Salleh labeled the enzyme with the mechanism based inactivator 2-deoxy-2-fluoro-β-D-glucopyranuronosyl fluoride (Figure 4.3). 2-Deoxy-2-fluoro-β-D-glucopyranuronosyl fluoride inactivates the glucuronidase by reacting with the catalytic nucleophile, as described previously (Scheme 1.3). The catalytic nucleophile was identified as glutamate 476 following enzyme digestion and LC-MS/MS analysis of the fragments by Shouming He (not published). Dr. Hamzah Mohd. Salleh then carried out site-directed mutagenesis to generate three mutant enzymes in which glutamate 476 was replaced with glycine, alanine, and serine.

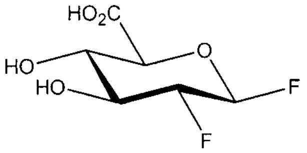

Figure 4.3 Diagram of 2-deoxy-2-fluoro-β-D-glucopyranuronosyl fluoride.

4.2.1 Synthesis of Donor Sugars: α-D-Galactopyranuronosyl Fluoride and α-D-Glucopyranuronosyl Fluoride

The donor sugars α-D-galactopyranuronosyl fluoride **(4.6)** and α-D-glucopyranuronosyl fluoride **(4.9)** were synthesized for use in the glycosynthase reaction (Figure 4.4). Both fluoro-sugars were synthesized using the same synthetic route, beginning with the corresponding acid.

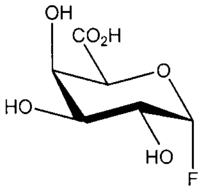

4.6

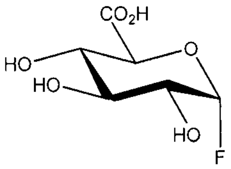

4.9

Figure 4.4 Diagram of α-D-galactopyranuronosyl fluoride **(4.6)** and α-D-glucopyranuronosyl fluoride **(4.9)**.

Shown in Scheme 4.2 is the synthesis of α-D-galactopyranuronosyl fluoride **(4.6)**. D-Galacturonic acid was dissolved in dry methanol and (TMS)diazomethane was added drop wise to yield the methyl ester **4.3**. The methyl ester **4.3** was subsequently acetylated to provide the acetylated methyl ester **4.4** in 60 % yield over the two steps. Reaction with HF/pyridine yielded the protected α-fluoride **4.5** in 32 % yield after purification by recrystallization. The anomeric stereochemistry was assigned on the basis of ^{1}H NMR coupling constants. Deprotection proceeded with the addition of hydrogen peroxide and lithium hydroxide in 7:3 THF:H_2O to first saponify the ester. Once the methyl ester was converted to the acid salt, the remaining acetyl groups were deprotected with sodium hydroxide in methanol to yield α-D-galactopyranuronosyl fluoride **(4.6)** in 49 % yield. These specific conditions are important because the methyl ester causes H-5 to be relatively acidic. Addition of a strongly basic deprotecting agent would risk elimination of the 4-OAc group, particularly in the case of the galacto-isomer, where the 4-OAc group is trans-diaxial to H-5.

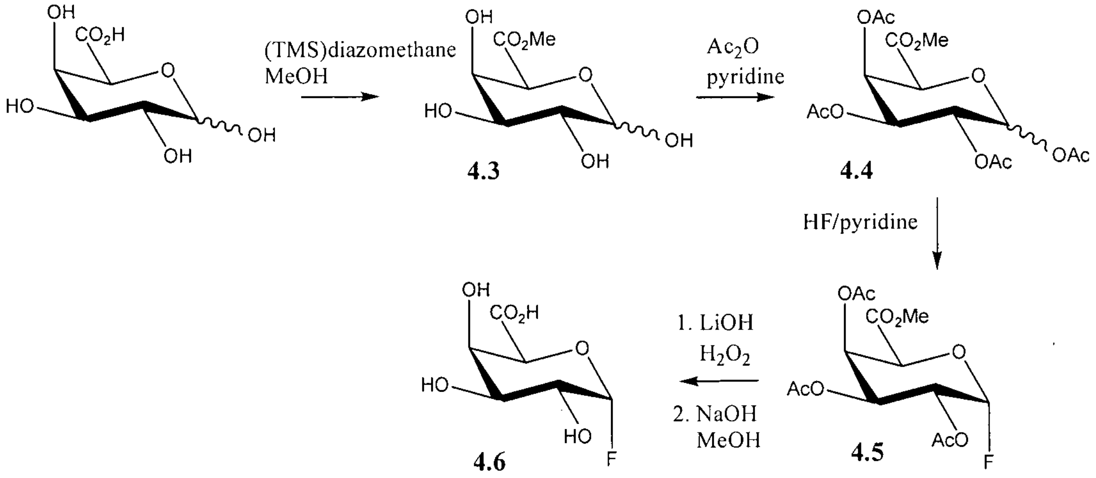

Scheme 4.2 The synthesis of galactopyranuronosyl fluoride **(4.6)**.

4.2.2 Glucuronosynthase Reactions

Test reactions performed by Dr. Hamzah Mohd. Salleh indicated that the E476A and E476G mutants catalyze a glycosynthase reaction between α-D-glucopyranuronosyl fluoride and pNP-glucoside. The E476S mutant did not function as a glycosynthase. Interestingly, with the original Abg glycosynthase[92] and a mannosynthase from *Cellulomonas fimi*,[93] the serine mutant is a better glycosynthase than the alanine mutant. It is not clear why the serine mutant is a better glycosynthase, yet this is not the case with the glucuronosynthase. The alanine mutant was selected for reaction scale-up and further study. A glycosynthase reaction using the E476A mutant is shown in Scheme 4.3.

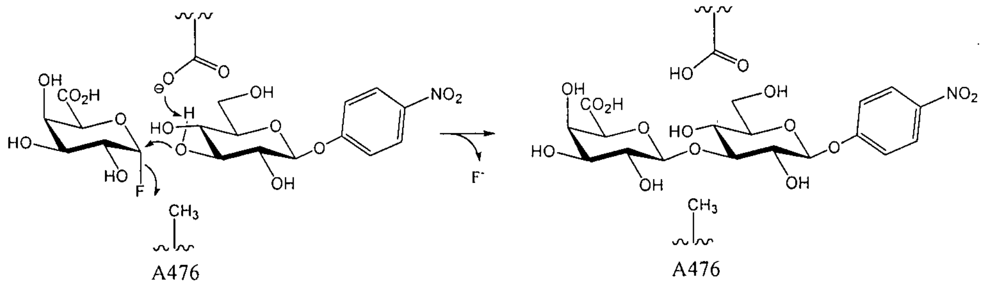

Scheme 4.3 A glycosynthase reaction catalyzed by the E476A mutant of β-glucuronidase.

Although the enzyme is a glucuronidase, the donor could be of either gluco- or galacto- stereochemistry; both α-D-glucopyranuronosyl fluoride (α-GluF, **4.9**) and α-D-galactopyranuronosyl fluoride (α-GalF, **4.6**) functioned as donors. PNP β-D-glucoside **(4.10)**, pNP β-D-xyloside **(4.11)**, and pNP β-D-cellobioside **(4.12)** were good acceptors. Glycosynthase reactions with the two donors and three acceptors were initally carried out by Dr. Hamzah Mohd. Salleh and later repeated by the author to produce more compound for product characterization. Table 4.1 shows glucuronosynthase reaction yields obtained by Dr. Hamzah Mohd. Salleh. The product of a glycosynthase reaction can act as an acceptor in additional glycosynthase reactions (provided excess donor is present), resulting in longer oligosaccharides over time. Thus tri and tetrasaccharides were isolated where two to three donor units were added to the oligosaccharide chain (Table 4.1).

Table 4.1 E476A Glucuronidase Glycosynthase Reaction Yields

Donor	Acceptor	disaccharide	trisaccharide	tetrasaccharide
α-GalF **(4.6)**	pNP β-D-glucoside **(4.10)**	83 %	7 %	n.d.*
	pNP β-D-xyloside **(4.11)**	32 %	6 %	n.d.
	pNP β-D-cellobioside **(4.12)**	--	60 %	n.d.
α-GluF **(4.9)**	pNP β-D-glucoside **(4.10)**	55 %	43 %	1 %
	pNP β-D-xyloside **(4.11)**	12 %	48 %	4 %
	pNP β-D-cellobioside **(4.12)**	--	72 %	10 %

* n.d. = not done

The products resulting from the addition of one glucuronic acid or galacturonic acid unit to an acceptor (disaccharides for pNP β-D-glucoside and pNP β-D-xyloside, and trisaccharides for pNP β-D-cellobioside, **4.13-4.18**) were selected for characterization (Table 4.2).

Table 4.2 E476A Glucuronidase glycosynthase products selected for characterization

Donor	Acceptor	Product selected for characterization
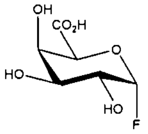 **4.6**	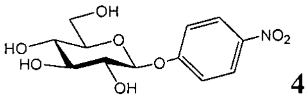 **4.10**	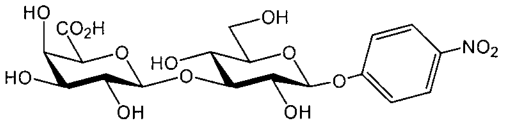 **4.13**
	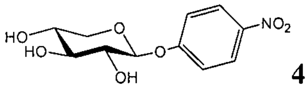 **4.11**	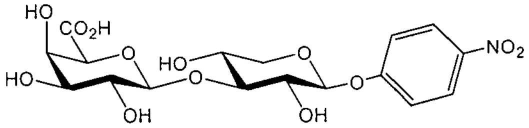 **4.14**
	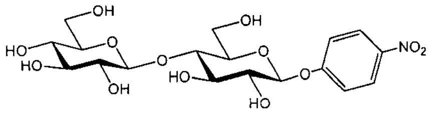 **4.12**	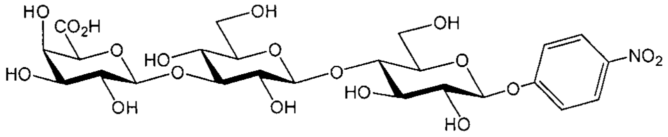 **4.15**
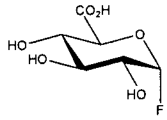 **4.9**	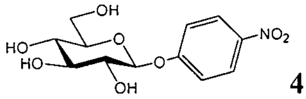 **4.10**	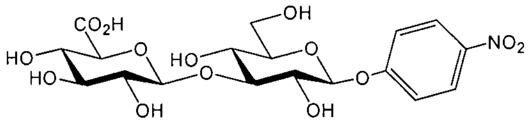 **4.16**
	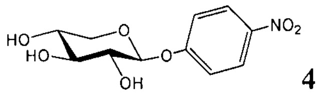 **4.11**	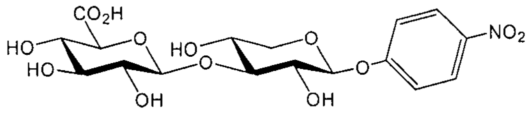 **4.17**
	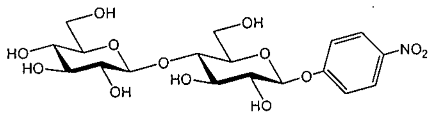 **4.12**	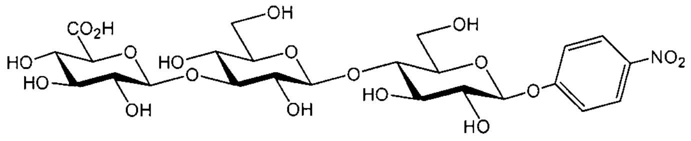 **4.18**

The products **4.13-4.18** were derivatized to their acetylated methyl esters **4.19-4.24** for characterization. The reaction scheme for the derivatization of compound **4.13** is shown in Scheme 4.4. Salts and enzyme were removed from the lyophilized mixture by passing the material through a C-18 Sep-Pak® cartridge. The material was acetylated with acetic acid and catalytic trifluoroacetic acid, and then esterified with (TMS)diazomethane in methanol. Through ^1H-^1H COSY NMR the linkages formed between donor and acceptor were identified as β-(1,3) in all cases.

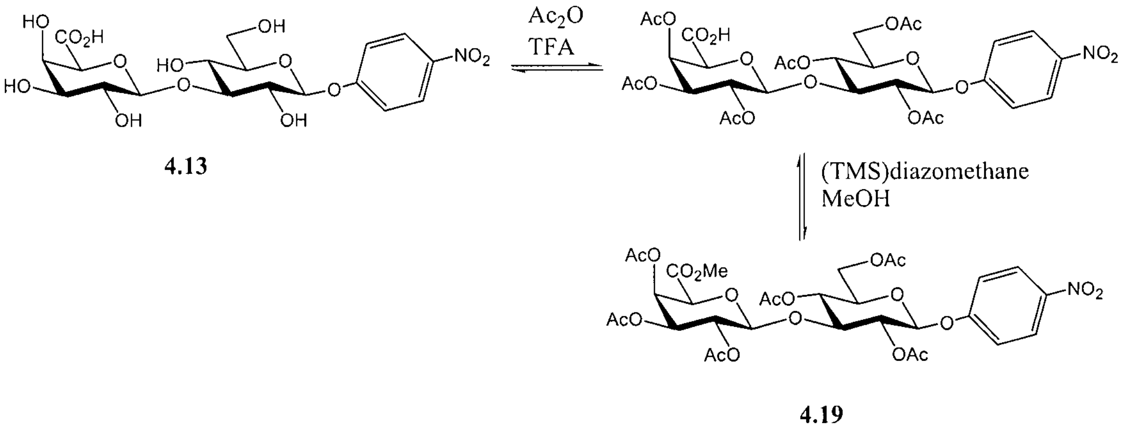
HO
CO2H
O
HO
HO
O
OH
OH
O
OH
O
NO2
4.13
Ac2O
TFA
AcO
CO2H
O
AcO
AcO
O
AcO
OAc
O
OAc
O
NO2
(TMS)diazomethane
MeOH
AcO
CO2Me
O
AcO
AcO
O
AcO
OAc
O
OAc
O
NO2
4.19

Scheme 4.4 The acetylation and esterification of compound **4.13**.

4.2.3 Attempts to Synthesize Glycosaminoglycan Fragments

In order to synthesize glycosaminoglycan fragments, an acceptor containing a 2-amino group would be necesserary. Unfortunately, *N*-acetyl-D-glucosamine (GlcNAc) **(4.25)**, pNP *N*-acetyl-β-D-glucosaminide (pNP-GlcNAc) **(4.26)**, pNP β-D-glucosamine **(4.27)** and NAG-thiazoline **(2.2)** do not function as acceptors (Figure 4.5).

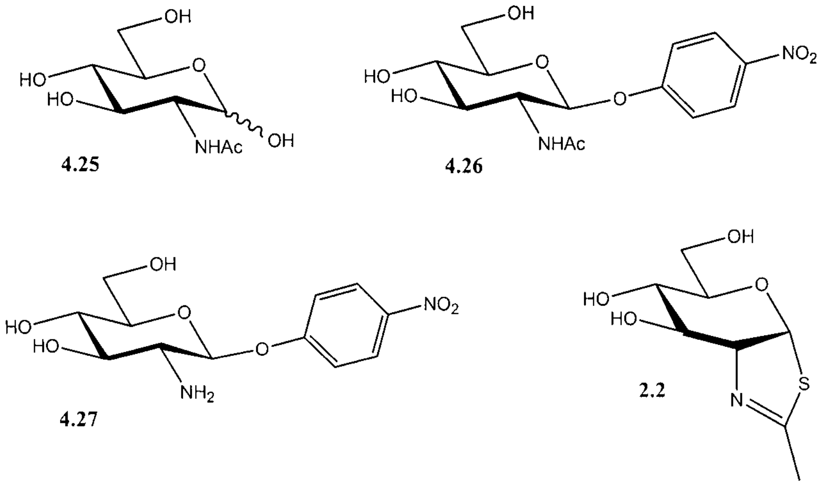

Figure 4.5 The compounds that did not function as acceptors for the E476A glucuronosynthase.

An additional test showed that glucose does not function as an acceptor, suggesting that the pNP group is necessary for acceptor binding. Because glucose did not function as an acceptor, it is not surprising that GlcNAc **(4.25)** and NAG-thiazoline **(2.2)**, which lack the apparently needed pNP group, also did not act as acceptors. The fact that pNP-GlcNAc and pNP-glucosamine do not function as acceptors suggests that the active site of the glucuronosynthase does not tolerate the added size of an amino or *N*-acetyl group relative to a hydroxyl group at the 2 position.

The problems presented by the fact that the E476A β-glucuronidase does not use 2-amino sugars as acceptors could be overcome with further enzyme mutations. The amino acid residues involved in binding the acceptor could be mutated to create space for the needed amino or *N*-acetyl group. Examining the active site in an X-ray crystal structure could provide candidate amino acids for mutation. Unfortunately, the structure of the *T. maritima* β-glucuronidase is not available. However, the structures of the related family 2 human β-glucuronidase[94] and *E. coli* β-galactosidase[95,96] are available, making a molecular modelling study possible. A molecular model of the wild-type β-glucuronidase from *T. maritima* was created using DeepView/Swiss-PdbViewer[97] based on the structure of the human β-glucuronidase[94], which is the most closely related enzyme with a structure available (34 % identity and 50 % similarity of amino acid sequence) (Figure 4.6). To provide further insight into binding, a bound carbohydrate was added to the model. There are no structures available for the human β-glucuronidase with bound inhibitor, however a structure of an enzyme/inhibitor complex of the homologous *E. coli* β-galactosidase[96] is available. The structure contains a 2-deoxy-2-fluoro galactosyl moiety covalently linked to the catalytic nucleophile formed by pre-incubating *E. coli* β-galactosidase with the inactivator 2,4-dinitrophenyl 2-deoxy-2-fluoro-β-D-galactopyranoside. The model of the *T. maritima* β-glucuronidase was overlaid onto the structure of the *E. coli* β-galactosidase with covalently bound 2-deoxy-2-fluoro galactosyl moiety. The overlaid structure of the β-galactosidase was then removed from the model, leaving a picture of the 2-deoxy-2-fluoro galactosyl moiety attached to the catalytic nucleophile E476 of the *T. maritima* β-glucuronidase (Figure 4.6). The geometry of the covalently bound 2-deoxy-2-fluoro galactosyl moiety approximates the geometry of an α fluoride donor sugar bound in the active site of the E476A nucleophile mutant used in the glycosynthase reactions. A space filled version of the model (Figure 4.7) shows the pocket where the acceptor sugar binds, and the residues involved in binding the acceptor sugar. The acceptor sugar could sit 'right side up' with the 2-hydroxyl (or desired 2-amino) group pointed downward in the picture, or the acceptor sugar could sit 'up side down', with the 2-group pointed upwards in the picture. The residues in the model that create the pocket where the acceptor sugar binds are Phe140, Tyr444, Tyr440, Thr475, Asn438, and Met426 (Figure 4.7). These residues are candidates for further site-directed mutagenesis studies on the E476A glucuronosynthase to allow the use of acceptors with 2-amino groups.

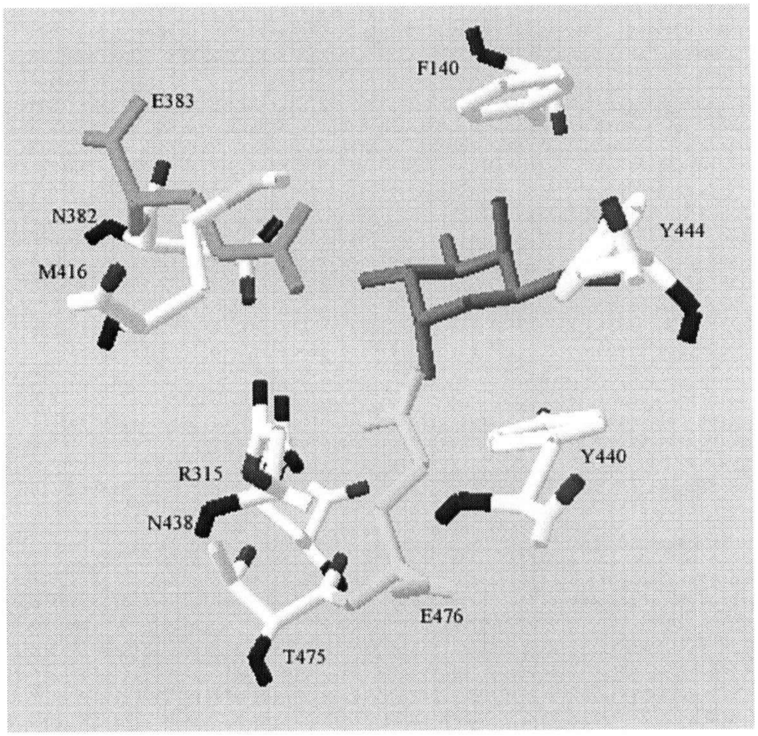
F140
E383
N382
Y444
M416
R315
Y440
N438
E476
T475

Figure 4.6 Molecular model of *T. maritima* β-glucuronidase with bound 2-deoxy-2-fluoro galactosyl moiety (green). Shown in yellow is the catalytic nucleophile (E476) and shown in blue is the catalytic acid/base residue (E383).

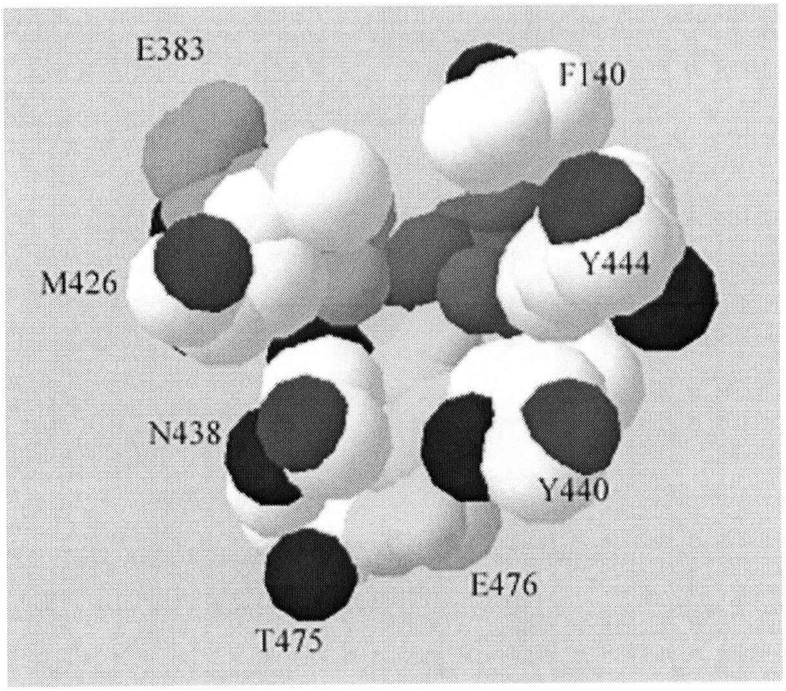
E383
F140
M426
Y444
N438
Y440
E476
T475

Figure 4.7 Space-filled model of *T. maritima* β-glucuronidase.

Another approach to creating mutants that can accommodate 2-amino containing acceptors is directed evolution. Members of the Withers group are currently working on directed evolution of glycosynthases to improve reaction rates, using a screen with a coupled assay that recognizes the product once it is formed. This approach could lead to mutations far removed from the active site that cause the small changes in active site geometry needed to accommodate acceptors with 2-amino groups and allow the synthesis of glycosaminoglycan fragments.

4.3 Conclusion

A glycosynthase was developed from the β-glucuronidase from *T. maritima.* Although the synthesis of a glycosaminoglycan fragment was not achieved, six novel oligosaccharides were synthesized and characterized, thus adding to the repertoire of compounds that can be synthesized by glycosynthases.

5 Materials and Methods

5.1 Enzymology

5.1.1 Sp. Hex. Kinetics

Sp. Hex. was cloned and overexpressed in *E. coli* as described previously[58] by Jiyoung Hwang, an undergraduate student in the Withers laboratory. Continuous spectrophotometric assays for *Sp. Hex.* were performed on a Varian Cary 4000 or Varian Cary 300 UV-Vis spectrophotometer, using *para*-nitrophenyl β-D-*N*-acetylglucosaminide (pNP-GlcNAc) as substrate. The buffer used for kinetic studies was 25/50 mM sodium citrate/sodium phosphate, 75 mM NaCl, pH 5.0. Kinetic assays were carried out at 37 °C. The concentration of enzyme used was 1.18 nM. The release of *para*-nitrophenol was measured at 360 nm. The extiction coefficient used for *para*-nitrophenol[57] was 2.05 $mM^{-1}cm^{-1}$. Michaelis-Menten parameters were determined using GraFit version 4.0.19.[60] The graphs and resulting Michaelis-Menten parameters are in the Appendix.

5.1.2 Human β-Hexosaminidase A and B Kinetics

Human β-hexosaminidases A and B were provided by the group of Dr. Don Mahuran (Hospital for Sick Children, Toronto). The buffer used was 20/40 mM sodium citrate/sodium phosphate, 0.1 % HSA, pH 4.50. 4-Methylumbelliferyl-*N*-acetyl-β-D-glucosaminide (MUG) was used as substrate. Stopped assays for Hex A and Hex B were performed as follows. Substrate/buffer solutions were pre-incubated at 37 °C in eppendorf tubes. Enzyme was added to a concentration of 0.23 nM for Hex A and 0.084 nM for Hex B. At fixed time intervals 20 μL aliquots of reaction mixture were removed and diluted into a cuvette containing 1 mL of 0.1 M 2-amino-2-methyl-1-propanol (pH 10.0). The fluorescence resulting from release of methylumbelliferone was measured on a Varian Cary Eclipse fluorimeter.

The instrument parameters were set as follows:

```
Ex. Wavelength (nm)              365.00
Em. Wavelength (nm)              450.00
Ex. Slit (nm)                    5
Em. Slit (nm)                    5
Ave Time (sec)                   0.1000
Excitation filter                Auto
Emission filter                  Open
PMT Voltage (V)                  Medium
```

An equation (equation 5.1) to convert data from units of fluorescence to units of concentration was created by measuring the fluorescence of solutions of known concentrations of methylumbelliferone, plotting the data, and fitting the data to a linear fit using GraFit version 4.0.19.[60]

$$\text{Fluorescence} = (5.83 \times 10^{8}) \times [\text{methylumbelliferone}] \qquad \text{(Equation 5.1)}$$

Michaelis-Menten parameters were calculated using GraFit version 4.0.19.[60] The graphs and resulting Michaelis-Menten parameters are in the Appendix.

5.1.2.1 Determination of k_{cat}/K_m Values for pNP-GlcNAc and pNP-GalNAc

k_{cat}/K_m values for *para*-nitrophenyl β-D-*N*-acetylglucosaminide (pNP-GlcNAc) and *para*-nitrophenyl β-D-*N*-acetylgalactosaminide (pNP-GalNAc) were determined using the substrate depletion method as follows. A continuous spectrophotometric assay was performed at 37 °C on a Varian Cary 4000 UV-Vis spectrophotometer. The substrate concentration used was 13.0 μM (Km ~ 500 μM). Enzyme concentrations were 0.77 nM for Hex B and 1.4 nM for Hex A. The change in absorbance was measured at 360 nm over ~ 40 minutes. The data were fitted to a first-order rate equation using the Cary WinUV kinetics application version 3.00, giving values for the pseudo-first-order rate constant. Equation 5.2 shows a modified Michaelis-Menten equation for the conditions of low substrate concentration ([S] << K_m). The k_{obs} values correspond to $[E]k_{cat}/K_m$, and thus the k_{cat}/K_m values can be extracted by dividing the observed rate constants by the enzyme concentration.

$$v = \frac{k_{cat}[E][S]}{K_m} \qquad \text{(Equation 5.2)}$$

5.1.3 Glucocerebrosidase Kinetics

Glucocerebrosidase was donated in the form of used vials of Cerezyme® (produced by Genzyme) from a patient currently undergoing enzyme replacement therapy. The buffer used for kinetics was 50 mM acetate buffer, pH 5.5, containing 0.125 % Thesit® or Triton X-100®, 0.30 % sodium taurocholate, and 1 mM EDTA. 2,4-Dinitrophenyl β-D-glucopyranoside was used as substrate for continuous spectrophotometric assays. Kinetic assays were carried out at 37 °C. The concentration of enzyme used was 29.0 nM. The release of the 2,4-dinitrophenol was measured at 400 nm. The extiction coefficient used for 2,4-dinitrophenol[70] was 10.7 $mM^{-1}cm^{-1}$. Michaelis-Menten parameters were determined using GraFit version 4.0.19.[60] The graphs and resulting Michaelis-Menten parameters are presented in the Appendix.

5.1.4 Competitive Inhibition

All inhibition kinetics were performed by measuring the reaction rate at a fixed concentration of artificial substrate while varying the concentration of inhibitor. K_i values were determined by fitting the data to the equation for competitive inhibitrion (Equation 5.3) using GraFit version 4.0.19.[60]

$$v = \frac{V_{\max} \cdot [S]}{K_m\left(1+\frac{[I]}{K_i}\right)+[S]} \qquad \text{(Equation 5.3)}$$

K_i values were graphically represented by creating a plot of the inverse of the reaction rate against the concentration of inhibitor (Dixon plot). The line for $1/V_{max}$ intersects the lines for different substrate concentrations at $K_i = -[I]$. The theory for this method of representing K_i, taken from Segel,[97] is presented below.

For competitive inhibition,

$$v = \frac{V_{max}[S]}{[S] + K_m(1 + [I]/K_i)}$$

The reciprocal of this equation is

$$\frac{1}{v} = \frac{K_m[I]}{V_{max}[S]K_i} + \frac{1}{V_{max}}\left(1 + \frac{K_m}{[S]}\right)$$

When $\frac{1}{v} = \frac{1}{V_{max}}$,

$$\frac{1}{V_{max}} = \frac{K_m[I]}{V_{max}[S]K_i} + \frac{1}{V_{max}}\left(1 + \frac{K_m}{[S]}\right)$$

and

$$1 = \frac{K_m[I]}{[S]K_i} + 1 + \frac{K_m}{[S]}$$

so,

$$-\frac{K_m[I]}{[S]K_i} = \frac{K_m}{[S]}$$

and

$$[I] = -K_i$$

5.1.5 Inactivation of Glucocerebrosidase

Glucocerebrosidase (0.441 μM) was incubated with an excess of 2-deoxy-2-fluoro-β-D-glucopyranosyl fluoride (2.47 mM) at room temperature. Aliquots of the enzyme/inactivator mixture were removed after 45 minutes, 3 hours, and 16 hours and enzyme activity was monitored as described above (5.1.3).

5.1.6 Thermal Denaturation Experiments

Thermal denaturation studies were performed by first determining a temperature at which the enzyme loses substantial activity within an hour. This was achieved by incubating the enzyme at 55 °C, and removing aliquots at fixed time intervals and measuring the enzyme activity with an artificial substrate. Different incubation temperatures were used until a suitable temperature was found. The enzyme was then incubated at this temperature in the presence or absence of inhibitor, and aliquots were removed at fixed time intervals and the enzyme activity with an artificial substrate was measured. The artificial substrates and assay conditions employed were identical to those used for previously described Michaelis-Menten and inhibition kinetics for each enzyme.

The concentration of inhibitor selected for all denaturation experiments was at least ten times its K_i value to ensure that the inhibitor occupied the vast majority of enzyme active sites. It was also ensured that the absolute concentration of inhibitor was always greater than the enzyme concentration. In all cases, when an aliquot of the enzyme/inhibitor mixture was diluted into a buffered solution of substrate for the kinetic assay, the dilution factor was large enough for the concentration of inhibitor to become sub-inhibitory. The table below summarizes the temperatures and concentrations used.

Table 5.1 Concentrations and temperatures used during thermal denaturation experiments.

		pre-incubation	pre-incubation	assay	assay			
Enzyme	Inhibitor	[Enzyme] (nM)	[Inhibitor] (μM)	[Enzyme] (nM)	[Inhibitor] (μM)	K_i (μM)	T (°C)	[substrate] (mM)
Sp. Hex.	NAG-thiazoline	38.2	240	1.18	7.41	20	55	0.666
Hex A	NAG-thiazoline	10.5	4.00	0.379	0.144	0.40	56	1.86
Hex B	NAG-thiazoline	10.6	2.40	0.341	0.0774	0.24	60	2.90
Glucocerebrosidase	*N*-octyl-1-epivalienamine	250	1.25	3.09	0.0154	0.10	53	2.05

5.1.7 Guanidine Hydrochloride Denaturation Experiments

Guanidine hydrochloride (99+%) was purchased from Sigma. The guanidine hydrochloride did not contain fluorescent impurities, and thus was not further purified. For each enzyme, the buffer used for kinetics was also used for denaturation experiments, except in the following cases where the buffers were found to interfere with fluorescence or CD. Phosphate buffers interfered with CD spectra, so the citrate/phosphate buffer used for *Sp. Hex.* was replaced with a 100 mM acetate buffer, pH 5.0, 75 mM NaCl, which did not affect enzyme activity. The Triton X-100® used in glucocerebrosidase buffer fluoresced significantly, and was replaced with Thesit®, which did not affect enzyme activity.

Guanidine hydrochloride concentrations were calculated by measuring the refractive index with a Spectronic Instruments model 334610 refractometer and using the following equation (from Creighton),[62] where ΔN is the difference in refractive index between the guanidine hydrochloride/buffer solution and the buffer alone at the sodium D line.

$$[\text{Gdm-HCl}] = 57.147(\Delta N) + 38.68(\Delta N)^2 - 91.60(\Delta N)^3 \qquad \text{(Equation 5.4)}$$

After adding enzyme or enzyme/inhibitor mixtures to the solutions of guanidine hydrochloride, solutions were allowed to equilibrate for at least 3 hours before fluorescence or CD readings were taken. Incubations for longer time periods showed no significant changes in fluorescence or CD measurements. For enzyme/inhibitor mixtures, the enzyme was pre-incubated with inhibitor for 10 minutes before addition to solutions of guanidine hydrochloride. In each case the inhibitor concentration was at least 10 x K_i to ensure that the vast majority of active sites were occupied. For glucocerebrosidase inactivation with 2-deoxy-2-fluoro-β-glucopyranosyl-fluoride, the enzyme/inactivator mixture was incubated at room temperature for 16 hours, at which time the enzyme was 90 % inactivated, prior to addition to solutions of guanidine hydrochloride. The table below summarizes the concentrations used. All data refer to fluorescence experiments except where noted.

Table 5.2 Concentrations used during guanidine hydrochloride denaturation experiments.

Enzyme	Inhibitor	[Enzyme] (μM)	[Inhibitor] (μM)	K_i (μM)
Sp. Hex.	NAG-thiazoline	0.66	230	20
Sp. Hex.[a]	NAG-thiazoline	3.0	230	20
Hex A	NAG-thiazoline	0.090	4.1	0.40
Hex B	NAG-thiazoline	0.098	2.5	0.24
Glucocerebrosidase	*N*-octyl-1-epivalienamine	0.44	28	0.10
Glucocerebrosidase	2-deoxy-2-fluoro-β-D-glucopyranosyl-fluoride	0.44	2500	NA

[a] concentrations used for CD measurements.

Circular dichroism measurements were taken on a JASCO J-810 spectropolarimeter.

Fluorescence measurements were taken on a Varian Cary Eclipse fluorimeter. A fluorescence excitation scan revealed a maximum at 280 nm, thus 280 nm was selected as the excitation wavelength. Fluorescence emission scans were corrected with a Savitzky Golay equation[98] using a filter size of 19 and an interval of 1.00. The instrument parameters were set as follows.

Scan mode	Emission
X Mode	Wavelength (nm)
Start (nm)	300.00
Stop (nm)	400.00
Ex. Wavelength (nm)	280.00
Ex. Slit (nm)	10
Em. Slit (nm)	10
Scan rate (nm/min)	600.00
Data interval (nm)	1.0000
Averaging Time (s)	0.1000

Excitation filter	Auto
Emission filter	Open
PMT voltage (V)	Medium

Chemical denaturation curves were fit to the equation for a sigmoidal curve (Equation 5.5) using GraFit version 4.0.19.[60]

$$y = Y_o + \frac{a}{1+e^{-\left(\frac{x-x_o}{b}\right)}} \qquad \text{(Equation 5.5)}$$

5.1.8 General Procedure for Glucuronidase Glycosynthase Reactions

In a typical preparative scale reaction 50 μL of 300 mM glucuronyl or galacturonyl fluoride and 200 μL of 50 mM acceptor were added to 750 μL of 3.5 mg/mL E476A β-glucuronidase in 50 mM pH 7 sodium phosphate buffer. Reaction concentrations were 15 mM donor, 10 mM acceptor, and 2.8 mg/mL E476A β-glucuronidase. The reactions were incubated for 18 hours at 37 °C and lyophilized before work-up. Test scale reactions were performed with a total volume of 100 μL, and preparative scale reactions were performed with a total volume of 1 mL. Reaction yields were calculated by separating a small portion of the material by HPLC (acetonitrile/water 9:1 to 1:1) and integrating the peaks of the HPLC profile. Compounds were detected by UV absorption of the *para*-nitrophenyl containing acceptors and products at 254 nm. The percent yield was calculated as the area of the peak due to the glycosynthase product divided by the sum of the areas of the glycosynthase product and acceptor peaks. Molecular weights of the oligosaccharide products were confirmed by ESI-MS.

5.2 Syntheses

5.2.1 General Synthesis

All reagents were purchased from Sigma/Aldrich unless otherwise stated. Solvents used were either reagent, certified, or spectral grade. Anhydrous solvents were prepared as follows: toluene, benzene, and acetonitrile were distilled over calcium hydride. Methanol was distilled from magnesium turnings in the presence of iodine. Tetrahydrofuran was distilled from sodium in the presence of benzophenone. Deionized water, purified with a Millipore Milli-Q® system, was used for all aqueous solutions.

Synthetic and enzymatic reactions were monitored by TLC using Merck Kieselgel F_{254} alumina based sheets (thickness 0.2 mm). Compounds were detected by ultraviolet light and/or by charring with 10 % ammonium molybdate in 2 M H_2SO_4. Column chromatography was performed with Merck Kieselgel (230-400 mesh) silica gel. NMR spectra were recorded on a Bruker Avance 300 MHz, Bruker Avance 400 MHz, or a Varian In̆ova 600 MHz spectrometer. Chemical shifts were reported on the δ scale in parts per million from tetramethylsilane (TMS). The abbreviations used in describing multiplicity are: s-singlet, d-doublet, t-triplet, m-multiplet, br-broad. ^{19}F NMR spectra were referenced to trifluoroacetic acid at 0 ppm. Low-resolution mass spectra were measured on an ESI PE Sciex API 300 spectrometer. High-resolution mass spectra were measured on an ESI Micromass LCT spectrometer by the mass spectrometry laboratory at the University of British Columbia. In each case analytical data for previously reported compounds was identical to the data reported in the reference provided with the compound title.

5.2.2 Generous Gifts

The group of Professor R. V. Stick (The University of Western Australia) provided the tetra-*O*-benzyl-1-epivalienamine for the synthesis of *N*-octyl-1-epivalienamine. The group of Professor Spencer Knapp (Rutgers, New Jersey) provided the XylNAc-isofagamine·HCl. NAGal-thiazoline and a portion of the NAG-thiazoline were synthesized by Dr. Hongming Chen in the Withers laboratory. A precursor to α-D-glucopyranuronosyl fluoride, methyl (1,2,3,4-tetra-*O*-acetyl-D-glucopyranosyl)uronate, was synthesized by Dr. Michael Jahn in the Withers laboratory. 2,4-Dinitrophenyl β-D-glucopyranoside was synthesized by Dr. Michael Jahn and Fathima Shaikh in the Withers laboratory.

5.2.3 NAG-Thiazoline[13] *(2.2)*

Tri-*O*-acetyl-1,2-dideoxy-2′-methyl-α-D-glucopyranoso-[2,1-*d*]-Δ2′-thiazoline (tri-*O*-acetyl NAG-thiazoline) (2.1)

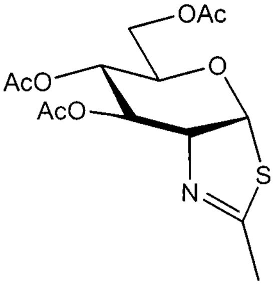

2-Acetamido-2-deoxy-β-D-glucopyranose 1,3,4,6-tetra-acetate (2.92 g, 7.50 mmol) was dissolved in dry toluene (35 mL). Lawesson's reagent (2.5 g, 6.18 mmol) was added and the mixture was heated to reflux and stirred at 110 °C under argon for 3.5 hours at which point the reaction was judged complete by TLC. The solvent was evaporated *in vacuo* and the material was purified by column chromatography (petroleum ether/ethyl acetate 2:1 to 1:2) to yield tri-*O*-acetyl NAG-thiazoline **(2.1)** as an oil (1.87 g, 5.41 mmol, 72 %). ^{1}H NMR (300 MHz, CDCl$_3$) δ: 6.23 (d, 1 H, $J_{1,2}$ = 7.1 Hz, H-1), 5.55 (m, 1 H, H-3), 4.94 (br d, 1 H, $J_{4,5}$ = 9.5 Hz, H-4), 4.48-4.43 (m, 1 H, H-2), 4.11 (d, 2 H, $J_{6a,5}$ = $J_{6a,5}$ = 4.4 Hz, H-6$_a$, H-6$_b$), 3.54 (dt, 1 H, H-5), 2.31 (d, 3 H, $J_{Mc,2}$ = 2.1 Hz, Me), 2.12, 2.07, 2.06 (3 s, 9 H, 3 OAc).

1,2-Dideoxy-2′-methyl-α-D-glucopyranoso-[2,1-*d*]-Δ2′-thiazoline (NAG-thiazoline) (2.2)

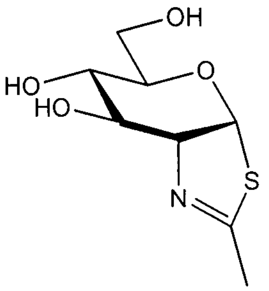

The per-*O*-acetylated thiazoline **2.1** (1.87 g, 5.41 mmol) was dissolved in dry methanol (50 mL) and sodium methoxide (catalytic amount) was added. The mixture was stirred under argon for 2 hours at which time the reaction was judged complete by TLC. Acetic acid was added dropwise until the mixture was acidic and the solvent was evaporated *in vacuo*. The material was dry loaded onto silica and purified by column chromatography (ethyl acetate/methanol/water 10:1:0 to 7:3:1) to yield NAG-thiazoline **(2.2)** as a gummy solid (0.902 g, 4.11 mmol, 76 %). ^{1}H NMR (400 MHz, D_2O) δ: 6.20 (d, 1 H, $J_{1,2}$ = 7.0 Hz, H-1), 4.35-4.32 (m, 1 H, H-2), 4.14 (dd, 1 H, $J_{3,2}$ = 4.5, $J_{3,4}$ = 3.2 Hz, H-3), 3.65 (dd, $J_{6a,6b}$ = 12.4, $J_{6a,5}$ = 2.4 Hz, H-6$_a$), 3.52 (dd, 1 H, $J_{4,5}$ = 9.1 Hz, H-4), 3.51 (dd, 1 H, $J_{6b,5}$ = 7.2 Hz, H-6$_b$), 3.24 (ddd, 1 H, H-5), 2.16 (d, 3 H, $J_{Me,2}$ = 2.1 Hz, Me). ^{13}C NMR (100 MHz, D_2O, referenced to MeOH) δ: 171.54 (SC=N), 87.83, 77.85, 74.11, 71.52, 69.41, 61.63 (6 ring C's), 19.47 (CH_3). HRMS (ESI) *m/z* 242.0462 [M + Na]$^+$. Calculated for $C_8H_{13}NNaO_4S$ 242.0463.

5.2.4 2-Deoxy-2-Fluoro-β-D-Glucopyranosyl Fluoride[71] *(3.3)*

3,4,6-Tri-*O*-acetyl-2-deoxy-2-fluoro-α-D-glucopyranosyl bromide (3.1)

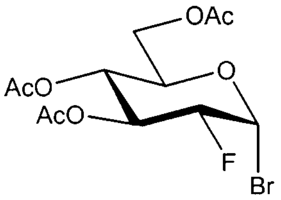

Tri-*O*-acetyl-D-glucal (15.0 g, 55.1 mmol) was dissolved in acetic acid (100 mL) and acetic anhydride (20 mL) was added. The mixture was heated to 60 °C and Selectfluor® (20.0 g, 56.4 mmol) was added. After stirring for 1 hour at 60 °C DMF (10 mL) was added to facilitate dissolving. Acetic acid (30 mL) and acetic anhydride (15 mL) were added and the mixture was stirred for 6 hrs at 60 °C. The reaction was judged incomplete by TLC, so another portion of Selectfluor® (5.0 g, 14 mmol) was added and the reaction mixture was stirred for 14 hours at 60 °C. The solvent was evaporated *in vacuo*, and the mixture was diluted with water (200 mL). The material was extracted with DCM (2 x 150 mL), and washed with water and saturated sodium bicarbonate solution. The organic layer was dried over $MgSO_4$ and concentrated to yield 14.5 g (41.4 mmol) of a mixture of the α-gluco, β-gluco and β-manno isomers of 1,3,4,6-tetra-*O*-acetyl-2-deoxy-2-fluoro-D-pyranose. The residue was purified by column chromatography (petroleum ether/ethyl acetate 3:1 to 1:1), yielding a mixture of the α and β anomers of 1,3,4,6-tetra-*O*-acetyl-2-deoxy-2-fluoro-D-glucopyranose (2.0 g, 5.7 mmol, 10 %).

The 1,2,4,6-tetra-*O*-acetyl-2-deoxy-2-fluoro-D-glucopyranose (2.0 g, 5.7 mmol) was dissolved in dichloromethane (8 mL) and cooled in an ice bath under N_2. HBr in acetic acid (30 wt. %, 5.0 mL, 25 mmol) was added and the reaction mixture was stirred for 16 h at RT under N_2. The material was diluted into ice water (100 mL) and ethyl acetate (40 mL) was added. The organic layer was washed with saturated sodium bicarbonate solution and brine, then dried over $MgSO_4$ and concentrated *in vacuo* to yield 3,4,6-tri-*O*-acetyl-2-deoxy-2-fluoro-α-D-glucopyranosyl bromide **(3.1)** (1.7 g, 4.6 mmol, 80 %). ^{1}H NMR (400 MHz, $CDCl_3$) δ: 6.51 (d, 1 H, $J_{1,2} = 4.2$ Hz, H-1), 5.61 (ddd, 1 H, $J_{3,F} = 11.2$, $J_{3,4} = 9.9$, $J_{3,2} = 9.4$ Hz, H-3), 5.10 (dd, 1 H, $J_{4,5} =$

9.8 Hz, H-4), 4.52 (ddd, 1 H, $J_{2,F}$ = 49.4 Hz, H-2), 4.34-4.28 (m, 2 H, H-6$_a$, H-6$_b$), 4.13-4.08 (m, 1 H, H-5), 2.03, 2.05, 2.07 (3 s, 9 H, 3 O-Ac).

3,4,6-Tri-*O*-acetyl-2-deoxy-2-fluoro-β-D-glucopyranosyl fluoride (3.2)

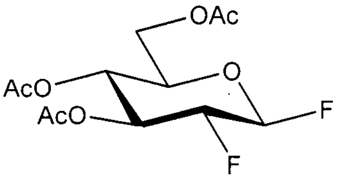

The α-bromide **3.1** (1.7 g, 4.6 mmol) was dissolved in dry acetonitrile (50 mL) and silver fluoride (1.70 g, 13.4 mmol) was added. After stirring for 16 h the reaction was judged incomplete by TLC, so another portion of silver fluoride (0.50 g, 3.9 mmol) was added. The mixture was stirred for 5 h at which point the reaction was judged complete by TLC. The material was filtered through Celite and the solvent was evaporated *in vacuo*. The residue was dissolved in ethyl acetate (50 mL) and washed with water and brine. The organic layer was dried over $MgSO_4$, the solvent was evaporated *in vacuo*, and the residue crystallized from ethyl acetate/heptane to yield 3,4,6-tri-*O*-acetyl-2-deoxy-2-fluoro-β-D-glucopyranosyl fluoride **(3.2)** (1.0 g, 3.2 mmol, 70 %). ^{1}H NMR (300 MHz, $CDCl_3$) δ: 5.42 (ddd, 1 H, $J_{1,F\text{-}1}$ = 51.9, $J_{1,2}$ = 6.2, $J_{1,F\text{-}2}$ = 3.8 Hz, H-1), 5.31 (m, 1 H, H-3), 5.11 (dd, 1 H, $J_{4,5}$ = 9.7, $J_{4,3}$ = 9.3 Hz, H-4), 4.49 (dddd, 1 H, $J_{2,F\text{-}2}$ = 56.1, $J_{2,F\text{-}1}$ = 11.0, $J_{2,3}$ = 7.9 Hz, H-2), 4.26 (dd, 1 H, $J_{6a,6b}$ = 12.5, $J_{6a,5}$ = 4.8 Hz, H-6$_a$), 4.18 (dd, $J_{6b,5}$ = 2.7 Hz, H-6$_b$), 3.88 (ddd, 1 H, H-5), 2.08 (s, 6 H, 2 O-Ac), 2.03 (s, 3 H, O-Ac).

2-Deoxy-2-fluoro-β-D-glucopyranosyl fluoride (3.3)

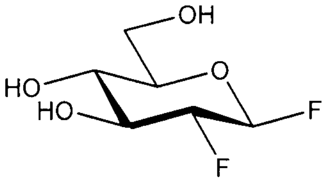

A portion of the 3,4,6-tri-*O*-acetyl-2-deoxy-2-fluoro-β-D-glucopyranosyl fluoride **(3.2)** (0.422 g, 1.36 mmol) was dissolved in dry methanol (40 mL). Sodium methoxide (2 spatula tips) was added and the mixture was stirred for 1 hour at which point the reaction was judged complete by TLC. Amberlite® H$^+$ IR 120 resin was added, and the mixture was filtered and then the solvent was evaporated *in vacuo*. The residue was purified by column chromatography (ethyl acetate/methanol/water 27:2:1) to yield 2-deoxy-2-fluoro-β-D-glucopyranosyl fluoride as a solid **(3.3)** (0.250 g, 1.16 mmol, 85 %). ^{1}H NMR (400 MHz, D_2O) δ: 5.38 (ddd, 1 H, $J_{1,\mathrm{F-1}} = 53.1$, $J_{1,2} = 7.0$, $J_{1,\mathrm{F-2}} = 3.3$ Hz, H-1), 4.21 (dddd, 1 H, $J_{2,\mathrm{F-2}} = 51.5$, $J_{2,\mathrm{F-1}} = 13.5$, $J_{2,3} = 9.1$ Hz, H-2), 3.79 (ddd, 1 H, $J_{6a,6b} = 12.5$, $J_{6a,5} = 2.2$, $J_{6a,\mathrm{F-1}} = 0.9$ Hz, H-6_a), 3.71 (dddd, 1 H, $J_{3,\mathrm{F-2}} = 15.4$, $J_{3,4} = 9.0$, $J_{3,\mathrm{F-1}} = 0.8$ Hz, H-3), 3.64 (ddd, 1 H, $J_{6b,5} = 5.3$, $J_{6b,\mathrm{F-1}} = 1.0$ Hz, H-6_b), 3.50 (dddd, 1 H, $J_{5,4} = 9.9$, $J_{5,\mathrm{F-1}} = 0.8$ Hz, H-5), 3.41 (dd, 1 H, H-4). ^{19}F NMR (282 MHz, D_2O, referenced to TFA) δ: -125.97 (dt, $J_{\mathrm{F-2,F-1}} = 16.9$ Hz, F-2), -67.37 (dt, F-1). ESI MS m/z 207.1 [M + Na]$^+$. Calculated for $C_6H_{10}F_2NaO_4$ 207.0.

5.2.5 N-Octyl-1-Epivalienamine (3.6)

(1*R*,4*R*,5*S*,6*S*)-4,5,6-tribenzyloxy-3-(benzyloxymethyl)-1-(octylamino)-2-cyclohexene (tetra-*O*-benzyl-*N*-octyl-1-epivalienamine) (3.5)

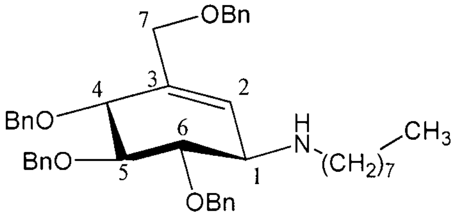

Tetra-*O*-benzyl-1-epivalienamine[77] [(1*R*,4*R*,5*S*,6*S*)-4,5,6-tribenzyloxy-3-(benzyloxymethyl)-1-amino-2-cyclohexene] **(3.4)** (0.408 g, 0.761 mmol) was dissolved in dry benzene (100 mL). Octyl aldehyde (130 μL, 0.832 mmol) and *p*-toluenesulfonic acid monohydrate (catalytic amount) were added and the mixture was heated at reflux with a Dean-Stark apparatus. After approximately 50 % of the solvent had distilled off, another portion of octyl aldehyde (100 μL, 0.640 mmol) was added and the mixture was stirred under reflux until a further 50 % of the solvent had distilled off. Dry methanol (20 mL) and sodium borohydride (catalytic amount) were added. The mixture was stirred for 5 minutes and acetic acid was added dropwise until no fizzing was visible in the reaction mixture. The solvent was evaporated *in* *vacuo* and the material was dissolved in dichloromethane (100 mL) and washed with saturated sodium bicarbonate and brine. The organic layer was dried over $MgSO_4$, filtered, and the solvent was evaporated *in vacuo*. The residue was purified by column chromatography (toluene/ethyl acetate/triethylamine 95:5:1 to 50:50:1) to yield tetra-*O*-benzyl-*N*-octyl-1-epivalienamine **(3.5)** (0.319 g, 0.492 mmol, 65 %). ^{1}H NMR (400 MHz, $CDCl_3$) δ: 7.33-7.24 (m, 20 H, CH_2-*Ph*), 5.70 (s, 1 H, H-2), 4.96 (t, 2 H, J = 11.7 Hz, CH_2-Ph), 4.84 (d, 1 H, J = 10.9 Hz, CH_2-Ph), 4.81 (d, 1 H, J = 10.9 Hz, CH_2-Ph), 4.70 (t, 2 H, J = 10.9 Hz, CH_2-Ph), 4.50 (d, 1 H, J = 11.9 Hz, CH_2-Ph), 4.43 (d, 1 H, J = 11.9 Hz, CH_2-Ph), 4.32 (br d, 1 H, $J_{4,5}$ = 7.6 Hz, H-4), 4.25 (br d, 1 H, $J_{7a,7b}$ = 12.0 Hz, H-7$_a$), 3.90-3.86 (m, 2 H, H-7$_b$, H-5), 3.59 (dd, 1 H, $J_{6,1}$ = 9.8, $J_{6,5}$ = 8.6 Hz, H-6), 3.36-3.34 (br d, 1 H, H-1), 2.52-2.39 (m, 2 H, NH-CH_2), 1.35-1.23 (m, 12 H, NH_2-CH_2-(CH_2)$_6$), 0.87 (t, 3 H, J = 6.6 Hz, (CH_2)$_7$-CH_3). ^{13}C NMR (75 MHz, $CDCl_3$) δ: 138.70, 138.66 (4 quaternary Ph C), 138.43 (C-2/3), 135.55 (C-2/3), 128.71, 128.59, 128.51, 128.31, 128.02, 127.99, 127.78, 127.69 (15 C, Ph), 85.30 (C-4/5/6), 81.07 (C-4/5/6), 80.45 (C-4/5/6), 75.32, 75.19, 74.54, 72.27, 70.51 (4 C, Ph-*C*H_2, C-7), 59.71 (C-1), 46.46 (NH-*C*H_2), 31.98, 30.55, 29.67, 29.41, 27.48, 22.81 (6 C, CH_2), 14.24 (CH_3). HRMS (ESI) *m/z* 648.4061 $[M + H]^+$. Calculated for $C_{43}H_{54}NO_4$ 648.4053.

(1*R*,4*R*,5*S*,6*S*)-4,5,6-hydroxy-3-(hydroxymethyl)-1-(octylamino)-2-cyclohexene (*N*-Octyl-1-epivalienamine)[76] (3.6)

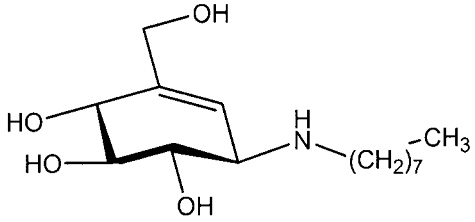

The protected *N*-octyl-1-epivalienamine **3.5** (0.319 g, 0.492 mmol) was dissolved in dry THF (25 mL) and stirred under nitrogen. Ammonia gas was condensed onto the mixture at -78 °C until a precipitate began to form. Sodium (4 small chunks) was added and the mixture was stirred for 1 hour after a deep blue colour had formed in the reaction mixture. Ammonium chloride was added until the solution became colourless. The mixture was allowed to warm to room temperature while stirring under nitrogen with a vent open to the atmosphere for the ammonia gas to vent. The remaining solvent was evaporated *in vacuo*. The residue was dissolved in methanol, filtered through Celite, and the solvent was again evaporated *in vacuo*. A portion of the product/salt mixture was further purified. The material was first purified by column chromatography (dichloromethane/methanol 6:1, 0.5 % triethylamine). The solvent was evaporated *in vacuo* and the residue was dissolved in H_2O and loaded onto a Sep-Pak® C-18 column as per the Sep-Pak® instruction manual. The Sep-Pak® C-18 column was flushed with H_2O and then methanol was used to elute the compound. The solvent was evaporated *in vacuo* and the material was redissolved in methanol and purified by anion exchange chromatography with a Bio-Rad AG® 1-X8 resin 200-400 mesh anion exchange column. The solvent was evaporated *in vacuo* to yield pure *N*-octyl-1-epivalienamine **(3.6)** as a solid. ^1H NMR (400 MHz D_2O) δ: 5.57 (s, 1 H, H-2), 4.13-4.03 (m, 3 H, H-1, H-7_a, H-7_b), 3.82 (dt, 1 H, $J_{4,5}$ = 9.2, $J_{4,7a} = J_{4,7b}$ = 2.5 Hz, H-4), 3.63 (dd, 1 H, $J_{5,6}$ = 10.2 Hz, H-5), 3.48 (dd, 1 H, $J_{6,1}$ = 8.3 Hz, H-6), 3.06-2.93 (m, 2 H, NH-CH_2), 1.55-1.65 (m, 2 H, NH-CH_2-CH_2), 1.27-1.12 (m, 10 H, 5 CH_2), 0.72 (t, 3 H, J = 7.0 Hz, CH_3). ^{13}C NMR (100 MHz, D_2O, referenced to MeOH) δ: 145.00 (C-4), 114.80 (C-5), 75.76 (C-1), 71.51 (C-6/7), 69.97 (C-2), 61.03 (C6/7), 59.78 (C-3), 44.77 (NH-CH_2), 31.23, 28.40, 25.95, 22.21 (6 CH_2), 13.63 (CH_3). HRMS (ESI) *m/z* 288.2173 $[M + H]^+$. Calculated for $C_{15}H_{30}NO_4$ 288.2175.

5.2.6 α-D-Galactopyranuronosyl Fluoride (4.6)

Methyl (2,3,4-tri-*O*-acetyl-α-D-galactopyranosyl fluoride)uronate (4.5)

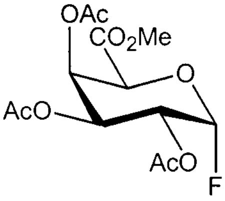

D-Galacturonic acid (2.10 g, 10.7 mmol) was dissolved in dry methanol and (TMS)diazomethane (10 mL, 2.0 M in hexanes, 20 mmol) was added dropwise until the solution retained a yellow colour. 10% Acetic acid in methanol was added dropwise until the solution became colourless. The solvent was evaporated, and then co-evaporated once with toluene yielding the methyl ester **(4.3)** as a thick brown oil (2.71 g). The methyl ester was dissolved in pyridine (30 mL) and cooled to 0 °C in an ice bath. Acetic anhydride (15 mL, 160 mmol) was added and the reaction mixture was stirred for 4.5 hours at which time the reaction was judged complete by TLC. Methanol (15 mL) was added slowly to quench the acetic anhydride. The solvent was evaporated to near dryness and the material was dissolved in dichloromethane (50 mL) and washed with 1 M HCl, saturated sodium bicarbonate, and brine. The organic layer was dried over $MgSO_4$ and the solvent was evaporated. The material was purified by column chromatography (petroleum ether/ethyl acetate 4:1 to 1:3) yielding methyl (1,2,3,4-tetra-*O*-acetyl-D-galactopyranosyl)uronate **(4.4)** as a foam (2.42 g, 6.43 mmol, 60 %).

The per-*O*-acetylated methyl ester **4.4** (2.42 g, 6.43 mmol) was dissolved in dichloromethane and transferred to a 50 mL Teflon tube. The solvent was evaporated and 70 % HF-pyridine (15 mL) was added dropwise. The reaction mixture was stirred for 70 h, and then the reaction mixture was added dropwise to 400 mL of saturated sodium bicarbonate solution. The product was extracted with ethyl acetate (200 mL) and washed with saturated sodium bicarbonate, 1 M HCl, and brine. The organic layer was dried over $MgSO_4$ and the solvent was evaporated. The material was purified by column chromatography (petroleum ether/ethyl acetate, 5:1 to 1:1), and crystallized from ethyl acetate/heptane to yield methyl (2,3,4-tri-*O*-acetyl-α-D-galactopyranosyl fluoride)uronate **(4.5)** (0.698 g, 2.08 mmol, 32 %). ^{1}H NMR (400 MHz, $CDCl_3$) δ: 5.90 (dd, 1 H, $J_{1,F}$ = 52.5, $J_{1,2}$ = 2.7 Hz, H-1), 5.82 (m, 1 H, H-4), 5.39 (dd, 1 H, $J_{3,2}$ = 10.9, $J_{3,4}$ = 3.3 Hz, H-3), 5.22 (ddd, 1 H, $J_{2,F}$ = 23.9 Hz, H-2), 4.76 (d, 1 H, $J_{5,4}$ = 1.2 Hz, H-5), 3.76 (s, 3 H, O-C*H*$_3$), 2.10, 2.09, 2.00 (3 s, 9 H, 3 O-Ac). ^{13}C NMR (100 MHz, $CDCl_3$) δ: 169.95, 169.67, 169.45 (3 s, 3 CO), 166.09 (s, C-6), 104.24 (d, $J_{1,F}$ = 230.0 Hz, C-1), 70.32, 68.32 (2 s, C-3/4/5), 66.83 (d, $J_{2,F}$ = 23.5 Hz, C-2), 66.51 (s, C-3/4/5), 52.82 (s, O-CH_3), 20.49 (s, 2 x CO-*C*H$_3$), 20.36 (s, CO-*C*H$_3$). ^{19}F NMR (282 MHz, $CDCl_3$) δ: -75.62 (dd). ESI MS m/z 359.4 [M + Na]$^+$. Calculated for $C_{13}H_{17}FNaO_9$ 359.3.

α-D-Galactopyranuronosyl Fluoride (4.6)

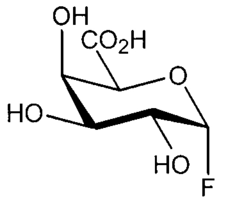

The protected galactopyranuronosyl fluoride **4.5** (0.698 g, 2.08 mmol) was dissolved in 7:3 THF:H_2O (23 mL) and cooled in an ice bath. H_2O_2 (8.8 mL, 30 % in H_2O, 114 mmol) and 1.25 M LiOH (4.0 mL, 5.0 mmol) were added and the mixture was stirred for 3 hours at 0 °C and 2 hours at room temperature. Methanol (9.4 mL) and 4.0 M NaOH (4.5 mL, 18 mmol) were added and the mixture was stirred at RT until the reaction was judged complete by TLC (3 hours). Amberlite® H^+ IR 120 resin was added, the mixture was filtered, and the solvent was evaporated *in vacuo*. The material was dry loaded on to silica with methanol and purified by column chromatography (ethyl acetate/petroleum ether/water + 0.2 % acetic acid, 5:1:0 to 6:3:1) to yield α-D-galactopyranuronosyl fluoride **(4.6)** as a solid (200 mg, 1.02 mmol, 49 %). ^{1}H NMR (400 MHz, D_2O) δ: 5.68 (dd, 1 H, $J_{1,F}$ = 53.2 Hz, $J_{1,2}$ = 2.8 Hz, H-1), 4.63 (d, 1 H, $J_{5,4}$ = 1.5 Hz, H-5), 4.31 (dd, 1 H, $J_{4,3}$ = 3.3 Hz, H-4), 3.90 (dd, 1 H, $J_{3,2}$ = 10.0 Hz, H-3), 3.78 (ddd, 1 H, $J_{2,F}$ = 25.6 Hz, H-2). ^{13}C NMR (100 MHz, D_2O, referenced to MeOH) δ: 171.82 (s, CO), 107.43 (d, $J_{1,F}$ = 224.9 Hz, C-1), 72.69 (s, C-3), 69.77, 68.53 (s, C-4/5), 67.52 (d, $J_{2,F}$ = 24.2 Hz, C-2). ^{19}F NMR (282 MHz, referenced to TFA) δ: -77.17 (dd). ESI MS *m/z* 219.3 $[M + Na]^+$. Calculated for $C_6H_9FNaO_6$ 219.1.

5.2.7 α-D-Glucopyranuronosyl Fluoride (4.9)

Methyl (2,3,4-tri-*O*-acetyl-α-D-glucopyranosyl fluoride)uronate (4.8)

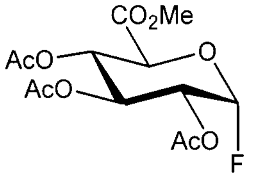

Methyl (1,2,3,4-tetra-*O*-acetyl-D-glucopyranosyl)uronate **(4.7)** (5.1 g, 13.5 mmol) was placed in a 50 mL Teflon tube. 70 % HF-pyridine (10 mL) was added dropwise. The mixture was stirred at room temperature for 2 hours. The reaction was incomplete by TLC, so more 70 % HF-pyridine (7 mL) was added and the mixture was stirred for 24 hours at which time the reaction was judged complete by TLC. The reaction mixture was added dropwise to 600 mL of saturated sodium bicarbonate solution. The product was extracted with ethyl acetate (300 mL) and washed with saturated sodium bicarbonate, 1 M HCl, and brine. The organic layer was dried over $MgSO_4$ and the solvent was evaporated *in vacuo*. The material was purified by column chromatography (petroleum ether/ethyl acetate, 5:1 to 1:1), and crystallized from ethyl acetate/heptane to yield methyl (2,3,4-tri-*O*-acetyl-α-D-glucopyranosyl fluoride)uronate **(4.8)** (2.62 g, 7.79 mmol, 58 %). ^{1}H NMR (400 MHz, $CDCl_3$) δ: 5.79 (dd, 1 H, $J_{1,F} = 53.0$, $J_{1,2} = 2.7$ Hz, H-1), 5.53 (dd, 1 H, $J_{3,2} = 10.2$, $J_{3,4} = 9.9$ Hz, H-3), 5.21 (dd, 1 H, $J_{4,5} = 10.3$ Hz, H-4), 4.95 (ddd, 1 H, $J_{2,F} = 24.2$ Hz, H-2), 4.47 (d, 1 H, H-5), 3.74 (s, 3 H, O-CH_3), 2.08 (s, 3 H, O-Ac), 2.02 (s, 6 H, 2 O-Ac). ^{19}F NMR (282 MHz, $CDCl_3$) δ: -73.36 (dd). ESI MS *m/z* 359.0 [M + Na]$^+$. Calculated for $C_{13}H_{17}FNaO_9$ 359.3.

α-D-Glucopyranuronosyl fluoride (4.9)

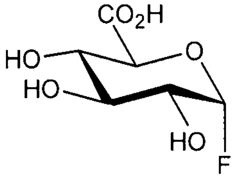

The α-fluoride **4.8** (2.62 g, 7.79 mmol) was dissolved in 7:3 THF:H_2O (80 mL) and cooled in an ice bath. H_2O_2 (30.5 mL, 30 % in H_2O, 394 mmol) and 1.25 M LiOH (14.0 mL, 17.5 mmol) were added and the mixture was removed from the ice bath and stirred for 2 hours at room temperature. Methanol (32.5 mL) and 4.0 M NaOH (15.5 mL, 62.0 mmol) were added and the mixture was stirred at 4 °C for 2 hours, allowed to warm to room temperature, then stirred for a further 2 hours at room temperature. Amberlite® H^+ IR 120 resin was added, the mixture was filtered, and the solvent was evaporated *in vacuo*. The material was dry loaded on to silica with methanol and purified by column chromatography (ethyl acetate/petroleum ether/water + 0.2 % acetic acid, 5:1:0 to 6:3:1) to yield α-D-glucopyranuronosyl fluoride **(4.9)** as a solid (460 mg, 2.35 mmol, 30 %). ^{1}H NMR (400 MHz, D_2O) δ: 5.59 (dd, 1 H, $J_{1,F}$ = 53.1, $J_{1,2}$ = 2.7 Hz, H-1), 4.05 (d, 1 H, $J_{5,4}$ = 10.1 Hz, H-5), 3.64 (dd, 1 H, $J_{3,2}$ = 9.8, $J_{3,4}$ = 9.5 Hz, H-3), 3.54 (ddd, 1 H, $J_{2,F}$ = 25.9 Hz, H-2), 3.48 (dd, 1 H, H-4). ^{19}F NMR (282 MHz, D_2O) δ: -73.81 (dd). ESI MS *m/z* 219.4 $[M + Na]^+$. Calculated for $C_6H_9FNaO_6$ 219.1.

5.2.8 General Procedure for Derivatization of Glycosynthase Products

Salts and enzyme were removed from the lyophilized mixture by passing the material through a C-18 Sep-Pak® cartridge according to the instruction booklet. The C-18 cartridge was flushed with methanol (6 mL), followed by water (6 mL). The reaction mixture was loaded with water and the cartridge was flushed with water (6 mL). The compound was then eluted with methanol and the solvent was evaporated *in vacuo*. The residue was dissolved in a minimum amount of acetic anhydride, and 3 drops of trifluoroacetic acid were added. The reaction mixture was allowed to stir at RT overnight, and then the solvent was evaporated *in vacuo*. A few drops of acetonitrile and 10 % HCl were added to cleave the mixed anhydride that may have formed, then the material was dissolved in chloroform and washed with 10 % HCl and brine. The organic layer was dried over $MgSO_4$, evaporated, and the residue dissolved in HPLC grade MeOH and (TMS)diazomethane added dropwise until a yellow colour persisted. The mixture was stirred for 5 minutes, and acetic acid (one drop) was added, causing the solution to become colourless. The solvent was evaporated *in vacuo* and the material was purified by column chromatography (toluene/ethyl acetate 3:1 to 3:2).

5.2.9 Assignment of Protons in ^1H NMR Specra of Derivatized Glycosynthase Products

The protons of the derivatized glycosynthase products were assigned using ^1H NMR COSY spectra. Assignments were made by examining the couplings within the ring system. The location of the glycosidic bond was determined on the basis of the chemical shift of the ring protons. The acetate groups are more electron withdrawing than a glycosidic likage; hence the proton attached to a carbon involved in the glycosidic bond is found more upfield. The configuration of the anomeric linkage (α or β) was assigned based on the $J_{1,2}$ coupling constants.

5.2.10 Characterization of Glycosynthase Products

***Para*-nitrophenyl 3-*O*-(methyl 2,3,4-tri-*O*-acetyl-β-D-galacturonate)-2,4,6-tri-*O*-acetyl-β-D-glucoside (4.19)**

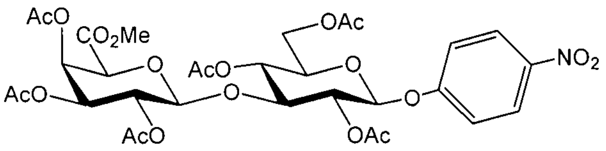

^{1}H NMR (400 MHz, $CDCl_3$): δ 8.18, 7.02 (2 d, 4 H, $J = 9.2$ Hz, Ar), 5.63 (d, 1 H, $J_{4',3'} = 3.5$ Hz, H-4′), 5.33-5.28 (m, 1 H, H-2), 5.14-5.08 (m, 2 H, H-2′, H-4), 5.03-4.99 (m, 2 H, H-1, H-3′), 4.59 (d, 1 H, $J_{1',2'} = 7.8$ Hz, H-1′), 4.26-4.20 (m, 3 H, H-5′, H-6_a, H-6_b), 4.06 (t, 1 H, $J_{3,4} = J_{3,2} = 9.5$ Hz, H-3), 3.96-3.88 (m, 1 H, H-5), 3.74, (s, 3 H, O-

CH_3) 2.22, 2.11, 2.09, 2.06, 2.03, 1.97 (6 s, 18 H, 6 O-Ac). HRMS (ESI) *m/z* 766.1802 $[M + Na]^+$. Calculated for $C_{31}H_{37}NNaO_{20}$ 766.1807.

Para-nitrophenyl 2,4-di-_O_-acetyl-3-_O_-(methyl 2,3,4-tri-_O_-acetyl-β-D-galacturonate)-β-D-xyloside (4.20)

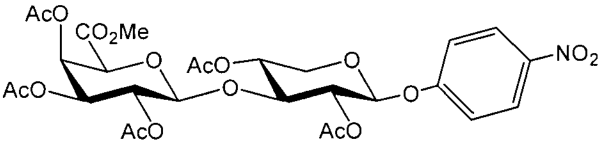

^{1}H NMR (*J* couplings from 400 MHz, assigned with 600 MHz, $CDCl_3$): δ 8.19, 7.12 (2 d, 4 H, $J = 9.3$ Hz, Ar), 5.69 (dd, 1 H, $J_{4',3'} = 3.5$, $J_{4',5'} = 1.4$ Hz, H-4′), 5.36 (d, 1 H, $J_{1,2} = 3.4$ Hz, H-1), 5.26 (dd, 1 H, $J_{2',3'} = 10.4$, $J_{2',1'} = 8.1$ Hz, H-2′), 5.11-5.02 (m, 3 H, H-4, H-3′, H-2), 4.31 (d, 1 H, H-5′), 4.67 (d, 1 H, H-1′), 4.20 (dd, 1 H, $J_{5a,5b} = 12.6$, $J_{5a,4} = 3.3$ Hz, H-5$_a$), 4.03 (t, 1 H, $J_{3,4} = J_{3,2} = 5.3$ Hz, H-3), 3.72 (s, 3 H, O-CH_3), 3.64 (dd, 1 H, $J_{5b,4} =$ 4.5 Hz, H-5$_b$), 2.15, 2.13, 2.11, 2.04, 1.99 (5 s, 15 H, 5 O-Ac). HRMS (ESI) *m/z* 694.1612 $[M + Na]^+$. Calculated for $C_{28}H_{33}NNaO_{18}$ 694.1595.

Para-nitrophenyl 4-_O_-(3-_O_-[methyl 2,3,4-tri-_O_-acetyl-β-D-galacturonate]-2,4,6-tri-_O_-acetyl-β-D-glucoside)-2,3,4-tri-_O_-acetyl-β-D-glucoside (4.21)

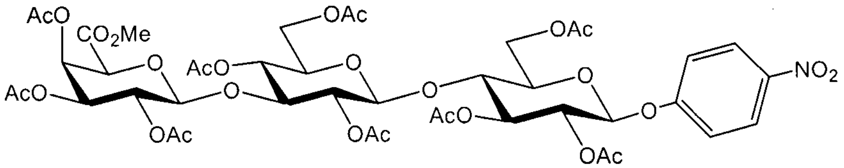

^{1}H NMR (400 MHz, $CDCl_3$): δ 8.18, 7.03 (2 d, 4 H, $J = 9.2$ Hz, Ar), 5.62 (dd, 1 H, $J_{4'',3''} = 3.5$, $J_{4'',5''} = 1.1$ Hz, H-4″), 5.26 (t, 1 H, $J_{3,4} = J_{3,2} = 8.8$ Hz, H-3), 5.19 (dd, 1 H, $J_{2,1} = 7.4$ Hz, H-2), 5.15 (d, 1 H, H-1), 5.05 (dd, 1 H, $J_{2'',3''} = 10.4$, $J_{2'',1''} = 7.8$ Hz, H-2″), 5.05-4.95 (m, 3 H, H-4′, 2′, 3″), 4.52 (d, 1 H, H-1″), 4.46-4.43 (m, 1 H, H-6$_a$), 4.34-4.29 (m, 1 H, H-6′$_a$), 4.32 (d, 1 H, $J_{1',2'} = 8.1$ Hz, H-1′), 4.23 (d, 1 H, H-5″), 4.12-4.05 (m, 2 H, H-6$_b$, H-6′$_b$), 3.90 (t, 1 H, $J_{3',4'} = J_{3',2'} = 9.5$ Hz, H-3′), 3.85-3.78 (m, 2 H, H-4, H-5), 3.71 (s, 3 H, O-CH_3), 3.67-3.63 (m, 1 H, H-5′), 2.18, 2.10, 2.09, 2.08, 2.07, 2.03, 2.02, 2.01, 1.96 (9 s, 27 H, 9 O-Ac). HRMS (ESI) *m/z* 1054.2632 $[M + Na]^+$. Calculated for $C_{43}H_{53}NNaO_{28}$ 1054.2652.

Para-nitrophenyl 3-*O*-(methyl 2,3,4-tri-*O*-acetyl-β-D-glucuronate)-2,4,6-tri-*O*-acetyl-β-D-glucoside (4.22)

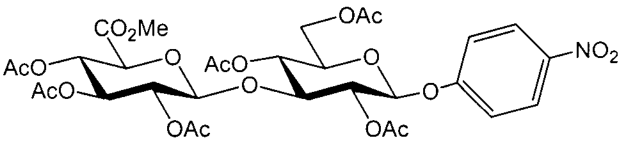

^{1}H NMR (400 MHz, $CDCl_3$): δ 8.18, 7.01 (2 d, 4 H, J = 9.2 Hz, Ar), 5.29 (dd, 1 H, $J_{2,3}$ = 9.4, $J_{2,1}$ = 7.9 Hz, H-2), 5.20 (dd, 1 H, $J_{3',4'}$ = 9.6, $J_{3',2'}$ = 9.2 Hz, H-3′), 5.12 (dd, 1 H, $J_{4',5'}$ = 9.7 Hz, H-4′), 5.06 (dd, 1 H, $J_{4,5}$ = 9.6, $J_{4,3}$ = 9.1 Hz, H-4), 5.02 (d, 1 H, $J_{1,2}$ = 7.9, H-1), 4.89 (dd, 1 H, $J_{2',1'}$ = 8.1 Hz, H-2′), 4.65 (d, 1 H, H-1′), 4.20-4.18 (m, 2 H, H-6$_a$, H-6$_b$), 3.99 (d, 1 H, H-5′), 3.98 (dd, 1 H, J = 9.4 Hz, H-3), 3.87-3.83 (m, 1 H, H-5), 3.72 (s, 3 H, O-CH_3), 2.13, 2.12, 2.04, 2.02, 1.99, 1.98 (6 s, 18 H, 6 O-Ac). HRMS (ESI) *m/z* 766.1813 $[M + Na]^+$. Calculated for $C_{31}H_{37}NNaO_{20}$ 766.1807.

Para-nitrophenyl 2,4-di-*O*-acetyl-3-*O*-(methyl 2,3,4-tri-*O*-acetyl-β-D-glucuronate)-β-D-xyloside (4.23)

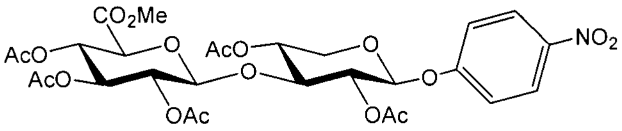

^{1}H NMR (400 MHz, $CDCl_3$): δ 8.18, 7.08 (2 d, 4 H, J = 9.2 Hz, Ar), 5.31 (d, 1 H, $J_{1,2}$ = 4.4 Hz, H-1), 5.24 (dd, 1 H, $J_{3',4'}$ = 9.5, $J_{3',2'}$ = 9.1 Hz, H-3′), 5.19 (dd, 1 H, $J_{4',5'}$ = 9.6 Hz, H-4′), 5.06 (dd 1 H, $J_{2,3}$ = 6.5 Hz, H-2), 5.04 (dd, 1 H, $J_{2',1'}$ = 7.8 Hz, H-2′), 5.01 (m, 1 H, H-4), 4.73 (d, 1 H, H-1′), 4.16 (dd, 1 H, $J_{5a,5b}$ = 12.7, $J_{5a,4}$ = 9.0 Hz, H-5$_a$), 4.04 (d, 1 H, H-5′), 3.98 (dd, 1 H, $J_{3,4}$ = 5.9 Hz, H-3), 3.73 (s, 3 H, O-CH_3), 3.58 (dd, 1 H, $J_{5b,4}$ = 5.4 Hz, H-5$_b$), 2.13, 2.11, 2.03 (3 s, 9 H, 3 O-Ac), 2.01 (s, 6 H, 2 O-Ac). HRMS (ESI) *m/z* 694.1614 $[M + Na]^+$. Calculated for $C_{28}H_{33}NNaO_{18}$ 694.1595.

Para-nitrophenyl 4-_O_-(3-_O_-[methyl 2,3,4-tri-_O_-acetyl-β-D-glucuronate]-2,4,6-tri-_O_-acetyl-β-D-glucoside)-2,3,4-tri-_O_-acetyl-β-D-glucoside (4.24)

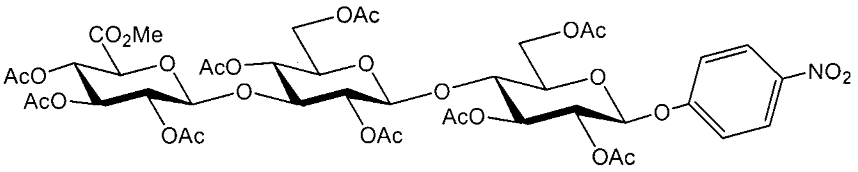

^{1}H NMR (400 MHz, CDCl$_3$): δ 8.18, 7.03 (2 d, 4 H, J = 9.2 Hz, Ar), 5.25 (t, 1 H, $J_{3,2}$ = $J_{3,4}$ = 8.2 Hz, H-3), 5.23-5.12 (m, 3 H, H-2, H-1, H-3″), 5.10, (dd, 1 H, $J_{4'',5''}$ = 9.7 Hz, $J_{4'',3''}$, H-4″), 4.88-4.83 (m, 2 H, H-2′, H-4′), 4.85 (dd, 1 H, $J_{2'',3''}$ = 9.3, $J_{2'',1''}$ = 8.1 Hz, H-2″), 4.57 (d, 1 H, H-1″), 4.45 (m, 1 H, H-6$_a$), 4.32 (d, 1 H, $J_{1',2'}$ = 8.0 Hz, H-1′), 4.31-4.26 (m, 1 H, H-6′$_a$), 4.13-4.07 (m 1 H, H-6$_b$), 4.05 (dd, 1 H, $J_{6'b,6'a}$ = 12.3, $J_{6'b,5'}$ = 2.1 Hz, H-6′$_b$), 3.98 (d, 1 H, H-5″), 3.85, 3.80 (m, 3 H, H-5, H-3′, H-4), 3.71 (s, 1 H, O-CH$_3$), 3.62-3.58 (m,1 H, H-5′), 2.12-1.98 (m, 27 H, 9 O-Ac). HRMS (ESI) _m/z_ 1054.2656 [M + Na]$^+$. Calculated for $C_{43}H_{53}NNaO_{28}$ 1054.2652.

Appendix

Michaelis-Menten parameters and plots of reaction rate against substrate concentration

Table A1. Michaelis-Menten Parmeters

Enzyme	Substrate	K_{m} (mM)	k_{cat}
Sp. Hex.	pNP-GlcNAc	0.072	3.2 x 10^{2} s^{-1}
Hex A	MUG	0.85	4.5 x 10^{2} s^{-1}
Hex B	MUG	0.92	1.5 x 10^{3} s^{-1}
Glucocerebrosidase	2,4-DNP-glucoside	1.6	4.3 x 10^{3} min^{-1}

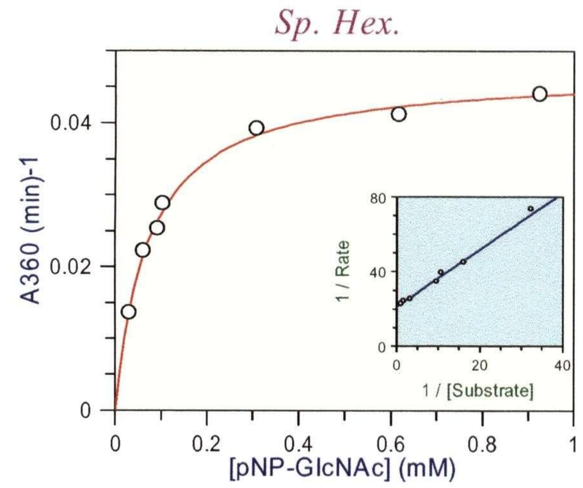

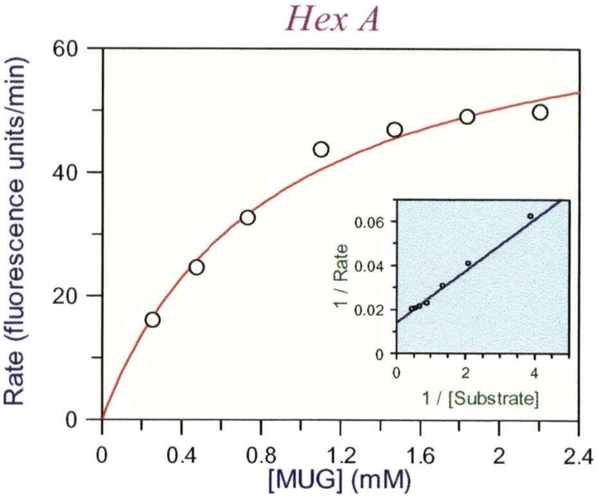

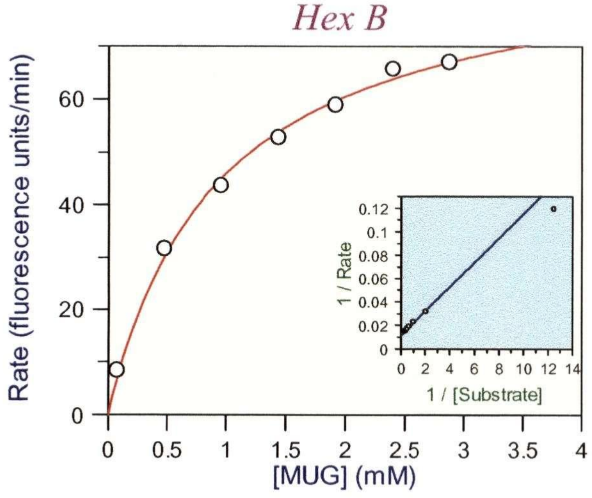

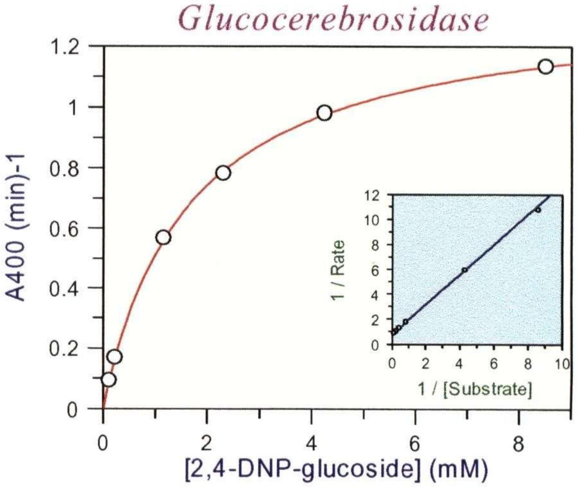

References

(1) Henrissat, B.; Bairoch, A. *Biochem. J.* **1996**, *316*, 695-696.

(2) Wolfenden, R.; Lu, X. D.; Young, G. *J. Am. Chem. Soc.* **1998**, *120*, 6814-6815.

(3) Koshland, D. E. *Biol. Rev.* **1953**, *28*, 416-436.

(4) Phillips, D. C. *Proc. Natl. Acad. Sci. U. S. A.* **1967**, *15*, 483-495.

(5) Sinnot, M. L.; Souchard, I. J. L. *Biochem. J.* **1973**, *133*, 89-98.

(6) McCarter, J. D.; Withers, S. G. *Curr. Opin. Struct. Biol.* **1994**, *4*, 885-892.

(7) White, A.; Tull, D.; Johns, K.; Withers, S. G.; Rose, D. R. *Nat. Struct. Biol.* **1996**, *3*, 149-154.

(8) Withers, S. G.; Warren, R. A. J.; Street, I. P.; Rupitz, K.; Kempton, J. B.; Aebersold, R. *J. Am. Chem. Soc.* **1990**, *112*, 5887-5889.

(9) Withers, S. G.; Aebersold, R. *Protein Sci.* **1995**, *4*, 361-372.

(10) Zechel, D. L.; Withers, S. G. *Acc. Chem. Res.* **2000**, *33*, 11-18.

(11) McIntosh, L. P.; Hand, G.; Johnson, P. E.; Joshi, M. D.; Korner, M.; Plesniak, L. A.; Ziser, L.; Wakarchuk, W. W.; Withers, S. G. *Biochemistry* **1996**, *35*, 9958-9966.

(12) Kempton, J. B.; Withers, S. G. *Biochemistry* **1992**, *31*, 9961-9969.

(13) Knapp, S.; Vocadlo, D.; Gao, Z. N.; Kirk, B.; Lou, J. P.; Withers, S. G. *J. Am. Chem. Soc.* **1996**, *118*, 6804-6805.

(14) Wolfenden, R. *Acc. Chem. Res.* **1972**, *5*, 10-18.

(15) Gruters, R. A.; Neefjes, J. J.; Tersmette, M.; Degoede, R. E. Y.; Tulp, A.; Huisman, H. G.; Miedema, F.; Ploegh, H. L. *Nature* **1987**, *330*, 74-77.

(16) Gubareva, L. V.; Kaiser, L.; Hayden, F. G. *Lancet* **2000**, *355*, 827-835.

(17) Goss, P. E.; Baker, M. A.; Carver, J. P.; Dennis, J. W. *Clin. Can. Res.* **1995**, *1*, 935-944.

(18) Ganem, B. *Acc. Chem. Res.* **1996**, *29*, 340-347.

(19) Look, G. C.; Fotsch, C. H.; Wong, C. H. *Acc. Chem. Res.* **1993**, *26*, 182-190.

(20) Truscheit, E.; Frommer, W.; Junge, B.; Muller, L.; Schmidt, D. D.; Wingender, W. *Angew. Chem. Int. Ed.* **1981**, *20*, 744-761.

(21) Clissold, S. P.; Edwards, C. *Drugs* **1988**, *35*, 214-243.

(22) Nicotra, F.; Panza, L.; Ronchetti, F.; Russo, G. *Gazz. Chim. Ital.* **1989**, *119*, 577-579.

(23) Nishikawa, T.; Ishida, N. *J. Antibiot.* **1965**, *18*, 132-133.

(24) Withers, S. G.; Namchuk, M.; Mosi, R. In *Iminosugars as Glycosidase Inhibitors; Nojirimycin and Beyond*; Stutz, A. E., Ed.; Wiley-VCH, 1999, pp 188-203.

(25) Umezawa, H.; Aoyagi, T.; Komiyama, T.; Morishima, H.; Hamada, M.; Takeuchi, T. *J. Antibiot.* **1974**, *17*, 963-969.

(26) Jespersen, T. M.; Dong, W. L.; Sierks, M. R.; Skrydstrup, T.; Lundt, I.; Bols, M. *Angew. Chem. Int. Ed.* **1994**, *33*, 1778-1779.

(27) Ichikawa, Y.; Igarashi, Y.; Ichikawa, M.; Suhara, Y. *J. Am. Chem. Soc.* **1998**, *120*, 3007-3018.

(28) Nishimura, Y.; Satoh, T.; Kudo, T.; Kondo, S.; Takeuchi, T. *Bioorg. Med. Chem.* **1996**, *4*, 91-96.

(29) Bols, M. *Acc. Chem. Res.* **1998**, *31*, 1-8.

(30) Withers, S. G.; Street, I. P.; Bird, P.; Dolphin, D. H. *J. Am. Chem. Soc.* **1987**, *109*, 7530-7531.

(31) Gravel, R. A.; Clarke, J. T. R.; Kaback, M. M.; Mahuran, D.; Sandhoff, K.; Suzuki, K. In *The Metabolic and Molecular Basis for Inherited Disease*; 7 ed., 1995; Vol. 2, pp 2839-2879.

(32) Gieselmann, V. *Biochim. Biophys. Acta-Mol. Bas. Dis.* **1995**, *1270*, 103-136.

(33) Voet, D.; Voet, J. G. *Biochemistry*; John Wiley and Sons, 1990.

(34) Sandhoff, K. In *Tay-Sachs Disease*, 2001; Vol. 44, pp 67-91.

(35) Svennerholm, L. *Biochem. Biophys. Res. Commun.* **1962**, *9*, 436-441.

(36) Okada, S.; O'Brien, J. S. *Science* **1969**, *165*, 698-700.

(37) Mahuran, D. J. *Biochim. Biophys. Acta-Mol. Bas. Dis.* **1999**, *1455*, 105-138.

(38) Mahuran, D. J. *Biochim. Biphys. Acta-Lip. Lip. Met.* **1998**, *1393*, 1-18.

(39) Ellgaard, L.; Molinari, M.; Helenius, A. *Science* **1999**, *286*, 1882-1888.

(40) Leinekugel, P.; Michel, S.; Conzelmann, E.; Sandhoff, K. *Hum. Genet.* **1992**, *88*, 513-523.

(41) Mark, B. L.; Mahuran, D. J.; Cherney, M. M.; Zhao, D. L.; Knapp, S.; James, M. N. G. *J. Mol. Biol.* **2003**, *327*, 1093-1109.

(42) Sharma, R.; Deng, H. N.; Leung, A.; Mahuran, D. *Biochemistry* **2001**, *40*, 5440-5446.

(43) Sharma, R.; Bukovac, S.; Callahan, J.; Mahuran, D. *Biochim. Biophys. Acta-Mol. Bas. Dis.* **2003**, *1637*, 113-118.

(44) Zhao, H.; Grabowski, G. A. *Cell. Mol. Life Sci.* **2002**, *59*, 694-707.

(45) Meikle, P. J.; Hopwood, J. J.; Clague, A. E.; Carey, W. F. *J. Am. Med. Assoc.* **1999**, *281*, 249-254.

(46) Barton, N. W.; Brady, R. O.; Dambrosia, J. M.; Dibisceglie, A. M.; Doppelt, S. H.; Hill, S. C.; Mankin, H. J.; Murray, G. J.; Parker, R. I.; Argoff, C. E.; Grewal, R. P.; Yu, K. T. *New Eng. J. Med.* **1991**, *324*, 1464-1470.

(47) Sawkar, A. R.; Cheng, W. C.; Beutler, E.; Wong, C. H.; Balch, W. E.; Kelly, J. W. *Proc. Natl. Acad. Sci. U. S. A.* **2002**, *99*, 15428-15433.

(48) Grabowski, G. A.; Gatt, S.; Horowitz, M. *Crit. Rev. Biochem. Mol. Biol.* **1990**, *25*, 385-414.

(49) Dvir, H.; Harel, M.; McCarthy, A. A.; Toker, L.; Silman, I.; Futerman, A. H.; Sussman, J. L. *EMBO Rep.* **2003**, *4*, 704-709.

(50) Grabowski, G. A.; Gatt, S.; Kruse, J.; Desnick, R. J. *Arch. Biochem. Biophys.* **1984**, *1*, 144-157.

(51) Butters, T. D.; Dwek, R. A.; Platt, F. M. *Chem. Rev.* **2000**, *100*, 4683-4696.

(52) Andersson, U.; Butters, T. D.; Dwek, R. A.; Platt, F. M. *Biochem. Pharmacol.* **2000**, *59*, 821-829.

(53) Morello, J.-P.; Petaja-Repo, U. E.; Bichet, D. G.; Bouvier, M. *Trends Pharmacol. Sci.* **2000**, *21*, 466-469.

(54) Sato, S.; Ward, C. L.; Krouse, M. E.; Wine, J. J.; Kopito, R. R. *J. Biol. Chem.* **1996**, *271*, 635-638.

(55) Fan, J. Q.; Ishii, S.; Asano, N.; Suzuki, Y. *Nature Med.* **1999**, *5*, 112-115.

(56) Matsuda, J.; Suzuki, O.; Oshima, A.; Yamamoto, Y.; Noguchi, A.; Takimoto, K.; Itoh, M.; Matsuzaki, Y.; Yasuda, Y.; Ogawa, S.; Sakata, Y.; Nanba, E.; Higaki, K.; Ogawa, Y.; Tominaga, L.; Ohno, K.; Iwasaki, H.; Watanabe, H.; Brady, R. O.; Suzuki, Y. *Proc. Natl. Acad. Sci. U. S. A.* **2003**, *100*, 15912-15917.

(57) Vocadlo, D. *Ph.D thesis*; The University of British Columbia, 2002.

(58) Mark, B. L.; Vocadlo, D. J.; Knapp, S.; Triggs-Raine, B. L.; Withers, S. G.; James, M. N. G. *J. Biol. Chem.* **2001**, *276*, 10330-10337.

(59) Mark, B. L.; Vocadlo, D. J.; Zhao, D. L.; Knapp, S.; Withers, S. G.; James, M. N. G. *J. Biol. Chem.* **2001**, *276*, 42131-42137.

(60) Leatherbarrow, R. J.; GraFit, Version 4.0.19, Erithacus Software Ltd., 2003.

(61) Benyoseph, Y.; Reid, J. E.; Shapiro, B.; Nadler, H. L. *Am. J. Hum. Genet.* **1985**, *37*, 733-740.

(62) Creighton, T. E. *Protein Structure: A Practical Approach, 2nd ed.*; Oxford University Press, **1997**.

(63) Tropak, M. B.; Reid, S. P.; Guiral, M.; Withers, S. G.; Mahuran, D. *J. Biol. Chem.* **2004**, *in press*.

(64) Miao, S. C.; McCarter, J. D.; Grace, M. E.; Grabowski, G. A.; Aebersold, R.; Withers, S. G. *J. Biol. Chem.* **1994**, *269*, 10975-10978.

(65) Withers, S. G.; Rupitz, K.; Street, I. P. *J. Biol. Chem.* **1988**, *263*, 7929-7932.

(66) Stevenson, A. D. *M.Sc. thesis*; The University of British Columbia, 1994.

(67) McCarter, J. D.; Adam, M. J.; Hartman, N. G.; Withers, S. G. *Biochem. J.* **1994**, *301*, 343-348.

(68) McCarter, J. D. *Ph.D. Thesis*; The University of British Columbia, 1995.

(69) Wong, A. W.; Adam, M. J.; Withers, S. G. *J. Labelled Compd. Radiopharm.* **2001**, *44*, 385-394.

(70) Wong, A. W. *Ph.D. Thesis*; The University of British Columbia, 2001.

(71) Hall, L. D.; Johnson, R. N.; Adamson, J. B.; Foster, A. B. *Can. J. Chem.* **1971**, *49*, 118-126.

(72) Albert, M.; Dax, K.; Ortner, J. *Tetrahedron* **1998**, *54*, 4839-4848.

(73) Rizzolo, L. J.; le Maire, M.; Reynolds, J. A.; Tanford, C. *Biochemistry* **1976**, *15*, 3433-3437.

(74) Cockle, S. A.; Epand, R. M.; Moscarello, M. A. *J. Biol. Chem.* **1978**, *253*, 8019-8026.

(75) Sun, Z. Y.; Pratt, E. A.; Simplaceanu, V.; Ho, C. *Biochemistry* **1996**, *35*, 16502-16509.

(76) Ogawa, S.; Ashiura, M.; Uchida, C.; Watanabe, S.; Yamazaki, C.; Yamagishi, K.; Inokuchi, J. *Bioorg. Med. Chem. Lett.* **1996**, *6*, 929-932.

(77) McAuliffe, J. C.; Stick, R. V. *Aust. J. Chem.* **1997**, *50*, 193-196.

(78) Kutney, J. P.; Abdurahman, N.; Gletsos, C.; Le Quesne, P.; Piers, E.; Vlattas, I. *J. Am. Chem. Soc.* **1970**, *92*, 1727-1735.

(79) Simon, P. M. *Drug Discovery Today* **1996**, *1*, 522-528.

(80) Laine, R. A. *Glycobiology* **1994**, *4*, 759-767.

(81) Palcic, M. M. *Curr. Opin. Biotechnol.* **1999**, *10*, 616-624.

(82) Mackenzie, L. F.; Wang, Q. P.; Warren, R. A. J.; Withers, S. G. *J. Am. Chem. Soc.* **1998**, *120*, 5583-5584.

(83) Williams, S. J.; Withers, S. G. *Aust. J. Chem.* **2002**, *55*, 3-12.

(84) Huber, R.; Langworthy, T. A.; Konig, H.; Thomm, M.; Woese, C. R.; Sleytr, U. B.; Stetter, K. O. *Arch. Microbiol.* **1986**, *144*, 324-333.

(85) Nelson, K. E.; Clayton, R. A.; Gill, S. R.; Gwinn, M. L.; Dodson, R. J.; Haft, D. H.; Hickey, E. K.; Peterson, L. D.; Nelson, W. C.; Ketchum, K. A.; McDonald, L.; Utterback, T. R.; Malek, J. A.; Linher, K. D.; Garrett, M. M.; Stewart, A. M.; Cotton, M. D.; Pratt, M. S.; Phillips, C. A.; Richardson, D.; Heidelberg, J.; Sutton, G. G.; Fleischmann, R. D.; Eisen, J. A.; White, O.; Salzberg, S. L.; Smith, H. O.; Venter, J. C.; Fraser, C. M. *Nature* **1999**, *399*, 323-329.

(86) Goyal, K.; Selvakumar, P.; Hayashi, K. *J. Mol. Cat. B-Enz.* **2001**, *15*, 45-53.

(87) Menzel, E. J.; Farr, C. *Canc. Lett.* **1998**, *131*, 3-11.

(88) Valla, S.; Li, J. P.; Ertesvag, H.; Barbeyron, T.; Lindahl, U. *Biochimie* **2001**, *83*, 819-830.

(89) Mulder, G. J. *Annu. Rev. Pharmacol. Toxicol.* **1992**, *32*, 25-49.

(90) Soliman, S. E.; Bassily, R. W.; El-Sokkary, R. I.; Nashed, M. A. *Carbohydr. Res.* **2003**, *338*, 2337-2340.

(91) Madaj, J.; Trynda, A.; Jankowska, M.; Wisniewski, A. *Carbohydr. Res.* **2002**, *337*, 1495-1498.

(92) Mayer, C.; Zechel, D. L.; Reid, S. P.; Warren, R. A. J.; Withers, S. G. *FEBS Lett.* **2000**, *466*, 40-44.

(93) Nashiru, O.; Zechel, D. L.; Stoll, D.; Mohammadzadeh, T.; Warren, R. A. J.; Withers, S. G. *Angew. Chem. Int. Ed.* **2001**, *40*, 417-420.

(94) Jain, S.; Drendel, W. B.; Chen, Z. W.; Mathews, F. S.; Sly, W. S.; Grubb, J. H. *Nat. Struct. Biol.* **1996**, *3*, 375-381.

(95) Juers, D. H.; Jacobson, R. H.; Wigley, D.; Zhang, X. J.; Huber, R. E.; Tronrud, D. E.; Matthews, B. W. *Protein Sci.* **2000**, *9*, 1685-1699.

(96) Juers, D. H.; Heightman, T. D.; Vasella, A.; McCarter, J. D.; Mackenzie, L.; Withers, S. G.; Matthews, B. W. *Biochemistry* **2001**, *40*, 14781-14794.

(97) Guex, N.; Peitsch, M.; Schwede, T.; Diemand, A.; 3.7 ed.

(98) Segel, I. H. *Enzyme Kinetics: Behaviour and Analysis of Rapid Equilibrium and Steady-State Enzyme Systems*; Wiley and Sons, 1993.

(99) Savitzky, A.; Golay, M. J. E. *Anal. Chem.* **1964**, *36*, 1627-1639.